AN OXYGEN ISOTOPIC STUDY OF SOIL WATER AND PEDOGENIC CLAYS IN HAWAII

Thesis by

Jean Chia Chin Hsieh

In Partial Fulfillment of the Requirements

for the Degree of

Doctor of Philosophy

California Institute of Technology

Pasadena, California

1997

(Thesis Defense: October 14, 1996)

Anything that can create itself by erupting out of the bowels of the Pacific Ocean is worth looking at.

- Hunter S. Thompson

Acknowledgements

There are many people to thank for help during my thesis work. The first is Oliver Chadwick. I don't know how to convey all my thoughts and so will only say "thanks." I don't think I would have made it without you. Many thanks need to be given to Sam Savin. Your patience with my numerous messages surprises me. To both Oliver and Sam, in the field and lab, there are no better mentors.

Official acknowledgements go out to Natural Science and Engineering Research Council of Canada and NASA Global Change graduate student fellowships for financial support. Research was supported by: JPL on contract to NASA's Mission to Planet Earth program (Oliver Chadwick), NSF grants EAR 91-05112 and EAR 94-18970 to Sam Savin, NSF grant EAR 92-18609 to Gene Kelly and the Colorado Agricultural Experimental Station, NSF grant EAR 93-17036 to Hugh Taylor, and internal funds from the Division of Geological and Planetary Sciences at Caltech.

Many thanks are required for help in Hawaii: Bob Gavenda, Chris Smith, and the gang in the SCS, sorry, NRCS-Kealakekua field office for use of vehicles and field logistics (thanks for your floor, Bob!), Monty Richards and Kahua Ranch for letting us dig holes in your fields and for pulling us out of the mud, the Kohala Ranch Water Company for collecting rain and ET-gauge readings (thanks Danny and Dave), the Kohala Ranch Estates for permission to dig holes without remediation, Ron Peyton and John Schlaegel for field logistics in Kauai, Tim Crews for pulling me out of the swamp, and Peter Vitousek, Amy Austin, and Margaret Torn for digging in that swamp, and finally thanks to all my diggers (Oliver Chadwick, Dana Chadwick, Bob Gavenda, Gene Kelly, Sam Savin, Robbie Savin, Don Banfield, Jason Hanchett, and Dave Evans).

Back on the mainland, many thanks for laboratory help to: Hugh Taylor, Xiahong Feng, Carey Gazis, Greg Holk, Cindy Grove, Xiaomei Xu, and Shannon McKinnon, and for paperwork, thanks to Kathy Lima, Mary Mellon, and Kerry Etheridge. Many thanks to all (Sylvie Giral, Linda Abel, Crawford Elliot, and Jim "Dr. A" Aronson) at Case

Western Reserve, my second home. I especially want to thank Linda Abel for all the help and great suggestions. Thanks to Bob Graham and his lab for letting me learn those soil chemistry tricks. Thanks to Kinga Revesz for azeotropic extractions and Hope for vacuum extractions. Discussions and encouragement was greatly appreciated from: Gene Kelly, Dave Hendricks, Rosemary Capo, Brian Stewart, Sue Trumbore, Ron Amundson, Ariel Anbar, Hope Jahren, Claudia Mora, Sam Epstein, George Rossman, and Lee Silver. Many thanks to Bruce Murray for suffering with me through the heat of Death Valley. I appreciate all your help and advice.

Finally, thanks to all fellow students at Caltech for moral support. Thanks to my officemates, Judy Zachariasen and Elizabeth Nagy, for actually living out the Zilchbrau skit, and all my housemates (at one time or another): Kim Mislick, Laura Wasylenki, Mihai Ducea, Nathan Niemi, and Jim Spotila (thanks, Spot, for your writing lessons). I also thank James Gleeson for putting up with my moods during the last few months and for lending me your shoulder. This thesis is dedicated to my parents, Mike and Sally, and especially for my brother, Wayne, this is for you!

Abstract

Soils result from complex interactions amongst the biosphere, atmosphere, hydrosphere, and lithosphere. In this project oxygen isotopes were used to trace the movement of water in soils and to determine the conditions of mineral formation during pedogenesis. Incoming rainwater and soil-water $\delta^{18}O$ values were monitored for two seasonal cycles in a series of soils along an arid-to-humid transect in Hawaii. The $\delta^{18}O$ values of halloysite separated from the soil profiles was related to depth profiles of soil-water $\delta^{18}O$ values. This is the first oxygen isotopic investigation of soil water and pedogenic clays from the same soil profiles.

A direct CO_2 equilibration method was developed to measure the $\delta^{18}O$ value of soil water. This method also has the advantage of requiring only one step compared with two steps for existing methods. Reproducibility of measurements using this method is as good as existing methods. Tests designed to investigate factors controlling equilibration determined that biological respiration, water content, and soil type were important. Samples should be irradiated to eliminate CO_2-respiring organisms. These results imply that water in soils can be partitioned into compartments such as bulk liquid water and adsorbed water and that these compartments may have unique isotopic compositions.

Application of this method to the soils in Hawaii showed that seasonal wetting and drying cycles affected the $\delta^{18}O$ value of soil water. During the dry season, the soil-water $\delta^{18}O$ values decrease with depth in the soil profile due

to evaporation of water from the surface. During the rainy season, they increase with depth as water infiltrates through the surface from storms. The $\delta^{18}O$ values of rainwater and soil-water generally increased as annual rainfall increased. Rainwater $\delta^{18}O$ values were 5‰ more negative soil-water $\delta^{18}O$ values at low rainfall sites and about 2‰ to 3‰ more negative at high rainfall sites. These trends are consistent with the current understanding of parameters that influence these $\delta^{18}O$ values.

The chemical treatments used to separate halloysite from bulk soil material did not alter the $\delta^{18}O$ values. Halloysite $\delta^{18}O$ values at low rainfall sites ranged between +20.4‰ to +23.6‰ and the two values at a high rainfall site ranged from +18.0‰ to +18.7‰. The data suggest halloysite formation in isotopic equilibrium with its environment and imply that it forms in a restricted range of conditions. A straightforward comparison of these data to soil-water $\delta^{18}O$ values suggests that halloysite formed between 50°C and 60°C, obviously an unrealistic circumstance. It is possible that independently calibrated mineral–water fractionation factors for low-temperature systems are incorrect or that climatic conditions in Hawaii are poorly constrained.

Table of Contents

List of Figures

Chapter 2

Chapter 3

Chapter 4

Chapter 5

Chapter 6

List of Tables

Chapter 2

Chapter 3

Chapter 5

Chapter 6

Chapter 1. Introduction to the Project.

Soils are formed at the interface of the biosphere, atmosphere, hydrosphere, and lithosphere. Variations in any of the four systems can be potentially recorded in a soil. Conversely, by examining soil properties, we may be able to learn about the history of those systems. Because the soil system is a complex mixture of organic material, mineral matter, and water, there is no simple way to isolate the effects of the biosphere, atmosphere, hydrosphere, and lithosphere. However, detailed characterization of soil material will lead to a better understanding of the process of soil formation. In this thesis project, I used the oxygen isotopic ratio, $^{18}O/^{16}O$, to trace the movement of water as it interacted with soil profiles and to determine the temperature and isotopic composition of the water present during pedogenic clay mineral formation.

1.1. Oxygen isotopic studies in modern soils.

Previous stable isotopic studies of soil material have primarily focused on soil water or on mineral matter in separate studies. In this project, I have combined these two types of studies. The incoming rainfall and soil-water $\delta^{18}O$ values were monitored for two seasonal cycles in a series of soils along an arid-to-humid transect in Hawaii. From these same soils, halloysite, the dominant clay mineral, was separated from the bulk soil material and its $\delta^{18}O$ value was measured. This is the first project to investigate oxygen isotopes in

coexisting soil water and pedogenic clay minerals at different depths in the same soil profiles.

Arid and semi-arid soils have been used to test theoretical models that describe the effect of soil-water evaporation on its stable isotopic composition (e.g. Allison et al., 1983). However, models which describe the effect of evaporation on soils formed in humid environments have not been fully investigated, in part because the process of evaporation is often interrupted by frequent rain storms. This project is the first documentation of soil-water $\delta^{18}O$ values in humid soils.

Most stable isotopic studies of pedogenic minerals have focused on the carbon isotopes of pedogenic carbonate (e.g. Cerling, 1992) to investigate possible changes in vegetative cover. Investigations of the role of oxygen isotopes in the process of mineral formation in soils have been few and have primarily focused on older soils composed of a significant amount of kaolinite (Bird et al., 1989, 1993; Giral, 1994; Giral et al., in prep.; Elliot et al., in prep). Critical to the interpretation of those values is the isolation of relatively pure kaolinite separate. In this project, I have investigated, for the first time, the oxygen isotopic behaviour of halloysite separated from bulk soil material.

1.2. Why study soils in Hawaii?

The soils studied for this project are located on the leeward side of the Kohala peninsula on the island of Hawaii. This location was chosen initially

to minimize the amount of clay material added through continental eolian dust. Hawaii is located in the middle of the Pacific ocean, far from large continental masses. The amount of eolian material is minimal, although there is some quartz and mica blown in from Asia and some locally reworked material. Furthermore, the basalt parent material in Hawaii also contains no naturally occurring clays. Thus, the amount of inherited clay material is also minimized. Halloysite, the dominant crystalline clay material in these soils is thus very likely to have formed *in situ*.

Other factors that influenced the site selection process can be visualized using the state factor theory of soil formation (Jenny, 1941):

$$S = f\,(cl, o, r, p, t, \ldots)$$

where S denotes the characteristics of the soil, *cl* the climatic factor, *o* the biotic factor, *r* the topographic factor, *p* the parent material factor, and *t* the time factor. The dots after *t* represent additional factors that might be important locally. In the approach used here, the importance of a single factor may be resolved by examining a suite of soils in which only that factor varies and all others have been held constant. By choosing sample sites with similar micro-topographic locations on lava flows of the same age, the factors *t*, *p*, and *r* are held constant. All sites were chosen in grassland environments and thus, *o* is also held constant. Therefore, the climate factor is the only one that varies among this series of soils, and this factor is primarily expressed as a difference in annual rainfall. By using the series of soils along an arid to humid transect, the effect of increasing annual rainfall on pedogenic

processes can be investigated through the use of oxygen isotopes as a geochemical tracer.

1.3. Description of chapters.

The standard technique by which soil-water $\delta^{18}O$ values are measured has been to first extract the soil water and then to measure its isotopic composition. However, the most widely used methods for water extraction from soils, namely azeotropic distillation and vacuum distillation can result in significantly different $\delta^{18}O$ values for the same sample when different temperatures and durations of extraction are used (Walker et al., 1994). For this project, a direct equilibration technique was successfully developed which avoids the errors intrinsic with bulk water extraction. This technique is presented in Chapter 2 and has been submitted as a paper to the journal *Geoderma* with co-authors Sam Savin, Gene Kelly, and Oliver Chadwick.

The idea of direct equilibration was suggested previously for soils (Jusserand, 1980) and tested more recently for the measurement of $\delta^{18}O$ values of plant material (Scrimgeour, 1995). The present study is the first application of the direct equilibration technique to soil material. Experiments were designed to test the effect of biological respiration, water content, and soil type on equilibration. Specific questions that were answered included: How does this method compare to standard methods in terms of reproducibility? Which is the most appropriate method to use? Are measurements of the

isotopic composition of soil water affected by the amount of water in the soil or by the type of soil?

After testing this technique, it was applied to samples of soil from the arid to humid transect in Hawaii. The $\delta^{18}O$ value of soil water and incoming precipitation, and the volumetric water content of the soil, were monitored for two seasonal cycles. The results of that study are presented in Chapter 3 and have been submitted to *Geoderma* with co-authors Oliver Chadwick, Gene Kelly, and Sam Savin. Questions that were answered in this investigation included: Do the observed patterns at the arid sites match theoretical calculations? What are the patterns at the humid sites? Are these patterns related to macroenvironmental parameters such as annual rainfall or evaporative demand? Are there any changes in the values through the year and if so, what causes them? What is the relationship between rainfall and soil-water $\delta^{18}O$ values?

The final part of this project is an investigation into the $\delta^{18}O$ values of pedogenic halloysite. It is presented in three chapters. Chapter 4 provides the background information regarding isotopic studies of clay minerals in soils. Chapter 5 describes the sample preparation techniques for separating halloysite. Chapter 6 presents the results from the soils on Kohala and our interpretations. The questions that were answered for this part of the project include: Can halloysite be separated from the bulk soil material? Is the $\delta^{18}O$ value affected by the separation treatments? Is there any systematic pattern in

the soil profiles? How do they compare to soil-water values? Is it possible to understand the conditions of formation from these $\delta^{18}O$ values?

Finally, the conclusions of all parts of this project are summarized and discussed in Chapter 7. The general questions addressed there include: Is annual rainfall important in controlling pedogenic processes? Are oxygen isotopes appropriate for tracing pedogenic processes? What have we learned about the formation of soils on Hawaii?

1.4. Definitions of isotopic terms.

A few basic definitions will be given here in lieu of a detailed discussion of the chemistry of oxygen isotopes which can be found in numerous sources (e.g. O'Neil, 1987, Sheppard, 1987, Savin and Lee, 1988, Sheppard and Gilg, 1996).

Isotope ratios are reported in δ-notation,

$$\delta = \left(\frac{R_{sample} - R_{std}}{R_{std}} \right) \times 1000$$

R_{sample} is the isotope ratio, e.g. $^{18}O/^{16}O$ ratio, of the sample and R_{std} is the isotope ratio of the standard to which the measurement is referred. All oxygen isotope ratios in this study are reported relative to Standard Mean Ocean Water (SMOW). Carbon isotope ratios are reported relative to the Pee Dee Belemnite (PDB) standard. The units of δ are permil (‰).

When a system is in isotopic equilibrium, an isotopic fractionation factor, α, can be defined:

$$\alpha_{i-ii} = \frac{1+\frac{\delta_i}{1000}}{1+\frac{\delta_{ii}}{1000}} = \frac{1000+\delta_i}{1000+\delta_{ii}}$$

where R_i and R_{ii} are isotope ratios of the same element in two compounds or phases, *i* and *ii*. In this dissertation, the term *fractionation factor* will be used to mean *equilibrium oxygen isotopic fractionation factor*. In fact, demonstrating that systems are actually in isotopic equilibrium is a ubiquitous problem in isotope geochemistry. This study is no exception. Like other preliminary investigations of new mineral-fluid systems, it is necessary to simply presume equilibrium, in the absence of direct evidence of disequilibrium, in order to establish preliminary patterns in the data.

Another term, $\Delta_{i\text{-}ii}$ (sometimes referred to informally as "big delta"), is expressed as:

$$\Delta_{i-ii} = 1000 \ln\left(\frac{R_i}{R_{ii}}\right)$$

When using $\Delta_{i\text{-}ii}$, there is no connotation of isotopic equilibrium.

Specific details about oxygen isotopes will be given when appropriate in later chapters.

1.5. References.

Allison, G.B., Barnes, C.J., and Hughes, M.W., 1983. The distribution of deuterium and ^{18}O in dry soils, 2. Experimental. Journal of Hydrology, 64: 377-397.

Bird, M.I., Chivas, A.R., and Andrew, A.S., 1989. A stable-isotope study of lateritic bauxites. Geochimica et Cosmochimica Acta, 53: 1411-1420.

Bird, M.I., Longstaffe, F.J., Fyfe, W.S., Kronber, B.I., and Kishida, A., 1993. An oxygen-isotope study of weathering in the eastern Amazon Basin, Brazil. In: P.K. Swart, K.C. Lohman, J. McKenzie, and S. Savin (editors), Climate Change in Continental Isotopic Records. A.G.U. Geophysical Monograph 78: 295-307.

Cerling, T.E., 1992. Development of grasslands and savannas in East Africa during the Neogene. Palaeogeography, Palaeoclimatology, Palaeoecology (Global Planetary Change Section), 97: 241-247.

Elliot, W.C., Savin, S.M., Dong, H., and Peacor, D.R., in preparation. Paleoclimate implications of the mineralogy and the oxygen isotope geochemistry of clay minerals formed in a saprolite from the Piedmont province, Virginia.

Giral, S., 1994. Variations des rapports isotopiques $^{18}O/^{16}O$ des kaolinites de deux profils latéritiques amazoniens: signification pour la pédologie et la paléoclimatologie. Ph.D. Thesis, Université de Droit, D'Économie et des Sciences d'Aix-Marseille.

Giral, S., Savin, S.M., Nahon, D.B., Girard, J.P., Lucas, Y., and Abel, L.J., in preparation. Oxygen isotope geochimistry of kaolinite in laterite-forming processes, Manaus, Amazonas, Brazil.

Jenny, H., 1941. Factors of soil formation. McGraw-Hill Book Company, Inc. New York, 281 pp.

Jusserand, C. 1980. Extraction de l'eau intersticielle des sediments et des sols. Comparaison des valeurs de l'oxygene 18 par differentes methodes. Premiers resultats. Catena, 7: 87-96.

O'Neil, J.R., 1987. Theoretical and experimental aspects of isotopic fractionation. In : J.W. Valley, H.P. Taylor, Jr., and J.R. O'Neil (editors), Stable isotopes in high temperature processes. Rev. in Min., v16: 1-40.

Savin, S.M., and Lee, M., 1988. Isotopic studies of phyllosilicates. In: S.W. Bailey (editor), Hydrous phyllosilicates (exclusive of micas). Rev. in Min., v19: 189-219.

Scrimgeour, C.M., 1995. Measurement of plant and soil water isotope composition by direct equilibration methods. Journal of Hydrology, 173: 261-274.

Sheppard, S.M.F., 1987. Characterization and isotopic variations in natural waters. In : J.W. Valley, H.P. Taylor, Jr., and J.R. O'Neil (editors), Stable isotopes in high temperature processes. Rev. in Min., v16: 165-183.

Sheppard, S.M.F., and Gilg, H.A., 1996. Stable-isotope geochemistry of clay-minerals. Clay Minerals, 31(1): 1-24.

Walker, G.R., Woods, P.H. and Allison, G.B., 1994. Interlaboratory comparison of methods to determine the stable isotope composition of soil water. Chemical Geology, 111: 297-306.

Chapter 2. Method for Measuring Soil-Water $\delta^{18}O$ Values.

The purpose of this chapter is to describe and test an alternative method for measuring the $\delta^{18}O$ value of soil water. This method uses direct equilibration with CO_2 instead of the standard two step procedure of soil-water extraction and subsequent isotopic measurement of the water. The reproducibility of the equilibration method is investigated, and other experiments were designed and performed to test the effect of irradiation treatment, soil type, and water content on the equilibration process.

2.1. Introduction.

The $\delta^{18}O$ value of soil water is commonly measured in a two step procedure. First, the water is extracted. Next, its isotopic composition is determined using a CO_2–water equilibration (Cohn and Urey, 1938; Epstein and Mayeda, 1953) or direct analysis by fluorination of the water (O'Neil and Epstein, 1966). The most widely used methods for water extraction are vacuum distillation and azeotropic distillation (Litaor, 1988; Revesz and Woods, 1990; Araguás-Araguás et al., 1995). For reasons explained below, the isotopic composition of water extracted using those methods may not be appropriate for use in studies where oxygen isotope ($^{18}O/^{16}O$) ratios of pedogenic minerals are to be related to the isotopic composition of soil water in the presence of which they formed or grew.

This method is a variant of the direct equilibration technique, first mentioned by Jusserand (1980) for soil material and more recently tested by Scrimgeour (1995) on plant materials. In this modification, CO_2 is equilibrated with soil that has been sterilized by radiation but is otherwise unmodified following collection in the field. Results of tests done using soils of different types and water content are reported. The results of the equilibration technique are compared with those obtained using azeotropic and vacuum distillation methods, and differences between the results of the methods are interpreted in terms of the existence of isotopic fractionations among the different physico-chemical forms of H_2O within the soil.

Water in soil can be visualized as a number of physico-chemically different, thermodynamically distinct forms (termed *compartments*), each of which can be described or identified on the basis of its relationship to the solid phase of the soil (Figure 2.1). The bulk liquid phase (which is called *liquid water*) moves about in response to a gradient in tension. Adsorbed water, which is held by mineral surfaces, and structural water, which is held loosely (as in smectite) or tightly (as in gypsum) in the crystal lattice of minerals, have different chemical and physical properties than liquid water (Sposito, 1984; Dunitz, 1994). In general, one may expect water in each compartment to have an $^{18}O/^{16}O$ ratio distinct from that of water in each of the other compartments.

The isotopic fractionations among different compartments of water are readily understood by analogy with brine systems that have received detailed study (Taube, 1954; Truesdell, 1974; Sofer and Gat, 1972, 1975; Horita and Gat,

1989). When a series of brines of varying solute concentrations is made by dissolving salts in distilled water, it is clear that the $\delta^{18}O$ values of the bulk solutions must be the same as that of the distilled water. However, the activity of ^{18}O in the liquid (as measured, for example, by the $\delta^{18}O$ value of water vapor or CO_2 in equilibrium with the solution) can indeed differ from that of the bulk solution. This reflects the fact that the water that forms coordination spheres around solute ions does not have the same isotopic composition as the "free" liquid water. Isotopically, the solution can be thought of as consisting of water in two compartments, free water and coordination water. If coordination spheres are enriched in ^{18}O relative to the free liquid, the free liquid becomes depleted in ^{18}O, and *vice versa*. If a significant fraction of total water occurs in spheres of coordination, the isotopic composition of the free water fraction may be significantly different (by a few ‰) than that of the total water of the solution. Similarly, in soils, the thermodynamic properties of water in the different compartments, and thus the $\delta^{18}O$ values of those compartments, ought to be different from one another and from that of the bulk water of the soil. Some evidence of fractionation is suggested by Araguás-Araguás et al. (1995) and Scrimgeour (1995).

If the water in each compartment is isotopically uniform, and if all of the compartments are in oxygen isotopic equilibrium with one another (conditions that seem reasonable except in the case of tightly held water of

crystallization), then the isotopic compositions of water in all of the compartments are related by the equations:

$$\delta_{total} = \Sigma\, x_i \delta_i$$

$$\alpha_{1-2} = R_1/R_2$$

$$\alpha_{1-3} = R_1/R_3$$

.

.

.

$$\alpha_{j-(j-1)} = R_j/R_{j-1}$$

where x_i is the mole fraction of water in the *i*th compartment ($\Sigma x_i=1$)

$\delta_i = [(R_i/R_{std}) - 1] \times 1000$

R_i is the $^{18}O/^{16}O$ ratio of the *i*th compartment, and R_{std} is the $^{18}O/^{16}O$ ratio of Standard Mean Ocean Water; and

α_{i-j} is the equilibrium fractionation factor between the water in the *i*th and *j*th compartments.

As a result of the partitioning of water among compartments within the soil, δ_{total} should approximate δ_{liquid} when most of the water is present in the liquid phase, but the two may differ significantly from one another when most of the soil water is not in the liquid phase.

In isotopic studies of mineral matter, a fractionation factor between the mineral and water is used to relate the two phases. Often, these fractionation factors are determined by isotopic measurement of the mineral and the liquid

water in which it was synthesized. Thus, when interpreting mineral $\delta^{18}O$ values, the most appropriate value to use for the isotopic composition of the water is the $\delta^{18}O$ value of liquid water. It is that value which is mostly likely obtained using the equilibration method.

2.2. *Materials and methods.*

Soils of three different types were used in this study: a clay loam, a silt loam and several coarse sandy loams. The clay loam is composed mainly of quartz and feldspar in the sand size fraction and smectite, kaolinite and minor amounts of iron and aluminum oxides in the clay size fraction. The silt loam is composed mainly of organic matter, non-crystalline material and poorly crystalline material such as ferrihydrite, imogolite and allophane in all size fractions. The coarse sandy loams are composed mainly of quartz and feldspar in the sand size fraction and illite in the clay size fraction. None of the soils contain carbonates. The clay loam and silt loam have high surface areas on which there can be a significant amount of adsorbed water (Hillel, 1980). The coarse sandy loams have less surface area. The clay loam also contains smectite, which has structural interlayer water. The silt and coarse sandy loams have relatively little smectite, and therefore little structural water.

Undisturbed soil samples were collected in the field, sealed in air-tight glass containers and coated with liquid Saran™ to further protect against loss of water by evaporation. In this study, some samples were also prepared by

adding water to dry soil. These were sealed in air-tight glass containers. To eliminate CO_2–respiring or metabolizing organisms, samples were sterilized by exposure to gamma radiation as soon as possible after collection; samples were refrigerated prior to irradiation to slow respiration. Each sample container was exposed to ^{137}Cs gamma radiation for a minimum dosage of 24 kGy at room temperature (Sparrow et al., 1967). To prevent reinnoculation of sterilized soil samples, all glass and metal equipment was autoclaved prior to use in the analysis.

An aliquot weighing 6 to 10 g is placed in a glass vacuum vessel fitted with a rubber septum (Figure 2.2). A larger soil sample is needed if the water content is low. This vessel is placed on a vacuum line and the soil is frozen with an ethanol-dry ice slurry. Once the sample is frozen (approximately 5 minutes), the vessel is opened to vacuum and evacuated. The stopcock to the vacuum is then closed and the sample is allowed to thaw, releasing any trapped gases into the head space. It is assumed to be thawed when it is not visibly frozen. Thawing time is variable and may take up to 30 minutes. The freeze-thaw process is repeated until no significant noncondensible gas is detected by a thermocouple vacuum gauge. At least 3 repetitions are required to release most of the soil gas. During the freeze-thaw process, the top of the glass vessel should be kept warmer than the soil to prevent condensation of water on the vessel walls. The top of the vessel is wrapped with electrical heating tape for this purpose. During freeze-thaw repetitions, water sometimes distills from the sample onto the sides of the vessel where it

freezes. This is most common for soils with higher water contents. Upon melting, it moves back into the soil. It is possible that this could result in some change in the distribution of water among different compartments that could affect the $\delta^{18}O$ value of the liquid water in the sample. This has not yet been investigated.

Tank CO_2 at a measured pressure (between 0.25 and 0.33 atm) is introduced into the vessel and allowed to exchange with the soil water in a thermostated bath at 25°C. To determine the time necessary for equilibration, an aliquot of CO_2 is taken with a gas-tight syringe through the rubber septum every few hours and analyzed on a mass spectrometer.

Isotopic results are reported in δ-notation as permil (‰) deviations from a standard. $^{18}O/^{16}O$ values are given relative to Standard Mean Ocean Water (SMOW) (Craig, 1961) and $^{13}C/^{12}C$ values are relative to the PDB standard. All soil-water contents (total water) are reported as a weight % (grams of water per gram of soil). The water contents are measured by weighing before and after drying in an oven at 110° overnight (Gardner, 1986) or fixed by adding known amounts of water to dry soil.

The $\delta^{18}O$ value of the water following equilibration with CO_2 may be calculated from the measured $\delta^{18}O$ value of CO_2 and $\alpha_{CO2\text{-}H2O}$ (1.0412 at 25°C according to Friedman and O'Neil, 1977). Because of isotopic exchange between CO_2 and water, however, δ^{f}_{H2O} is not identical to δ^{i}_{H2O}, the initial $\delta^{18}O$

value of the water. δ^i_{H2O} can be calculated from material balance considerations and the appropriate fractionation factors.

$$x_{CO2}\delta^i_{CO2} + \Sigma x_j \delta^i_{H2Oj} = x_{CO2}\delta^f_{CO2} + \Sigma x_j \delta^f_{H2Oj}$$

where the subscripts *i* and *f* denote initial (before equilibration) and final (after equilibration) conditions. The subscript *j* is used to index different compartments of water. Mole fractions of oxygen are indicated by *x*, appropriately subscripted.

In the simplest case, in which all of the water is present as liquid, the mass balance equation reduces to

$$x_{CO2}\delta^i_{CO2} + x_{H2O}\delta^i_{H2O} = x_{CO2}\delta^f_{CO2} + x_{H2O}\delta^f_{H2O}$$

and the initial value of the water is

$$\delta^i_{H2O} = [\delta^f_{CO2} - 1000(\alpha_{CO2\text{-}H2O} - 1)] / \alpha_{CO2\text{-}H2O} + (x_{CO2}/x_{H2O})(\delta^f_{CO2} - \delta^i_{CO2}).$$

x_{CO2} and x_{H2O} are calculated from n_{CO2} and n_{H2O}, the number of moles of oxygen in H_2O and CO_2 during equilibration. These, in turn, are calculated from sample weight and density, water content, volume of the equilibration vessel, pressure of CO_2 introduced into the vessel, and the ideal gas law.

$$n_{H2O} = \frac{\text{sample weight (g)} \times \text{water content (g H}_2\text{O / g sample)}}{18 \text{ g/mole H}_2\text{O}}$$

and

$$n_{CO2} = 2 \times \frac{PV}{RT}$$

where P is the pressure of CO_2, T is the absolute temperature, V is the volume and R is the gas constant. The factor of 2 is included because each molecule of CO_2 contains 2 atoms of oxygen.

$$V = V_{vessel} - V_{sample}$$

and

$$V_{sample} = \text{sample weight / bulk density}$$

Bulk density is the ratio of the mass of solids to the total volume (Blake and Hartge, 1986).

When water exists in more than one compartment, it is necessary to know the fractionation factors among the different compartments to solve for δ^i_{H2O} exactly. In the case of two water compartments, liquid and non-liquid,

$$\delta^i_{liq} = \left[\frac{1}{L}\cdot\frac{x_{CO2}}{(1-x_{CO2})} - \frac{1}{\alpha_{CO2-liq}}\right]\cdot\delta^f_{CO2} - \frac{1}{L}\cdot\frac{x_{CO2}}{(1-x_{CO2})}\cdot\delta^i_{CO2} + 1000\left(\frac{1}{\alpha_{CO2-liq}} - 1\right)$$

where

$$L = \frac{x_{liq}}{x_{liq}+x_{nonliq}} + \frac{1}{\alpha_{liq-nonliq}}\cdot\frac{x_{nonliq}}{x_{liq}+x_{nonliq}}$$

Neither the mole fractions of liquid and non-liquid water in a soil nor the fractionations among the different components are known. However, it is possible to estimate the magnitude of error introduced by intercompartmental fractionations on the value of δ^i_{liquid} calculated using the equilibration technique. It is unlikely, by analogy with what is known about

fractionations between liquid water, ice, and vapor, that the fractionation between liquid and non-liquid water in a soil is greater than 10‰. Using values of $\alpha_{liquid\text{-}nonliquid}$ between 0.99 and 1.01 and other values typical for the analyses reported in this paper (δ^f_{CO2} +20‰ to +40‰, δ^i_{CO2} +4‰, and x_{H2O} between 0.5 and 0.9), we calculate errors in δ^i_{liquid} ranging from 0 (when all of the water is liquid) to 0.36‰ (when all of the water is nonliquid). Errors in δ^i_{liquid} increase with increasing $\alpha_{liquid\text{-}nonliquid}$, $x_{nonliq}/(x_{liq} + x_{nonliq})$ and $(\delta^f_{CO2} - \delta^i_{CO2})$. Errors as large as 4.5‰ were calculated in a worst-case scenario in which a 50‰ fractionation between liquid and non-liquid was assumed, all of the water in the soil was non-liquid, x_{CO2} was 0.5, and the isotopic composition of the CO_2 shifted by 100‰ during the equilibration. These conditions are unlikely to occur in the analysis of naturally occurring samples.

The calculations for the case of two water compartments are equally valid when there are multiple compartments and the proportions of water in the various non-liquid compartments remain constant. For this study, because none of the fractionation factors between water compartments are known, all calculations were made assuming only one compartment of water.

2.3. Results and discussion.

2.3.1. Reproducibility.

Several aliquots taken from a single sample were analyzed to determine reproducibility of the method. Samples were prepared by adding

water to soil that had been oven dried at 110°C for 48 hours. The standard deviation was 0.4‰ (n=8) for the clay loam and 0.3‰ (n=7) for a coarse sandy loam. Revesz and Woods (1990) and Ingraham and Shadel (1992) reported a reproducibility of 0.2‰ for the azeotropic distillation method, Araguás-Araguás et al. (1995) reported a precision of 0.5‰ for the vacuum distillation method while Walker et al. (1994) reported an average precision of 0.3‰ for all methods that they compared.

2.3.2. Time of equilibration between CO_2 and soil water.

The time for oxygen isotope equilibration between CO_2 and soil water in three samples (two silt loams and a clay loam) was determined by analyzing a series of aliquots of CO_2 taken from each equilibration vessel. The two phases were deemed to be in equilibrium when the $\delta^{18}O$ of the CO_2 reached a value which did not change more than about 1‰ over a period of several days. Results are shown in Figure 2.3. The wetter silt loam reached oxygen isotope equilibrium in about 12 hours while it took about 24 hours for the clay loam and about 48 hours for the drier silt loam to reach equilibrium. We have not investigated the factors that affect equilibration time, but they probably include water content, pore size distribution, and the distribution of water among different compartments. We speculate that soils with significant amounts of liquid water may equilibrate with CO_2 more quickly than soils with only adsorbed and/or structural water. This is because of the rapidity with which dissolved HCO_3^- (formed by dissolution of CO_2 in liquid

water) exchanges with H_2O. We conclude that the time for oxygen isotope equilibration between CO_2 and soil water of each new soil needs to be determined prior to analyses of many samples of the same type.

2.3.3. Influence of biological respiration.

Biological respiration can affect the isotopic composition of soil water prior to analysis and biogenic CO_2 can exchange with the sample during analysis. Prior to analysis, respiration processes, illustrated schematically with glucose

$$C_6H_{12}O_6 + 6O_2 \rightarrow 6CO_2 + 6H_2O$$

result in formation of both H_2O and CO_2. If sufficient H_2O is produced and soil-water contents are low, the $\delta^{18}O$ value of the soil water may be changed prior to analyzing the sample. In addition, CO_2 produced within the sample jar will exchange with the soil water, possibly altering the isotopic composition of H_2O. Any CO_2 produced later in the equilibration vessel will also affect the $\delta^{13}C$ value of the CO_2. If the rate of production (or consumption if conditions in the vessel become anaerobic) of CO_2 in biological processes should be greater than the rate of equilibration of CO_2 and H_2O, the possibility also exists that the CO_2 will not come into oxygen isotopic equilibrium with the H_2O.

To test the necessity and efficacy of using gamma radiation to destroy any CO_2–producing or CO_2–consuming organisms prior to analysis, we analyzed a series of sterilized and unsterilized pairs of soil samples. Isotopic

analyses of the samples were done between 4 and 8 weeks after irradiation. Results are in Table 2.1.

The $\delta^{18}O$ values of all non-irradiated samples are more negative than those of irradiated samples, in some cases by as much as 2‰. No significant differences were noted in $\delta^{13}C$ values between the two sample sets. We tentatively conclude that these results are the consequence of respiration in the untreated samples after the irradiation of the treated samples but prior to analysis. During the analytical procedure, any respired CO_2 is removed prior to introduction of tank CO_2. The absence of differences in $\delta^{13}C$ values of the irradiated and untreated samples indicates that the amount of respired CO_2 produced during the 24 to 48 hours allowed for equilibration between CO_2 and soil water is small compared to the amount of tank CO_2 added to the equilibration vessel. However, any respired water produced between the time of sampling and the time of analysis of the untreated sample (or time of sampling and time of irradiation of the treated sample) is added to the original soil water. Thus, all soil samples should be refrigerated between the time of collection and time of irradiation, and be irradiated as soon as practical after collection to minimize production of respired water. This recommendation is made regardless of the technique that is to be used to analyze the soil water.

2.3.4. Long term changes in the isotopic composition of CO_2 in equilibrium with soil water.

One of the samples, a wet silt loam, was allowed to equilibrate with CO_2 for over three months. During that interval, the $\delta^{18}O$ value increased by approximately 1‰ from -11.8‰ to -10.7‰ and the $\delta^{13}C$ value increased by approximately 5‰ from -41.0‰ to -35.5‰. Soil organic matter is enriched in ^{13}C relative to tank CO_2 and the oxygen of the organic matter may be enriched in ^{18}O relative to the soil water. This suggests that the long term shifts in the isotopic ratio of the CO_2 were the result of very slow degradation of organic matter in the equilibration vessel even though the soil was sterilized.

2.3.5. Comparison of distillation extraction methods and the CO_2 equilibration method.

In many previous studies of the isotopic composition of soil water, water has been removed from soil samples prior to analysis. The $\delta^{18}O$ of the water is typically measured using the CO_2–water equilibration method of Epstein and Mayeda (1953).

The azeotropic distillation method is described by Revesz and Woods (1990) and Ingraham and Shadel (1992). A soil sample is placed in a flask of toluene and attached to a distillation apparatus. Water and toluene form an azeotropic mixture at 84.1°C but are immiscible at room temperature. The azeotrope is distilled from the soil sample by heating, after which it is

condensed and cooled to room temperature. The water and toluene can then be separated in a separatory funnel.

In the vacuum distillation technique (Ingraham and Shadel, 1992; Araguás-Araguás et al., 1995), a soil sample is frozen in a vessel on a vacuum line and non-condensables are pumped away. The sample is then heated and the water evolved is frozen in a separate vessel. Heating temperatures are variable ranging from 100°C for most samples up to 350°C (Araguás-Araguás et al., 1995).

The results of both the azeotrope and vacuum distillation methods are sensitive to operational details. Walker et al. (1994) conducted an interlaboratory comparison and reported that waters of different amounts, types and isotopic compositions were extracted when the same sample was analyzed in different laboratories. Variations in the details of the technique among the laboratories include the temperature and duration of the distillation process. Walker et al. (1994) concluded that there was a need for standard protocols for both the azeotropic and vacuum distillation methods.

In the direct soil-CO_2 equilibration method, the $\delta^{18}O$ value of liquid water is presumably measured while distillation extractions may remove some of the more strongly held water (Araguás-Araguás et al., 1995; Scrimgeour, 1995) resulting in a composite $\delta^{18}O$ value. To determine the significance of this, samples were sent to Dr. K. Revesz (U.S. Geological Survey) for analysis by azeotrope extraction and to A.H. Jahren (University of California at Berkeley) for analysis by vacuum distillation. All of these

samples were ones that had been dried and re-wetted with waters of known isotopic composition for a series of experiments discussed in more detail in the subsequent section.

Results are shown in Table 2.2. The $\delta^{18}O$ values obtained using azeotropic distillation range from 4.1‰ higher to 2.8‰ lower (n=4) than those obtained with direct CO_2 equilibration. Those obtained using vacuum distillation were between 3.4‰ higher and -0.5‰ lower than values obtained by the direct equilibration method. There is no systematic pattern in the discrepancies between the two methods and the water contents (16 or 32 weight %), or the nature of the samples (clay loam vs. coarse sandy loam). Part of the discrepancy probably reflects the factors responsible for interlaboratory differences in the results of the distillation methods (Walker et al., 1994) such as length of time of distillation, temperature of distillation, and complete recovery of water vapour. Another part of the discrepency probably reflects the fact that the direct equilibration technique measures the $\delta^{18}O$ value of only the liquid water while the distillation methods measure all extractable, more mobile water. A comprehensive comparative study is currently underway.

2.3.6. Results of adding water of known isotopic composition to previously dried soils.

In order to test the CO_2 equilibration method, analyses were made on soil samples that contained waters of known isotopic compositions. A series

of experiments were desinged in which two soils, a clay loam and a coarse sandy loam, were oven dried in air at 110°C for 12 hours and then re-wetted with waters of known amounts and isotopic compositions. Samples were incubated for an interval of between two weeks and two months prior to isotopic analyses. Results are given in Table 2.2 and, for the clay loam, are plotted in Figure 2.4.

The result for addition of 32% water of $\delta^{18}O$ +63.4‰ to the clay loam is clearly aberrant for reasons we do not understand, and is not considered further. With the exception of that result, as the water content of the soil increases, the measured isotopic composition of the soil water approaches that of the water added to the dried sample. In almost every case, however, measured $\delta^{18}O$ value of the soil water only approximated the $\delta^{18}O$ value the water added at the highest water content. In all other cases, forthe additions of ^{18}O-rich waters, measured $\delta^{18}O$ values were always at least 12‰ lower than that of the water added.

The data must reflect, in part, that some water remained in the samples dried at 110°C for 12 hours. However, mass balance calculations for a simple two-component system do not provide a satisfactory solution for the amount and isotopic composition of that water. Comparison of the results for addition of the heavy and light water indicates that the amount of residual water must be small (no more than 3 or 4 weight %) and of low $\delta^{18}O$ value (perhaps between -5‰ and -20‰). Failure to obtain consistent solutions for

material balance calculations indicates that, especially at low water contents, the soil must contain water in more than one compartment, and that isotopic fractionations must exist among the different compartments. Because the fractionations among compartments are not known, it is not possible to write and solve the appropriate material balance equation for the soil water. The reasonable agreement noted in the foregoing discussion of comparisons between the direct equilibration technique and the distillation technique for samples to which 32% ^{18}O-rich water was added supports the contention that soil water is partitioned among compartments and that water extracted by the distillation method is roughly comparable to the liquid water analyzed by the direct equilibration method.

These data may also reflect, in part, subtle differences in how the water was added into the dry soil. When small amounts of water are added to the soil, the adsorption of water onto the mineral surface is so rapid that water might be fractionated kinetically. Such small amounts of water also makes the physical mixing of the samples difficult. Because the soil is still very dry after introducing water, the isotopic exchange among waters of different compartments might be very slow. The poorer agreement among the results for the samples re-wet with small amounts of water may reflect a relatively slow rate of equilibration of water among the different compartments of those soils, especially for the lowest water contents (0.5%).

2.4. Conclusions.

Three main conclusions can be made from this study. The first is that a direct equilibration is a feasible method for measuring the $\delta^{18}O$ value of soil water. The reproducibility of this method is about 0.3‰ to 0.4‰, approximately the same as extraction methods. The single step of analysis and the lack of dangerous chemicals are advantages of this method.

A second conclusion is that biological respiration can cause significant changes in the measured $\delta^{18}O$ value of soil water. For this reason, sterilization of the sample is recommended prior to analyses. Samples should also be stored at low temperatures prior to sterilization to inhibit biological activity.

Finally, the effect of different amounts of water and soil type on the $\delta^{18}O$ value of soil water is an important discovery. The measured $\delta^{18}O$ value changes as water content and soil texture is changed. The most likely explanation for this is that soil water occurs in several forms or compartments such as bulk liquid water and adsorbed water. Each of these forms may have a different isotopic composition and they are likely in isotopic equilibrium with one another. The $\delta^{18}O$ value measured by the equilibration method is operationally defined as the $\delta^{18}O$ value of the bulk liquid water because the CO_2–liquid water fractionation factor is used to relate the two phases. Thus, changes in the measured $\delta^{18}O$ value are due to different proportions of liquid water relative to the amount of total water as water content and soil texture are varied. The liquid water $\delta^{18}O$ value should

be used when mineral–water fractionation factors are used to interpret the conditions under which pedogenic processes occur.

2.5. References.

Araguás-Araguás, L., Rozanski, K., Gonfiantini, R., and Louvat, D., 1995. Isotope effects accompanying vacuum extraction of soil water for stable isotope analyses. Journal of Hydrology, 168: 159-171.

Blake, G.R., and Hartge, K.H., 1986. Bulk density. In: (A. Klute, editor) Methods of soil analysis. Part 1. Physical and mineralogical methods. American Society of Agronomy, pp. 363-382.

Cohn, M., and Urey, H.C., 1938. Oxygen exchange reactions of organic compounds and water. Journal of the American Chemical Society, 60: 679-687.

Craig, H., 1961. Standard for reporting concentrations of deuterium and oxygen 18 in natural water. Science, 133: 1833.

Dunitz, J.D., 1994. The entropic cost of bound water in crystals and biomolecules. Science, 264: 670.

Epstein S., and Mayeda, T., 1953. Variations of ^{18}O content of waters from natural sources. Geochimica et Cosmochimica Acta, 4: 213-224.

Friedman, I., and O'Neil, J.T., 1977. Compilation of stable isotope fractionation factors of geochemical interest. USGS Professional Paper, 440-KK.

Gardner, W.H., 1986. Water content. In: (A. Klute, editor) Methods of soil analysis. Part 1. Physical and mineralogical methods. American Society of Agronomy, pp. 493-544.

Hillel, D., 1980. Fundamentals of Soil Physics. Academic Press. 413 pp.

Horita, J., and Gat, J.R., 1989. Deuterium in the Dead Sea: remeasurement and implications for the isotopic activity correction in brines. Geochimica et Cosmochimica Acta, 53: 131-133.

Ingraham, N., and Shadel, C., 1992. A comparison of the toluene distillation and vacuum/heat methods for extracting soil water for stable isotopic analysis. Journal of Hydrology, 140: 371-387.

Jusserand, C. 1980. Extraction de l'eau intersticielle des sediments et des sols. Comparaison des valeurs de l'oxygene 18 par differentes methodes. Premiers resultats. Catena, 7: 87-96.

Litaor, M.I., 1988. Review of soil solution samplers. Water Resources Research, 24: 727-733.

O'Neil, J.R., and Epstein, S., 1966. A method for oxygen isotope analysis of milligram quantities of water amd some of its applications. Journal of Geophysical Research, 71: 4955-5961.

Revesz, K., and Woods, P.H., 1990. A method to extract soil water for stable isotope analysis. Journal of Hydrology, 115: 397-406.

Scrimgeour, C.M., 1995. Measurement of plant and soil water isotope composition by direct equilibration methods. Journal of Hydrology, 173: 261-274.

Sofer, A. and Gat, J.R., 1972. Activities and concentrations of oxygen-18 in concentrated aqueous salt solutions: analytical and geophysical implications. Earth and Planetary Science Letters, 15: 232-238.

Sofer, A., and Gat J.R., 1975. The isotope composition of evaporating brines: effect of the isotopic activity ratio in saline solutions. Earth and Planetary Science Letters, 26: 179-186.

Sparrow, A.H., Underbink, A.G., and Sparrow, R.C., 1967. Chromosomes and cellular radiosensitivity. I. The relationship of D_o to chromosome volume and complexity in seventy-nine different organisms. Radiation Research, 32: 915-945.

Sposito, G., 1984. The surface chemistry of soils. Oxford University Press. pp. 234.

Taube, H., 1954. Use of oxygen isotope effects in the study of hydration of ions. Journal of Physical Chemistry, 58: 523-538.

Truesdell, A.H., 1974. Oxygen isotope activities and concentrations in aqueous salt solutions at elevated temperatures: consequences for isotope geochemistry. Earth and Planetary Science Letters, 23: 387-396.

Walker, G.R., Woods, P.H., and Allison, G.B., 1994. Interlaboratory comparison of methods to determine the stable isotope composition of soil water. Chemical Geology, 111: 297-306.

Table 2.1. Effect of different soil types and radiation treatment on the measured $\delta^{18}O$ and $\delta^{13}C$ values by the direct CO_2–equilibration method.

	8% water content		8% water content		4% water content
	not irradiated		irradiated		
Sample	$\delta^{13}C$	$\delta^{18}O$	$\delta^{13}C$	$\delta^{18}O$	$\delta^{18}O$
Clay Loam	-40.6	-12.4	-41.0	-11.8	-10.6
Coarse Sandy Loam 1	-40.6	-11.2	-40.6	-9.2	-9.2
Coarse Sandy Loam 2	-40.7	-10.3	-40.7	-9.2	-8.8
Coarse Sandy Loam 3	-40.6	-11.3	-40.7	-9.4	-8.9

Table 2.2. Results of drying/rewetting experiments (including comparisons of analyses done using different techniques).

	$\delta^{18}O$ of water added	64.4	64.4	63.4	65.4	65.4	-10.5	-10.5	-11.3	-9.8	-9.8
	Months between wetting and analysis	2	2	0.5	2	2	2	2	0.5	2	2
Sample	Water content (%)	Measured isotopic composition of soil water									
		$\delta^{18}O^{*}$	$\delta^{18}O^{\Psi}$	$\delta^{18}O^{*}$	$\delta^{18}O^{*}$	$\delta^{18}O^{\#}$	$\delta^{18}O^{*}$	$\delta^{18}O^{\Psi}$	$\delta^{18}O^{*}$	$\delta^{18}O^{*}$	$\delta^{18}O^{\#}$
Clay Loam	.5	-9.5		50.1	22.4		-21.6		1.0	4.2	
	1	0.5		41.6	28.4		-18.0		-7.4	-7.8	
	2	15.4		46.4	59.2		-15.7		-10.1	-3.5	
	4	23.3		51.9	53.8		-10.6		-9.8	-6.4	
	8			55.5	46.4		-11.8		-9.3	-5.2	
	16	50.4		60.1	54.6		-10.5		-9.9	-7.1	
	32	54.1	50.0	39.8	52.1	52.6	-13.4	-7.3	-13.6	-7.5	-10.9
Coarse Sandy Loam	.5	-8.3					-20.4				
	1	2.5					-17.9				
	2	15.2					-15.1				
	4	29.8					-8.8				
	8	41.6					-9.2				
	16	49.2	52.0				-10.2	-7.4			

Notes: * measured by CO_2 equilibration

$^{\Psi}$ measured using the azeotropic distillation method by Dr. K. Revesz, U.S. Geological Survey

$^{\#}$ measured using the vacuum distillation method (average of 3 analyses) by A.H. Jahren, University of California, Berkeley

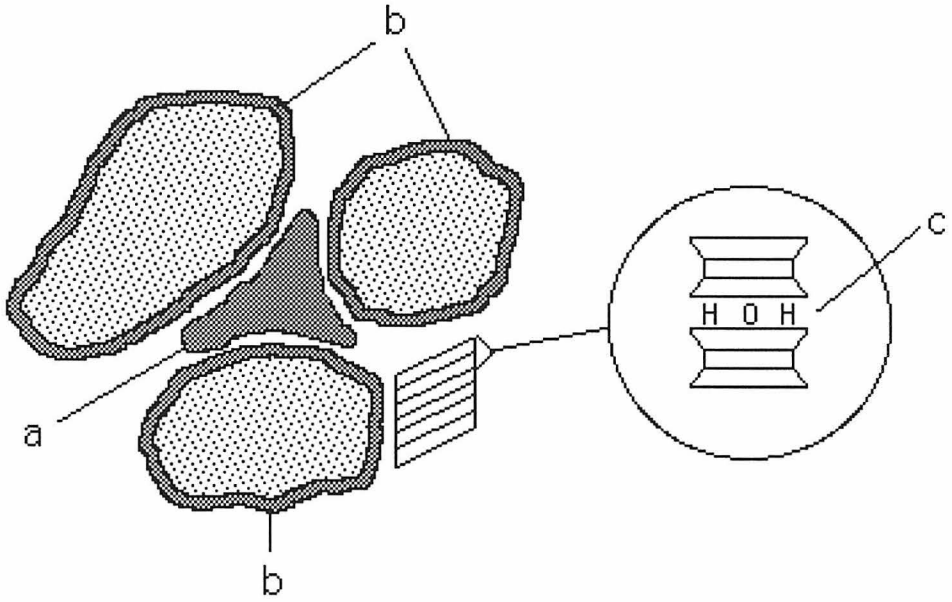

Figure 2.1. Different forms of water found in soils.
a) bulk liquid phase (liquid water);
b) adsorbed water;
c) structural water bound in minerals (e.g., interlayer water in clays)

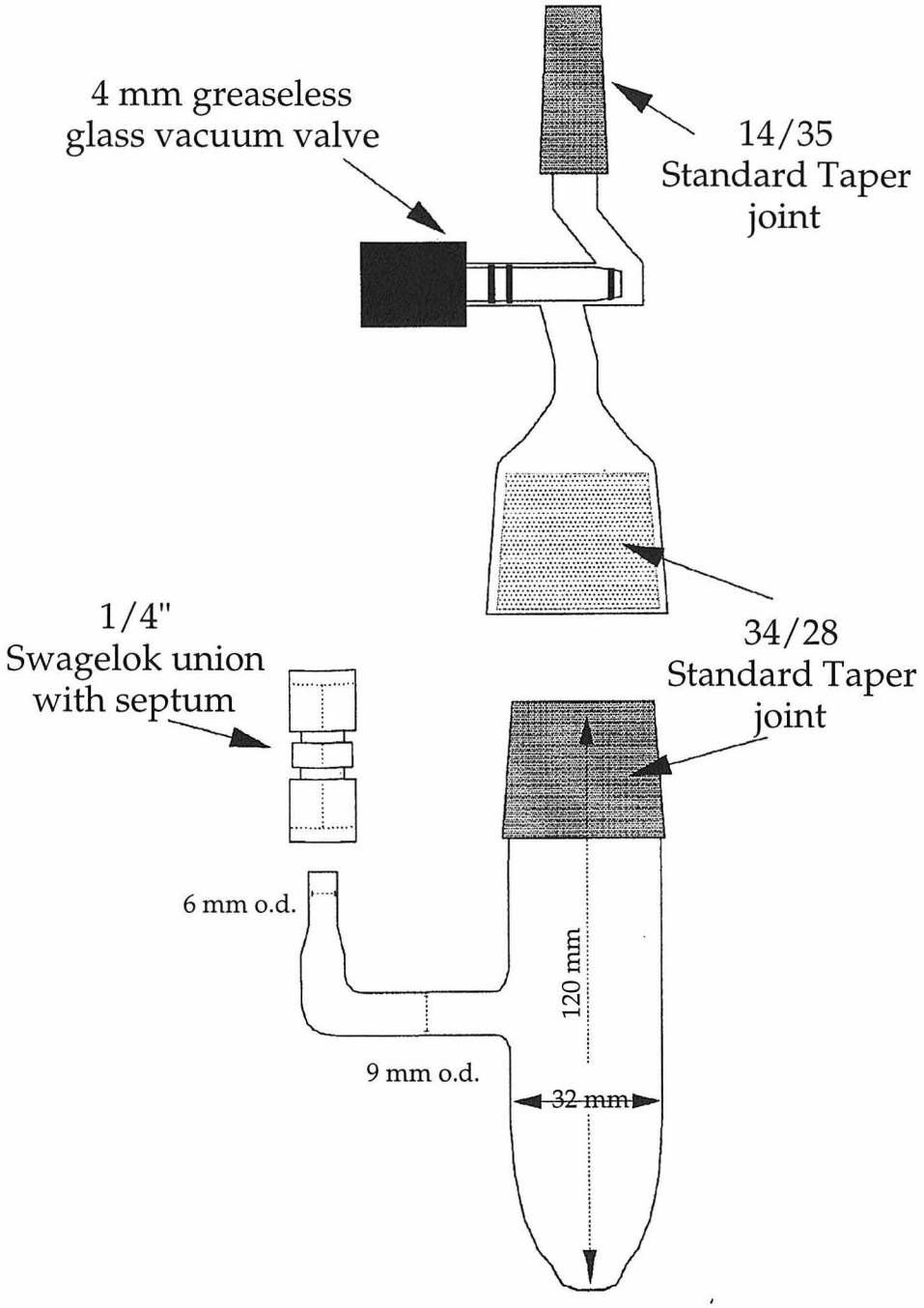

Figure 2.2. Direct CO_2–equilibration reaction vessel. A 1/4 inch brass union swagelok is fitted with a brass back ferrule, a Teflon front ferrule, and a 10 mm rubber septum (typically used for gas chromotography) on the end for gas aliquot extraction.

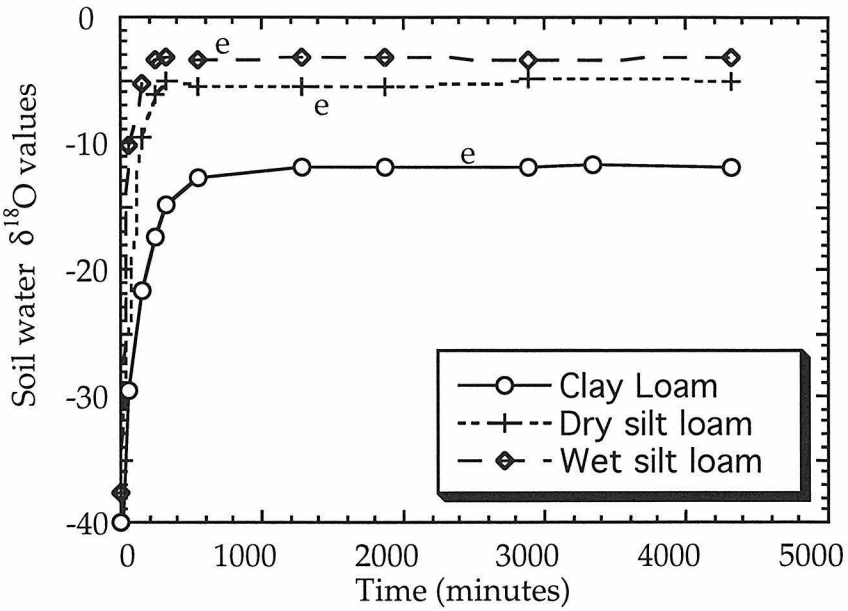

Figure 2.3. Equilibration rate comparison of a wet silt loam (88%), a drier silt loam (23% water), and clay loam (8% water). The x-axis represents the time of reaction and the y-axis represents the $\delta^{18}O$ value of the soil water. "e" represents the time at which equilibration is reached for each of the soil types.

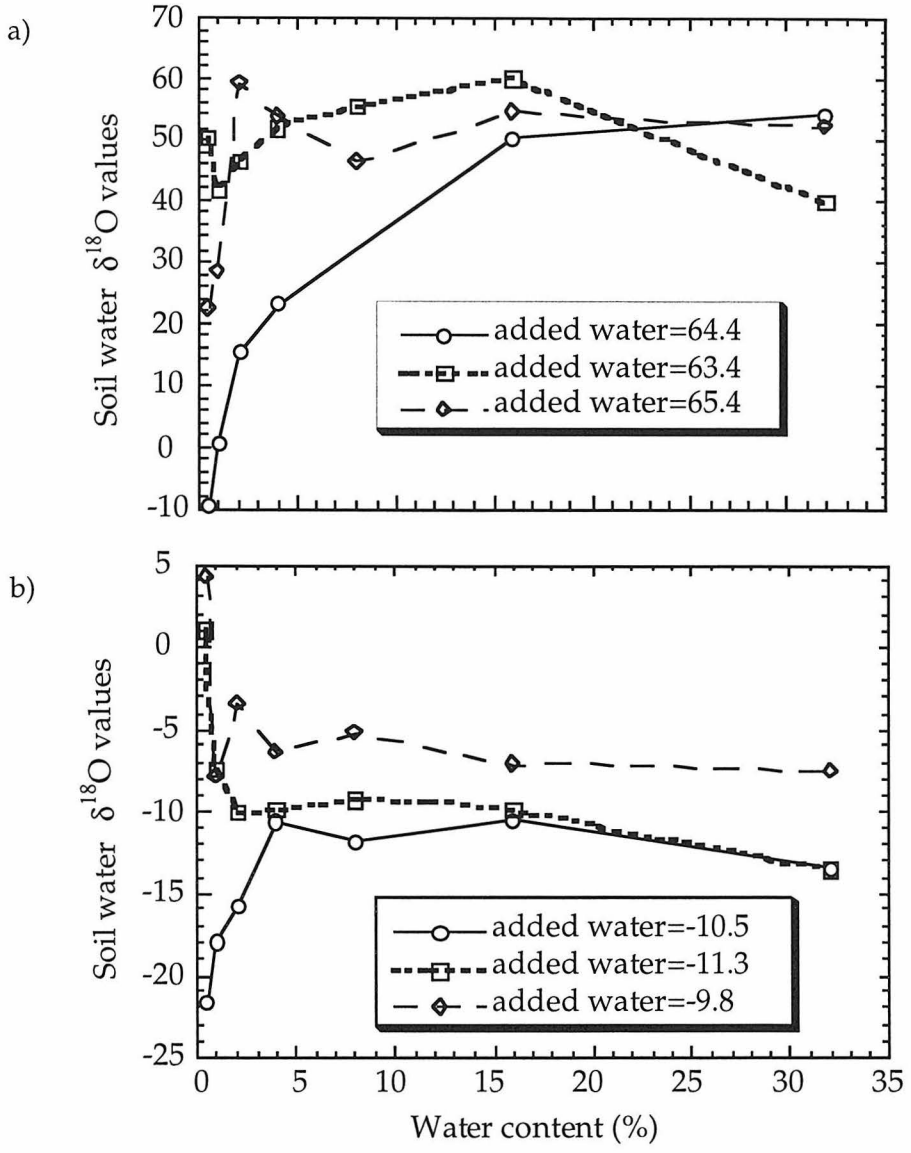

Figure 2.4. Comparison of $\delta^{18}O$ values measured using the CO_2 equilibration method in a series of drying and rewetting experiments. a) samples with a more ^{18}O-enriched added water composition; b) samples with a more ^{18}O-depleted added water composition.

Chapter 3. Monitoring the $\delta^{18}O$ Values of Soil Water.

This chapter documents the variations in the $\delta^{18}O$ values of soil water and incoming rainwater along an arid-to-humid transect on the leeward side of Kohala, Hawaii through two seasonal cycles. The investigation was the first application of the direct equilibration method for measuring $\delta^{18}O$ values of soil water (Chapter 2) and the first to document trends in non-arid climatic regimes. The results from this monitoring study were used for comparison with the results of the pedogenic mineral study that is presented in the following chapters.

3.1. Introduction.

Monitoring hydrologic fluxes among ecosystem components provides information on inputs, storage, and loss of water. The degree to which water loss in ecosystems is controlled by evaporation versus transpiration is important in understanding feedbacks between terrestrial ecosystems and the atmosphere. Geochemical characterization of soil water can provide insights into the dominant water loss processes. Water uptake from soil by plants does not result in isotopic fractionation (Zimmerman et al., 1967; Allison et al., 1985; White et al., 1985) until water evaporates from stomata in leaves (Allison et al., 1985; White et al., 1985; Bariac et al., 1991; Dawson and Ehleringer, 1993). Thus, during transpiration, only the soil-water content changes and the soil-water isotopic composition remains the same. In

contrast, evaporation of soil water changes both the soil-water content and soil-water isotopic composition.

A theoretical model describing the effect of soil-water evaporation on its oxygen and hydrogen isotopic composition was originally developed by Zimmerman and others (1967). This model was expanded, modified, and field tested on sand columns and non-vegetated arid and semi-arid soils by many authors (Heller, 1968; Allison, 1982; Allison and Hughes, 1983; Allison and Barnes, 1983; Barnes and Allison, 1983, 1984, 1988; Allison et al., 1983; Dincer and Davis, 1984; Walker et al., 1988). These studies validate the model when there is no antecedent soil moisture and evaporation is the dominant process controlling soil-water isotopic composition. However, use of sand and non-vegetated soils neglects transpiration. Plants are very efficient at extracting water from large volumes of arid soil and the importance of evaporation in water loss is not clear.

The soil-water evaporation models have not been tested in humid environments supporting nearly continuous plant cover that rapidly utilizes rainwater and that probably also minimizes loss of water by evaporation. The few published humid-environment soil-water isotopic studies were conducted for other reasons such as tracing groundwater recharge pathways (e.g., Darling and Bath, 1988). In this context, model testing is important because if there is significant near surface evaporative enrichment of ^{18}O, ground water reservoir and local precipitation isotopic values will differ.

In theory, we should be able to determine the fraction of water lost through evaporation and transpiration by monitoring both total water loss and isotopic composition of soil water. In practice, however, soil-water dynamics are so complicated that application of evaporation models has not gone beyond the simple case in which an initially dry soil is wetted and evaporation is allowed to proceed unhindered by further rewetting. In this study, we take an empirical approach. Water content and soil-water $\delta^{18}O$ values were monitored along an arid-to-humid bioclimatic transect in Hawaii through two annual cycles. We interpret seasonal $\delta^{18}O$ variations within soil profiles and among soil profiles in terms of antecedent moisture content, rainwater input, and evapotranspiration.

3.2. Geological setting and climate.

The soils monitored in this study are found on the leeward side of Kohala Peninsula on the Island of Hawaii (Figure 3.1). Kohala, located on the northern tip, is the oldest of the five volcanoes that make up the Island of Hawaii. The soil profiles sampled for this study are developed on Hawi lava flows that have a modal K/Ar age of 170 000 years old (Moreschalchi, Mertzman, and Elliot, unpublished data).

Kohala has a large variation in rainfall (Figure 3.1), decreasing from the mountain top down the leeward side into the mountain rain shadow; median annual rainfall and temperature values range from 300 cm and 17°C at the highest site, L (1254 m) to 16 cm, and 23°C at the lowest site, A (77 m).

There are three State of Hawaii rainfall monitoring stations near the crest and along the leeward side of Kohala: Middle Pen at 420 m, Headquarters at 992 m and Waterhead at 1200 m. A long-term average of monthly rainfall is compared with the rainfall values for the first annual cycle in Figure 3.2. In general, there is a rainy season that starts in December and lasts until late March. At lower elevations on the leeward side, rainfall and its distribution reflect input from large cyclonic storms, called Kona storms, during the winter but no significant rain from Tradewind sources. In some years, there may be only one or two Kona storms, and year to year variability is great. At higher elevations, there is gentle rain throughout the year resulting from the orographic rise of the easterly Tradewinds, and additional rain during the winter months due to the influx of Kona storms. Annual variability in the amount of rain is less than at lower elevations. Usually, the high elevation windward Waterhead station receives 224 cm/year compared with the high elevation leeward Headquarters station which receives 129 cm/year. During our sampling period, the Tradewinds were more variable than usual resulting in less continous cloud cover and approximately the same amount of rain at both stations.

The variability of the Tradewinds raises the concern that the first annual cycle (Dec., 1993 to Nov., 1994), in which more detailed sampling occurred, is not representative of the average climate on Kohala. However, a simple analysis of rainfall and wetting depths shows that it is a representative year. Table 3.1 includes mean monthly rainfall for the past 66 years

(calculated by taking the sum of rain and dividing by the number of years), the median monthly rainfall values, the monthly rainfall values for the first annual cycle, and the maximum rainfall values at two stations; station Middle Pen is close to Site B and station Headquarters is near Site J. The last column represents the number of years since 1930 in which rainfall in the indicated month was equal to or less than that measured in the first annual cycle.

Monthly precipitation amounts for the first annual cycle are similar to or greater than the median and mean values. The maximum montly rainfall amounts are even greater, up to 10 times greater than those measured during the first annual cycle of this study. Several years of lower than the mean rainfall must balance the extremely wet years to obtain the mean values. Thus, the climate on the leeward side of Kohala is predominantly dry, with occasional wet years. Over 1/3 of the years since 1930 at Site B had the same or less rain than the first annual cycle and even more for Site J, consistent with a dominantly dry climate.

This relatively simple analysis of rainfall shows that the weather patterns during the study period are within the range of variation seen since 1930. Thus, we assume that the weather patterns on Kohala for the study period are representative of climate since 1930 and that the conclusions of the soil-water $\delta^{18}O$ monitoring study are valid for this period.

This study focuses on soil sampling sites B, E, J and M (Figure 3.1). Selected soil properties are shown in Table 3.2. These soils are classified using

Soil Taxonomy (Soil Survey Staff, 1990) as: at Site B, a clayey-skeletal, halloysitic, hyperthermic Typic Anthrocambid; at Site E, a medial thermic Typic Anthrocambid; at Site J, a medial isothermic Humic Haplustand; and at Site M, a medial over hydrous isothermic Typic Hydrudand. At the low rainfall sites, the mineral part of the soil is predominantly halloysite with lesser amounts of allophane, imogolite, hematite, and gibbsite, and a thin layer of high Mg-calcite at Site B. At the high rainfall sites, the mineral part of the soil is predominantly allophane, imogolite, ferrihydrite with smaller amounts of halloysite and gibbsite. The amount of organic matter increases with increasing rainfall and the amount of coarse material (> 2mm) decreases with increasing rainfall. The available water capacity also increases with increasing rainfall. These soil properties reflect the influence of annual rainfall values over the history of soil formation while the soil-water parameters measured in this study were dominantly influenced by the short-term weather patterns.

3.3. Experimental design and methods.

Because the study sites are located a series of lava flows all approximately the same age, we assume that geological parent material and duration of the soil forming process are the same for all sites. The slope was held constant at approximately 0° by the selection of level areas on local high points in the landscape for all sampling sites. In this way, we have designed a

study to examine the effects of climate and vegetation on the soil-water oxygen isotopic composition.

At each site, a sampling region approximately 100 m^2 was defined. During each sampling, a small pit was dug and layers were channel sampled continuously along at least two, but often three, different walls of the pit. Because modelled depth profiles for the isotopic composition of soil water showed greater differences in the surface horizons (Zimmerman et al., 1967), a smaller sampling interval was chosen for the upper parts of the soil. At Sites B and E, samples were taken at 5 cm intervals for the first 20 cm, 10 cm intervals from 20 to 40 cm, and 15 cm intervals from 40 to the lava-soil interface. This interface was reached at 70 cm for Site B and at 85 cm for Site E.

Initially, a similar sampling strategy was employed for Sites J and M. Although these soils are much thicker, sampling was initially confined to the upper 90 cm. Samples were taken at 5 cm intervals for the first 20 cm, 10 cm intervals from 20 to 50 cm, and 20 cm intervals from 50 to 90 cm. However, when the isotopic results for the first 3 samplings were obtained, it was apparent that it would be useful to sample more deeply. The remaining samplings were deeper, up to 100 cm for Site J and 130 cm for Site M. During some of the drier months (August, 1994 and September, 1995), we only sampled up to 90 cm at Site M because digging became very difficult.

Sampling started in December, 1993, and continued at approximately six week intervals until November, 1994, and then at 3 month intervals until

September, 1995. A new pit was dug for every sampling. During this period, rainwater at these sites was also collected for isotopic analysis at approximately two week intervals during the rainy season (December to March) and after storms during the drier season (April to November). Rainwater was collected in 1L Nalgene bottles fitted with 150 mm diameter plastic funnels. Mineral oil was poured into the bottle to minimize the effects of evaporation during sample collection. The rainwater samples were then processed by filtration to remove oil and residues.

Rainwater samples were degassed under vacuum and equilibrated with tank CO_2 for the measurement of $\delta^{18}O$ values following the method of Cohn and Urey (1938) and Epstein and Mayeda (1953). The isotopic composition of soil water was determined using a modification of the Scrimgeour (1996) direct equilibration method (Chapter 2). This method elimates the necessity of removing water from the soil.

In the field, soil samples are collected and sealed to prevent evaporation. They are refrigerated to inhibit microbial activity. In the lab, the samples are sterilized using gamma radiation and directly equilibrated with CO_2 after degassing. The $\delta^{18}O$ value of soil water is calculated from the $\delta^{18}O$ value of equilibrated CO_2 using mass balance equations as described in Chapted 2. The analytical error of this method is ±0.3‰. Gravimetric water content of soil samples was determined for each sample by measuring the loss of water after heating for 12 hours at 110°C (Gardner, 1986). The analytical error is ±10% of the gravimetric water content value. All results are reported

as the volume percent occupied by water, which is the product of gravimetric water content, bulk density, and density of water. All $\delta^{18}O$ values are reported in per mil (‰) relative to Standard Mean Ocean Water (SMOW) (Craig, 1961).

Along the transect, potential evapotranspiration (PET) was measured using E-TGage™-Model A evaporimeters. Evaporimeters were set up adjacent to soil-water sampling sites and interspersed between these sites for complete coverage of the transect. The values from these gauges are equivalent to 70% of pan evaporation values (W. Parton, pers. commun., 1994). PET values are presented in mm of water loss day^{-1}. Data collection began in September, 1994, and ended in March, 1996; the data presented in this chapter are from September, 1994, to August, 1995.

All data are interpreted using the following assumptions. First, lateral variation of soil properties within our ~100 m^2 sampling sites is minimal. Visual inspection of the soil in each pit supported this assumption allowing the comparison of results from pit to pit, i.e., from sampling to sampling. Second, movement of water laterally is also minimal. The sites were chosen on level to nearly level landscape positions on local high points in order to minimize downslope movement of water. On a larger scale, there is lateral movement of water down the slope, but within the top meter of soil, visual inspection of the soil profiles after storms indicated that water moved primarily downwards due to gravity. Third, we assume that the $\delta^{18}O$ value of the collected rainfall is the same value as the water entering the soil column. The effect of cloud condensation onto grass leaves is neglected. The resulting

droplets could be enriched in ^{18}O by evaporation prior to dropping onto the soil surface. Fourth, liquid water and water vapor is distributed through the bulk soil. The soil structure at all sites is composed of weak to very weak, very fine to medium subangular blocks that do not support large pores. Thus, water does not flow preferentially in macropores. Instead, the distribution of water reflects uniform wetting processes. The uniform wetting depth viewed on all pit walls at Sites B and E after a large rainstorm (Feb. 15-17, 1994) supports this assumption.

3.4. Results.

3.4.1. Soil-water profiles.

The soil-water oxygen isotopic results at Site B are plotted on the upper row of Figure 3.3 and the volumetric water content is plotted below. The most significant change occurs from February 13, 1994, to February. 18, 1994, due to a large storm on February 15-17, 1994. Prior to the storm, volumetric water content increased from 10% at the surface of the profile to 20% at the bottom of the profile. The $\delta^{18}O$ value decreased from +2‰ at the surface to about -1‰ at the bottom of the profile. In both cases, values below about 40 cm depth did not vary much. After the storm, volumetric water content decreased from 25% at the surface to about 20% at 35 to 70 cm while the $\delta^{18}O$ values increased from -4‰ at the surface to -1‰ at 35 to 70 cm depth. Subsequent profiles had the same shape as the profiles prior to the storm.

The results for Site E (Figure 3.4) showed the same pattern, but with different volumetric water content and soil-water $\delta^{18}O$ values than Site B.

At Site J (Figure 3.5), the volumetric water content values decreased from between 50 and 95% (wetter in the rainy season) at the surface to a constant value of about 30% in the interval 30 cm to the bottom of the profile for all sampling periods except February where the value from 30 cm and below was 50%. The $\delta^{18}O$ values varied similarly to Site B and E except that it required a longer time to return to the pre-storm profile.

The volumetric water content profiles at Site M (Figure 3.6) showed the same pattern as seen at Sites B and E with three stormy periods: one in February, 1994, one in September, 1994, and a weaker one in March, 1995. Thus, the shape of the profile changed three times. The $\delta^{18}O$ value profiles at Site M (Figure 3.6) followed a pattern similar to the Site J profiles.

Depth-weighted average values for selected depth zones were calculated and plotted in a time series (Figure 3.7a-d). The upper graph in each pair shows the rain and soil-water oxygen isotope data and the lower graph shows the volumteric water content data. The start date for the time series is December 1, 1993.

The volumetric water content for the surficial zone (0-20 cm) at Site B peaked at around day 70 (Fig. 7a). The lower zones did not show such a pronounced spike, but instead were fairly constant. The trend of the soil-water $\delta^{18}O$ values for the surficial zone correlated with the rainfall $\delta^{18}O$

values. The lower zones did not show much variation except for a slight rise near the end of the sampling period.

The data for Site E (Fig. 7b) showed similar trends except that there was more scatter in volumetric water content for the lower zones and less difference between rainfall and soil-water $\delta^{18}O$ values.

The volumetric water content for Site J also reached a peak at day 70 (Figure 3.7c) and then the values remained constant with slight fluctuations. The soil-water $\delta^{18}O$ values for Site J reached a minimum around day 120 in the upper two zones. The lower zones exhibited little change in soil-water $\delta^{18}O$ values.

At Site M (Figure 3.7d), the volumetric water content slowly decreased and reached a constant value around day 120. However, at day 300, there was a sharp rise before falling once again. There was a slight minimum at day 70. Otherwise, the isotopic data varied little with time. At both Sites J and M (Figure 3.7c,d), the soil-water $\delta^{18}O$ values did not correlate with the rainfall $\delta^{18}O$ values. Instead the rainfall $\delta^{18}O$ values increased with time and leveled off at about -4‰. The difference between rainfall and soil-water $\delta^{18}O$ values has decreased from about 5‰ at Site B, to about 2‰ at these sites.

3.4.2. Macroenvironmental parameters.

Rainfall $\delta^{18}O$ values from each sample collector are plotted as a function of median annual rainfall (Figure 3.8a,b) for individual cyclonic Kona storms and a series of Tradewind storms. For both storm types, the $\delta^{18}O$

values decreased with increasing rainfall. However, the difference between the $\delta^{18}O$ values of the sites with lowest and highest median annual rainfall was larger for Tradewind storms than for Kona storms; rainfall $\delta^{18}O$ values ranged from -6 to -10‰ for Kona storms and from -3 to -12‰ for Tradewind storms.

Potential evapotranspiration values are plotted against the median annual rainfall (Figure 3.9a). PET decreases with increasing rainfall. Time-weighted average $\delta^{18}O$ values for 0-20 cm, 20-40 cm and 40+cm zones are plotted as a function of the PET and median annual rainfall values (Figure 3.9b,c). The average soil-water $\delta^{18}O$ values decrease as PET decreases and median annual rainfall increases. However, this change is more evident in the 0-20 cm zone than for the other zones. For the lower two zones (20-40 cm and 40+ cm), Sites E, J and M have approximately the same $\delta^{18}O$ values; only Site J and M are similar at depths from 0 to 20 cm.

3.5. Discussion of experimental results.

3.5.1 Soil-water profiles.

The soil-water measurements integrate the effects of evapo-transpiration, recharge by rain and mixing with existing water. At Sites B and E, the majority of the year is dry (Figure 3.2a) and evapotranspiration occurs continuously. Significant soil wetting is derived only from cyclonic Kona storms in the winter months bringing more ^{18}O depleted water. The higher volumetric water contents and lower $\delta^{18}O$ values are due to the mixture of

infiltrating rainfall with the water already present. The profiles for December, 1993, and February 13, 1994, reflect the end of a long period of evapotranspiration. The next two samplings show the influx of cyclonic storms. The beginning of the next cycle of evapotranspiration is reflected in the May, 1994, profiles. As the dry season progresses, there is continued evaporation but little transpiration from the dormant vegetation. The $\delta^{18}O$ values of the successive months continue to become more positive while volumetric water content change is insignificant.

At Sites J and M, the same pattern occurs but not on the same time scale. The rainfall pattern is different from Sites B and E (Figure 3.2a-c). They receive gentle rain throughout the year with an increase in duration and intensity of precipitation during late winter and early spring. Evapotranspiration occurs at all times, but the signal is complicated by the continual mixing and removal of water. Isotopic profiles show a change in shape from the drier to wetter seasons, but the differences are smaller. The profiles from December, 1993, reflects the end of the drier season while February and March, 1994, profiles reflect the pulse of increase rainfall. From May to August, the influence of incoming rain is overwhelmed by evapotranspiration which causes the $\delta^{18}O$ values to become more positive. For Site J, this process continues until November, while for Site M, there is an increase in rain during September initiating another cycle of recharge and drying.

The volumetric water content depth profiles are more difficult to interpret. Evapotranspiration is reflected in these profiles as a decrease in water content and recharge is reflected as an increase in water content. The overall increase from December to February and subsequent decrease from February to November is the result of these two processes. However, the shape of the profile only changes slightly for Site M. The volumetric water content decreases with depth for all months except the driest months at Site M. At Site J, there is no evidence for a drier surface horizon. Slow mixing of Tradewind mists into the soil along with the increased water holding capacity from large amounts of organic matter and non-crystalline material (see Table 3.2) most likely allows preservation of the shape of the profile. The soils at Site B and E do not have the water holding capability nor the constant mixing to preserve the shape of their volumetric water content profiles.

The evapotranspiration, recharge, and mixing effects are preserved in the integrated data. During the rainy season, volumetric water contents rise rapidly but, during the dry season, they fall less rapidly. The rapid rise is due to recharge by rain during a short period of time, while the fall is due to the slow uptake of water by plants and evaporation through the surface. The rate of rising and falling is controlled by mixing and macroclimatic events. The integrated volumetric water content and soil-water $\delta^{18}O$ values from deeper in the soil profiles show less change than those near the surface.

3.5.2. Macroenvironmental parameters.

The $\delta^{18}O$ values of rainwater are also plotted with the integrated data (Figure 3.7) and the isotopic values of representative storms are plotted in Figure 3.8. Rain in the wet season is more depleted in ^{18}O than during the rest of the year. The $\delta^{18}O$ value decreases as the intensity of the storm increases (Dansgaard, 1964). Large Kona rainstorms have a high downpour rate. Tradewind storms have less intensity and usually more positive $\delta^{18}O$ values than Kona storms especially at lower elevations on the leeward side (Figure 3.8). Because raindrops follow a long trajectory as they are blown over the top of Kohala by the Tradewinds, some evaporation occurs before hitting the ground. Thus, the remaining water in the raindrop is enriched in ^{18}O.

In nearly all cases, the rainfall $\delta^{18}O$ values are more negative than the soil-water $\delta^{18}O$ values. Evaporation and mixing with ^{18}O enriched residual soil water are responsible for the observed isotopic shift. Exceptions to this pattern occur after an extremely high rainfall period in the March sampling for Site J and in one of the pit-wall profiles in the March sampling for Site M. The soil water at the surface was derived from rain only; the antecedent water was flushed further down the profile. The same process created the profile at Site M.

An increase in temperature causes PET to increase while a decrease of relative humidity causes PET to increase. As the median annual rainfall increases, the temperature decreases and relative humidity increases. Thus,

there is an inverse correlation of PET with median annual rainfall as shown in Figure 3.9a.

Soil-water $\delta^{18}O$ values increase due to the loss of water by evaporation and by mixing with existing soil water that has already been enriched by evaporation. Soil-water $\delta^{18}O$ values decrease when rainfall with more negative $\delta^{18}O$ values infiltrates into the soil. The balance of these two processes determines the $\delta^{18}O$ values along the bioclimatic transect. Because there is a large gradient with elevation on the mountain in incoming rainfall and PET, there should be a reasonable gradient in soil-water $\delta^{18}O$ values. This is true for the values in the 0-20 cm zone, but not in the deeper zones (Figure 3.9 b,c). The balance of water addition, loss, and mixing results in similar $\delta^{18}O$ values of soil water in the deeper parts of Sites E, J, and M. Site B, however, has such a strong PET and little moisture recharge that values in the lower zone are different. The unique presence of pedogenic carbonate at that rainfall zone also testifies to its unusual combination of climatic parameters.

3.6. Conclusions.

Three main conclusions can be made from this monitoring study. The first conclusion is that depth profiles of volumetric water content and soil-water $\delta^{18}O$ values reflect infiltration and evaporation of water. During periods of rain, the volumetric water content decreases in value towards the bottom of the profile. The soil-water $\delta^{18}O$ values increase towards the bottom of the profile because the incoming rain $\delta^{18}O$ values are always more negative

than the soil water values. During dry periods, water is lost from the surface layers preferentially, resulting in volumetric water content profiles increase and $\delta^{18}O$ profiles that decrease towards the bottom of the soil profile.

The relative influence of short intense Kona storms and frequent gentle Tradewind storms at each site determines the mixing time scale which in turn controls the time scale of changes within the soil water depth profiles. The wetting and drying cycle is completed quickly at low elevations because there is a relatively short wet season followed by a significant drying period. The cycle is longer at higher elevations because there is a more continuous rainfall pattern. In all cases, however, it is only in the top 35 to 40 cm that the differences between seasons are evident. Below this level, volumetric water content and soil-water $\delta^{18}O$ values are relatively constant.

The second conclusion is that trends along the transect in measured isotopic values reflect the influence of macroenvironmental parameters. Measurements of PET show an inverse correlation with median annual rainfall and time-weighted average soil-water $\delta^{18}O$ values for surficial horizons (0-20 cm) show a correlation with these two climatic parameters. The soil-water $\delta^{18}O$ value becomes more negative as PET decreases and median annual rainfall increases. The $\delta^{18}O$ values of precipitation also decreases with increasing median annual rainfall.

Finally, there is a significant difference between incoming rainfall $\delta^{18}O$ values and soil-water $\delta^{18}O$ values. For all soils, the $\delta^{18}O$ values of rainwater are more negative than the $\delta^{18}O$ values of soil water. The difference at the

low rainfall sites is about 5‰, while at the high rainfall sites, it is about 2 ‰ to 3‰. Previous to this study, the $\delta^{18}O$ values of soil water were assumed to be the same as the $\delta^{18}O$ value of rainwater.

3.7. References.

Allison, G.B., 1982. The relationship between ^{18}O and deuterium in water in sand columns undergoing evaporation. Journal of Hydrology, 55: 163-169.

Allison, G.B., and Barnes, C.J., 1983. Estimation of evaporation from non-vegetated surfaces using natural deuterium. Nature, 301: 143-145.

Allison, G.B., Barnes, C.J., and Hughes, M.W., 1983. The distribution of deuterium and ^{18}O in dry soils, 2. Experimental. Journal of Hydrology, 64: 377-397.

Allison, G.B., Gat, J.R., and Leaney, F.W.J., 1985. The relationship between deuterium and oxygen-18 delta values in leaf water. Chemical Geology, 58: 145-156.

Allison, G.B., and Hughes, M.W., 1983. The use of natural tracers as indicators of soil-water movement in a temperate semi-arid region. Journal of Hydrology, 60: 157-173.

Bariac, T., Deleens, E., Gerbaurd, A., Andre, M., and Mariotti, A., 1991. La composition isotopique (^{18}O, ^{2}H) de la vapeur d'eau transpiré: étude en conditions asserviés. Geochimica et Cosmochimica Acta, 55: 3391-3402.

Barnes, C.J., and Allison, G.B., 1983. The distribution of deuterium and ^{18}O in dry soils. 1. Theory. Journal of Hydrology, 60: 141-156.

Barnes, C.J., and Allison, G.B., 1984. The distribution of deuterium and ^{18}O in dry soils. 3. Theory for non-isothermal water movement. Journal of Hydrology, 74: 119-135.

Barnes, C.J., and Allison, G.B., 1988. Tracing of water movement in the unsaturated zone using stable isotopes of hydrogen and oxygen. Journal of Hydrology, 100: 143-176.

Cohn, M., and Urey, H.C., 1938. Oxygen exchange reactions of organic compounds and water. Journal of the American Chemical Society, 60: 679-687.

Craig, H., 1961. Standard for reporting concentrations of deuterium and oxygen 18 in natural water. Science, 133: 1833.

Dansgaard, W., 1964. Stable isotopes in precipitation. Tellus, 16: 436-468.

Darling, W.G., and Bath, A.H., 1988. A stable isotope study of recharge processes in the English Chalk. Journal of Hydrology, 101: 31-46.

Dawson, T.E., and Ehleringer, J.R., 1993. Isotopic enrichment of water in the "woody" tissues of plants: implications for plant water source, water uptake, and other studies which use the stable isotopic composition of cellulose. Geochimica et Cosmochimica Acta, 57: 3487-3492.

Dincer, T., and Davis, G.H., 1984. Application of environmental isotope tracers to modeling in hydrology. Journal of Hydrology, 68: 95-113.

Epstein, S., and Mayeda, T., 1953. Variations of ^{18}O content of waters from natural sources. Geochimica et Cosmochimica Acta, 4: 213-224.

Gardner, W.H., 1986. Water content. In: A. Klute (editor), Methods of soil analysis. Part 1. Physical and mineralogical methods. American Society of Agronomy, pp. 493-544.

Heller, J.P., 1968. The drying through the top surface of a vertical porous column. Soil Science Society of America Proceedings, 32: 778-786.

Scrimgeour, C.M., 1995. Measurement of plant and soil water isotope composition by direct equilibration methods. Journal of Hydrology, 173: 261-274.

Soil Survey Staff, 1990. Keys to soil taxonomy, 4th edition. Soil Survey Staff Technical Monograph, 19. Blacksburg, VA.

Walker, G.R., Hughes, M.W., Allison, G.B., and Barnes, C.J., 1988. The movement of isotopes of water during evaporation from a bare surface. Journal of Hydrology, 987: 181-197.

White, J.W.C., Cook, W.R., Lawrence, J.R., and Broecker, W.S., 1985. The D/H ratios of sap in trees: implications for water sources and tree ring D/H ratios. Geochimica et Cosmochimica Acta, 49: 237-246.

Zimmerman, U., Ehhalt, D., And Münnich., K.O., 1967. Soil-water movement and evapotranspiration: changes in the isotopic composition of the water. Proc. I.A.E.A. Symposium on Isotopes in Hydrology, p. 567-585.

Table 3.1. State of Hawaii Monthly Rainfall Data.

	Rainfall (cm)				# of years*
Month	Mean	Median	1st cycle	Max	< 1st cycle
Site B					
Jan	5.2	2.9	1.0	34.3	19
Feb	3.1	1.7	6.4	16.6	51
March	3.1	2.2	2.4	14.2	39
April	2.1	1.0	0.0	21.8	15
May	2.8	2.1	2.0	12.7	33
June	1.8	0.5	2.0	10.0	45
July	1.4	0.7	0.0	8.7	20
Aug	1.6	1.0	1.8	8.7	45
Sept	2.5	1.3	3.9	22.9	55
Oct	2.2	0.8	0.8	12.9	31
Nov	2.3	1.2	0.0	14.2	18
Dec	3.5	2.2	0.0	26.8	10
Site J					
Jan	18.2	15.4	10.0	65.5	20
Feb	13.3	11.8	15.6	46.9	33
March	15.8	13.3	30.0	72.7	63
April	14.3	11.2	17.5	66.0	48
May	7.7	6.9	4.3	22.6	14
June	5.5	4.8	7.0	17.0	47
July	7.1	6.3	8.3	28.4	48
Aug	7.1	4.5	4.3	39.6	30
Sept	4.5	3.8	5.1	21.1	43
Oct	7.0	5.8	4.1	32.5	22
Nov	11.4	8.7	12.3	52.0	42
Dec	16.8	13.1	12.6	64.8	24

* The number of years since 1930 in which there was rainfall less than or equal to the amount received during the first annual cycle of the study year.

Table 3.2. Selected Properties of the Sampling Sites.

	Horizon	Depth	> 2 mm[&]	15 bar water content	Bulk density	O.M.*	Non-XL[#]	Halloysite
		(cm)	(%)	(%)	(g/cm^3)	(wt. %)	(wt. %)	(wt.%)
Site B	A	0-10	72	18.7	0.90	7.0	9.8	22.3
	Bw	10-37	65	21.7	0.90	5.2	11.2	19.9
Elev: 185 m	Bw2	37-65	85	26.5	0.90	4.4	11.8	21.3
MAR[a]: 18 cm	2Cr	65-100	90	17.9	1.56	3.8	15.7	22.4
MAT[b]: 23°C	R	100+	-	10.1	-	1.4	8.2	1.7
Site E	A	0-13	65	28.5	0.99	14.0	14.7	21.5
	Bt1	13-30	12	28.5	0.99	7.8	18.9	16.7
Elev: 674 m	Bt2	30-44	15	35.0	1.03	4.7	19.5	12.8
MAR[a]: 57 cm	Bt3	44-62	13	42.2	0.81	9.5	33.3	13.8
MAT[b]: 20°C	BC1	62-85	56	36.6	0.80	8.1	20.2	14.6
	BC2	85-103	50	33.5	0.94	7.2	10.8	23.8
Site J	A	0-22	3	75.1	0.48	25.5	25.1	8.4
	Bw	22-47	2	89.2	0.45	15.1	32.1	9.4
Elev: 1158 m	Bw2	47-67	6	95.9	0.58	7.5	45.4	10.6
MAR[a]: 138 cm	Bw3	67-92	39	78.4	0.58	9.1	39.8	11.4
MAT[b]: 18°C	Bt	92-125	24	54.2	0.62	3.6	40.1	13.6
	BCt	125-185	15	56.3	0.74	5.2	37.7	14.1
Site M	Ag	0-10	0	-	0.39	27.8	19.6	1.8
	Bw1	10-28	0	62.0	0.39	24.8	29.9	1.8
Elev: 1200 m	Bw2	28-42	0	134.1	0.35	18.9	32.3	1.9
MAR[a]: 250 cm	Bw3	42-58	0	120.4	0.37	14.9	31.7	2.0
MAT[b]: 17°C	Bw4	58-79	0	121.9	0.38	16.7	30.9	1.8
	2Cr	79-101	0	94.7	0.39	8.4	39.2	2.0
	3Ab	101-110	0	88.0	0.42	6.5	29.6	2.0
	3Bwb1	110-120	0	170.1	0.44	10.2	42.8	2.2
	3Bwb2	120-132	0	167.9	0.44	11.3	47.5	2.0

[a]Median Annual Rainfall, [b]Mean Annual Temperature

[&]Coarse fragment fraction, *Organic matter content, [#]Non-crystalline material

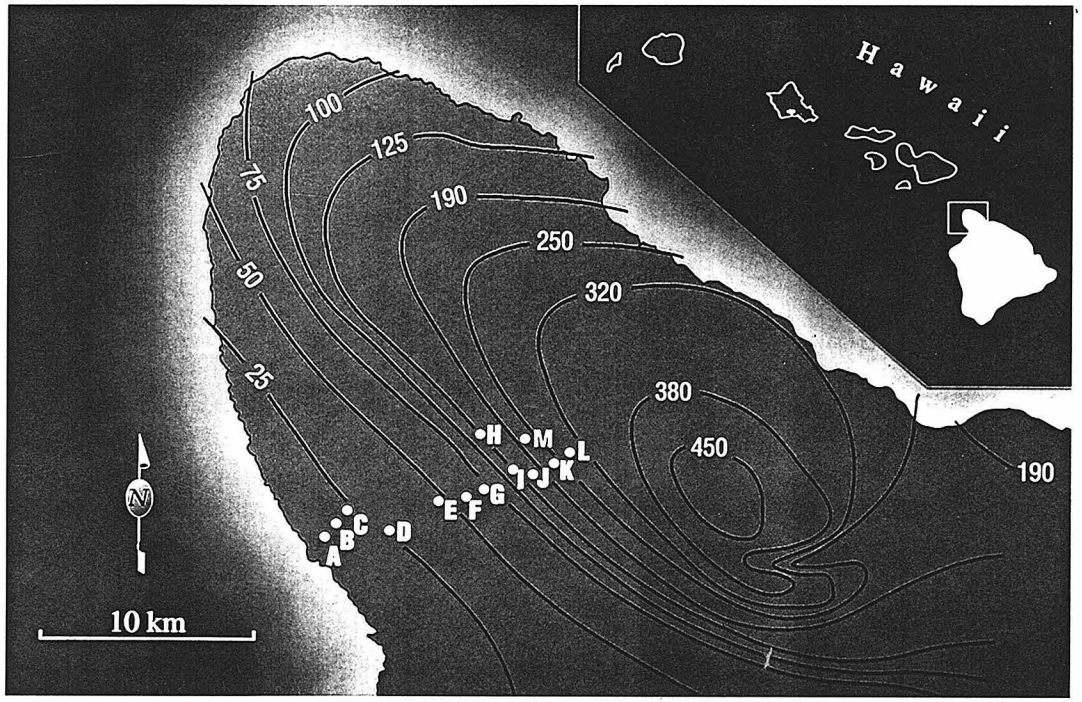

Figure 3.1. Location of the Kohala peninsula on the island of Hawaii. The bioclimatic transect is located on the leeward side of the peninsula. Contours of median annual precipitation are in cm.

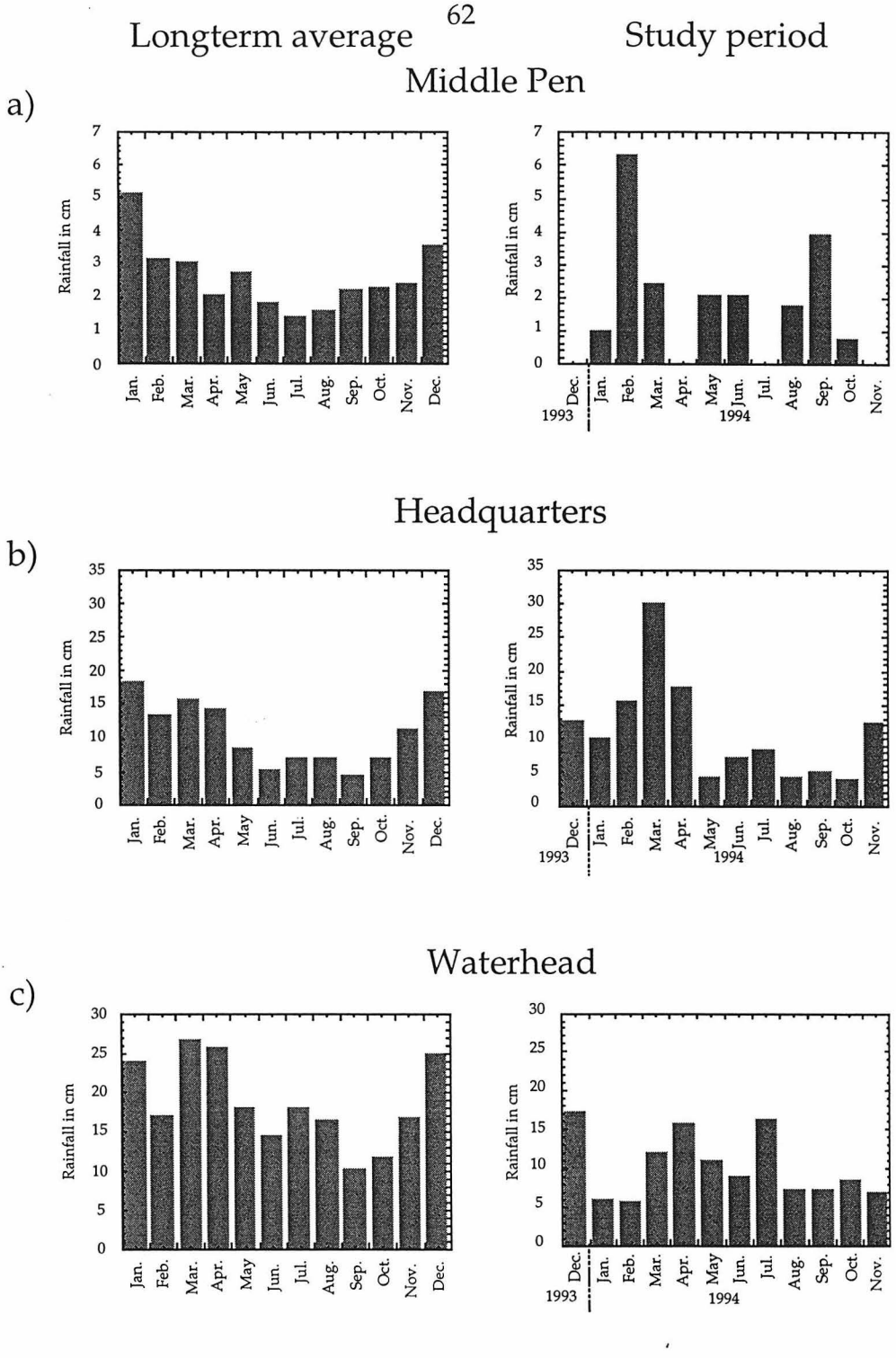

Figure 3.2. Monthly precipitation data from State of Hawaii rainfall monitoring stations along the leeward side of Kohala. Middle Pen (a) is located at 420 m, Headquarters (b) at 992 m, and Waterhead (c) 1200 m. Sixty-year long-term average values and values measured in the study period are presented for each station.

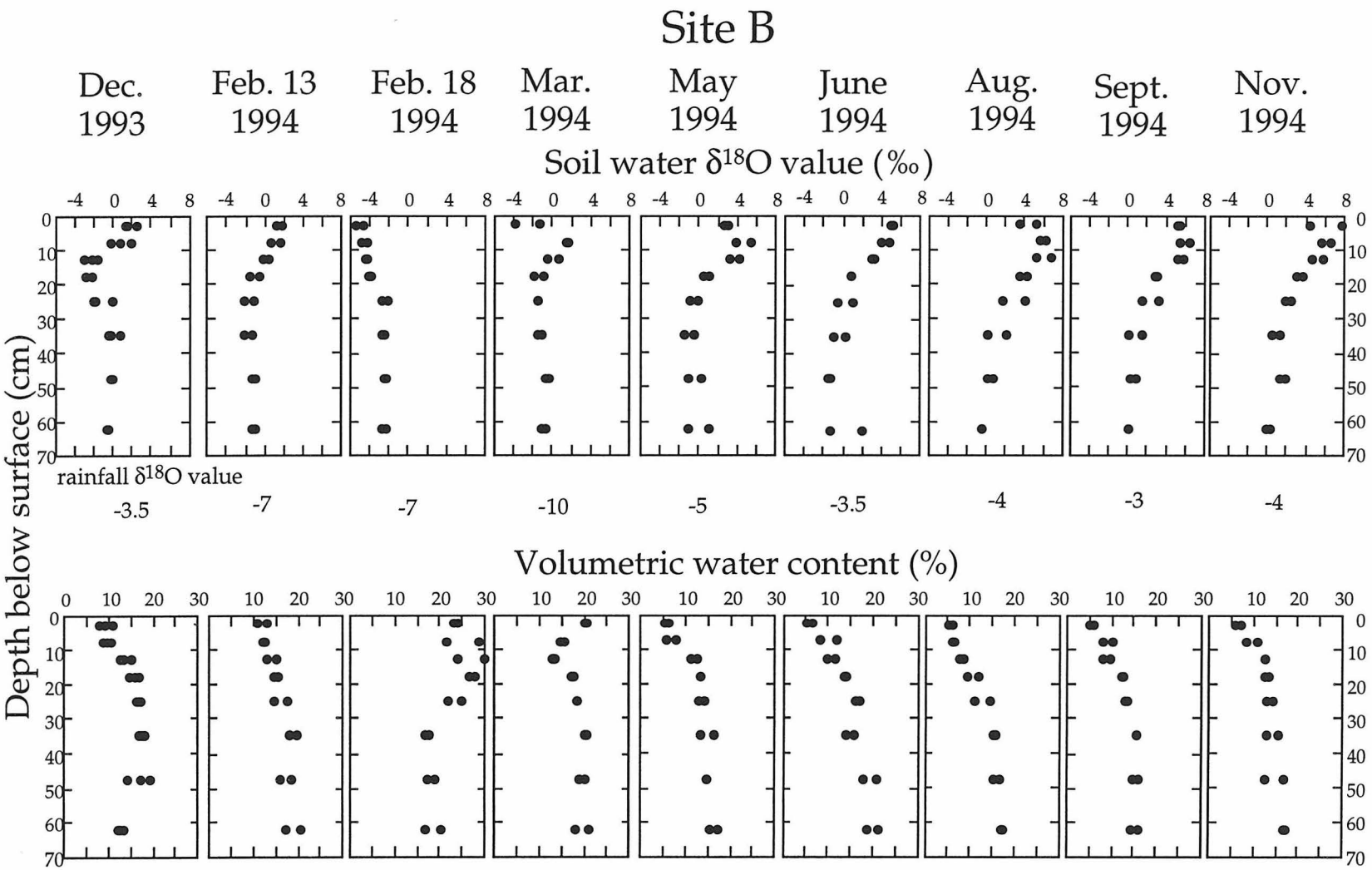
Site B
Dec. 1993
Feb. 13 1994
Feb. 18 1994
Mar. 1994
May 1994
June 1994
Aug. 1994
Sept. 1994
Nov. 1994
Soil water δ18O value (‰)
Depth below surface (cm)
rainfall δ18O value
-3.5
-7
-7
-10
-5
-3.5
-4
-3
-4
Volumetric water content (%)

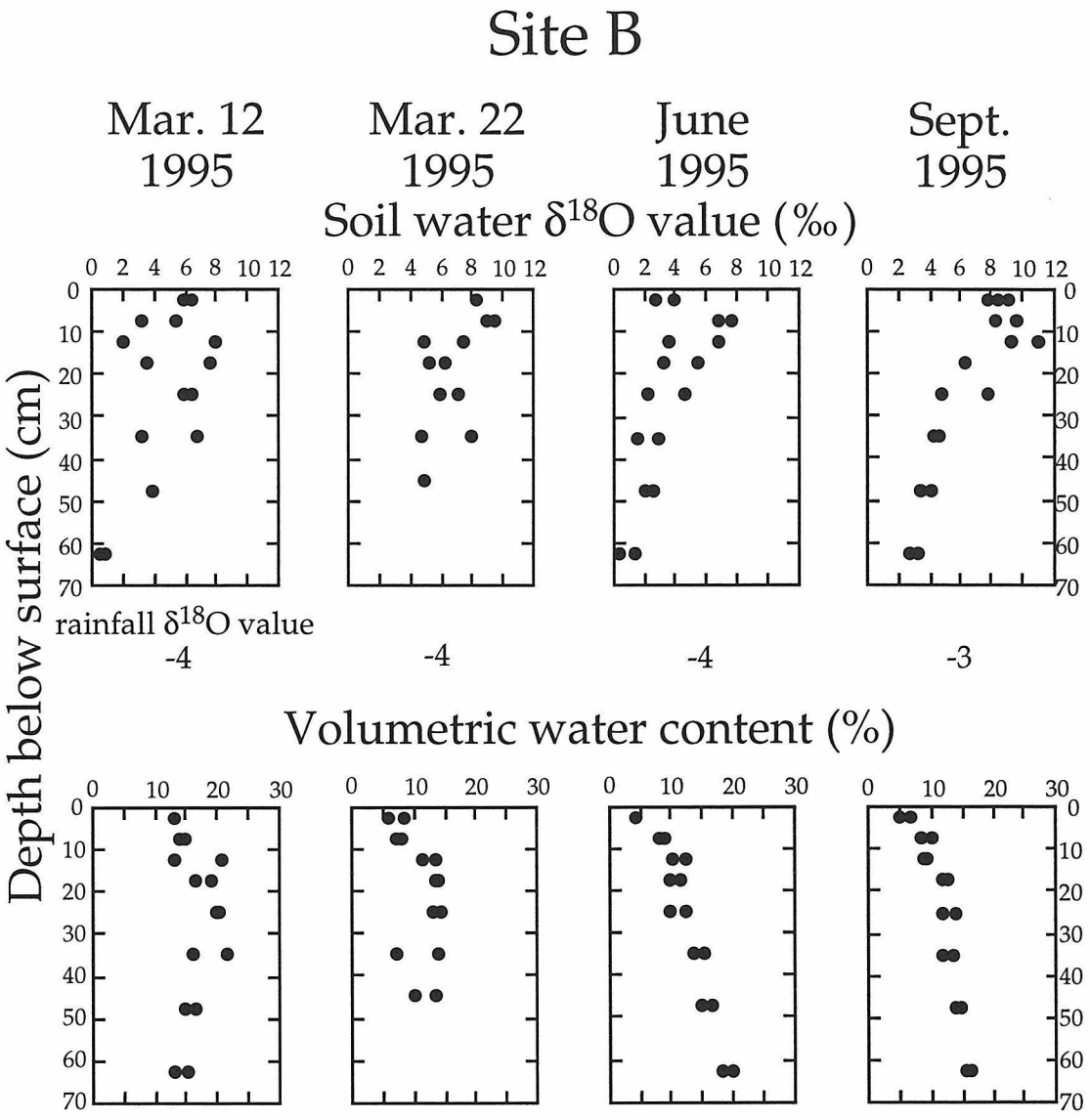

Figure 3.3. Site B results presented as y-axis depth plots with either soil water $\delta^{18}O$ values or volumetric water content on the x-axis. The $\delta^{18}O$ value of the rainfall during the measurement interval is reported below the graph of soil water $\delta^{18}O$ values. The date of sample collection is presented above each pair of graphs. Note scale change for soil water $\delta^{18}O$ values in 1995.

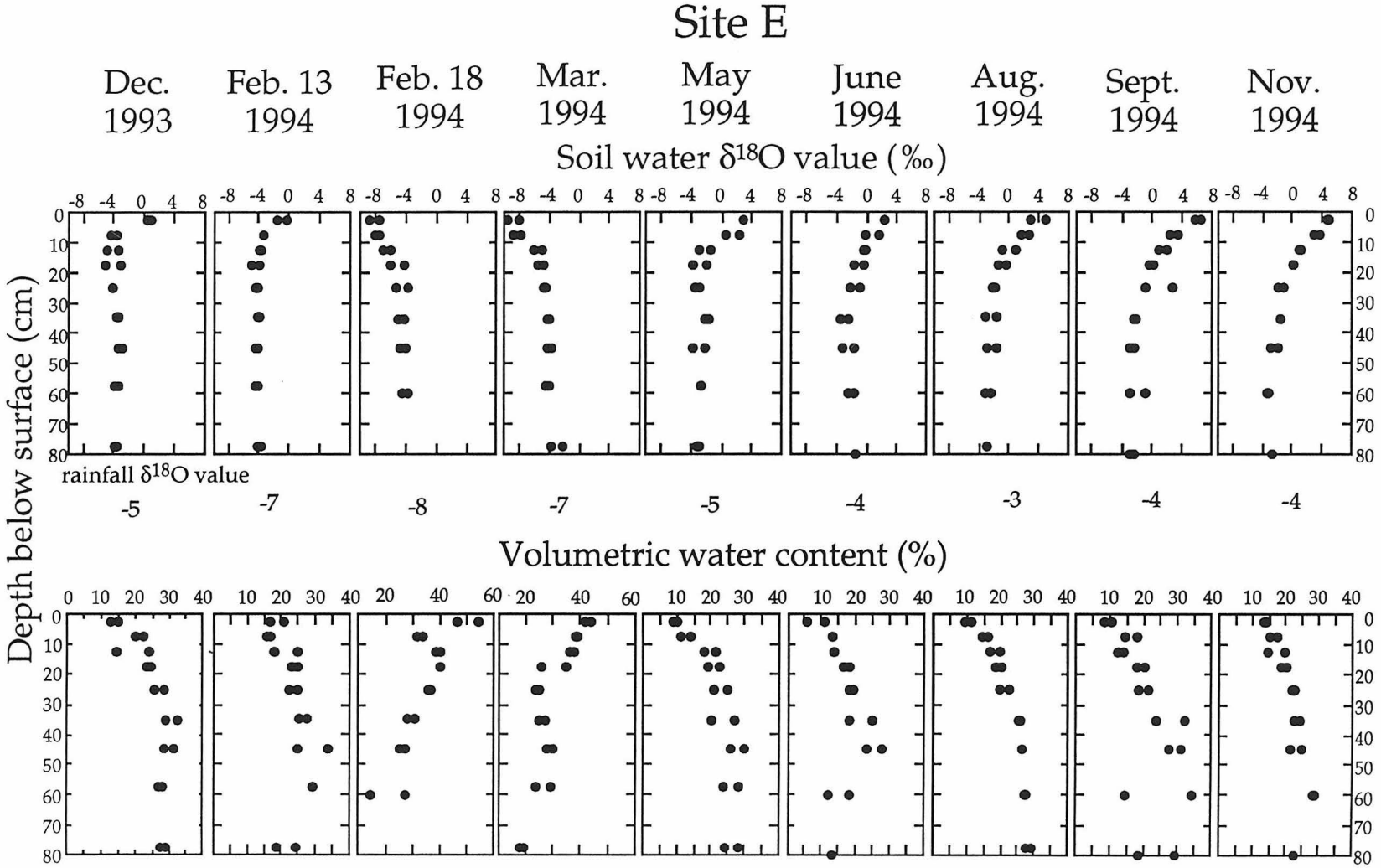
Site E
Dec. 1993
Feb. 13 1994
Feb. 18 1994
Mar. 1994
May 1994
June 1994
Aug. 1994
Sept. 1994
Nov. 1994
Soil water δ18O value (‰)
Depth below surface (cm)
rainfall δ18O value
-5
-7
-8
-7
-5
-4
-3
-4
-4
Volumetric water content (%)

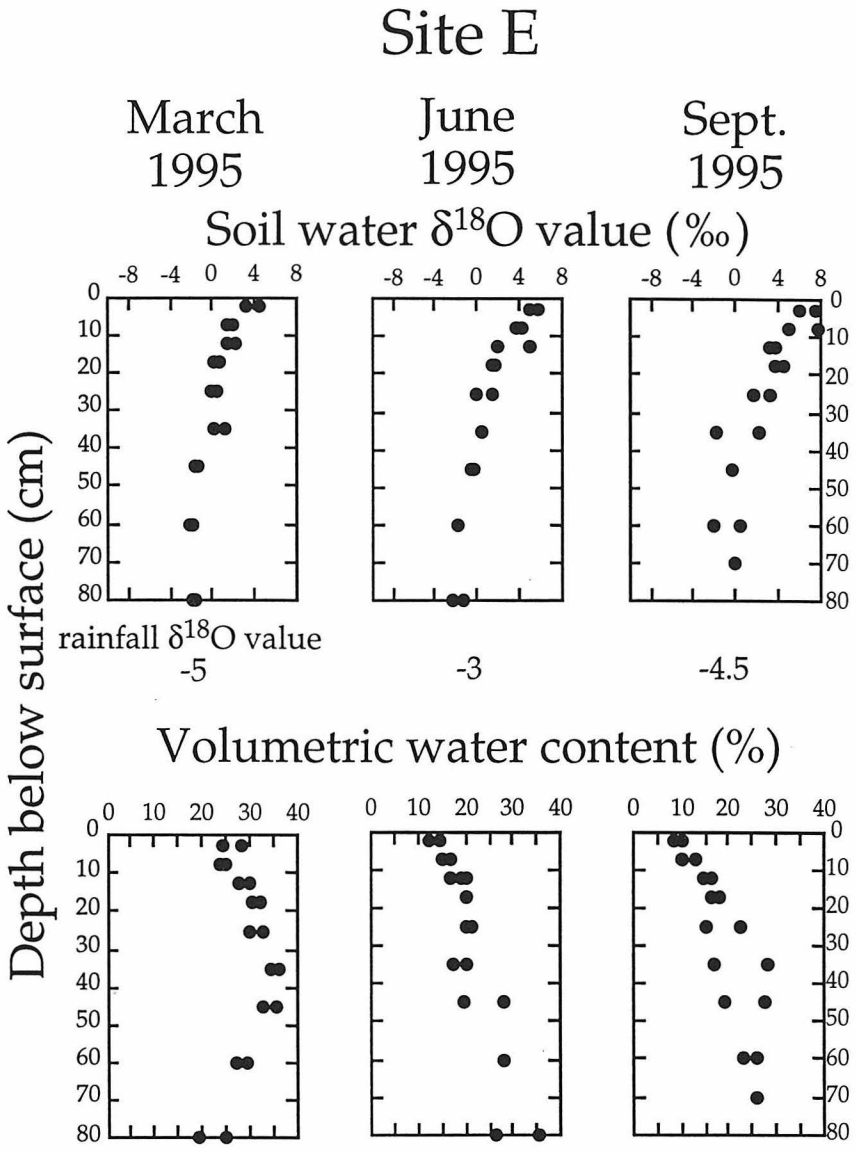

Figure 3.4. Site E results presented as y-axis depth plots with either soil water $\delta^{18}O$ values or volumetric water content on the x-axis. The $\delta^{18}O$ value of the rainfall during the measurement interval is reported below the graph of soil water $\delta^{18}O$ values. The date of sample collection is presented above each pair of graphs. Note scale change for volumetric water contents for February 18 and March in 1994.

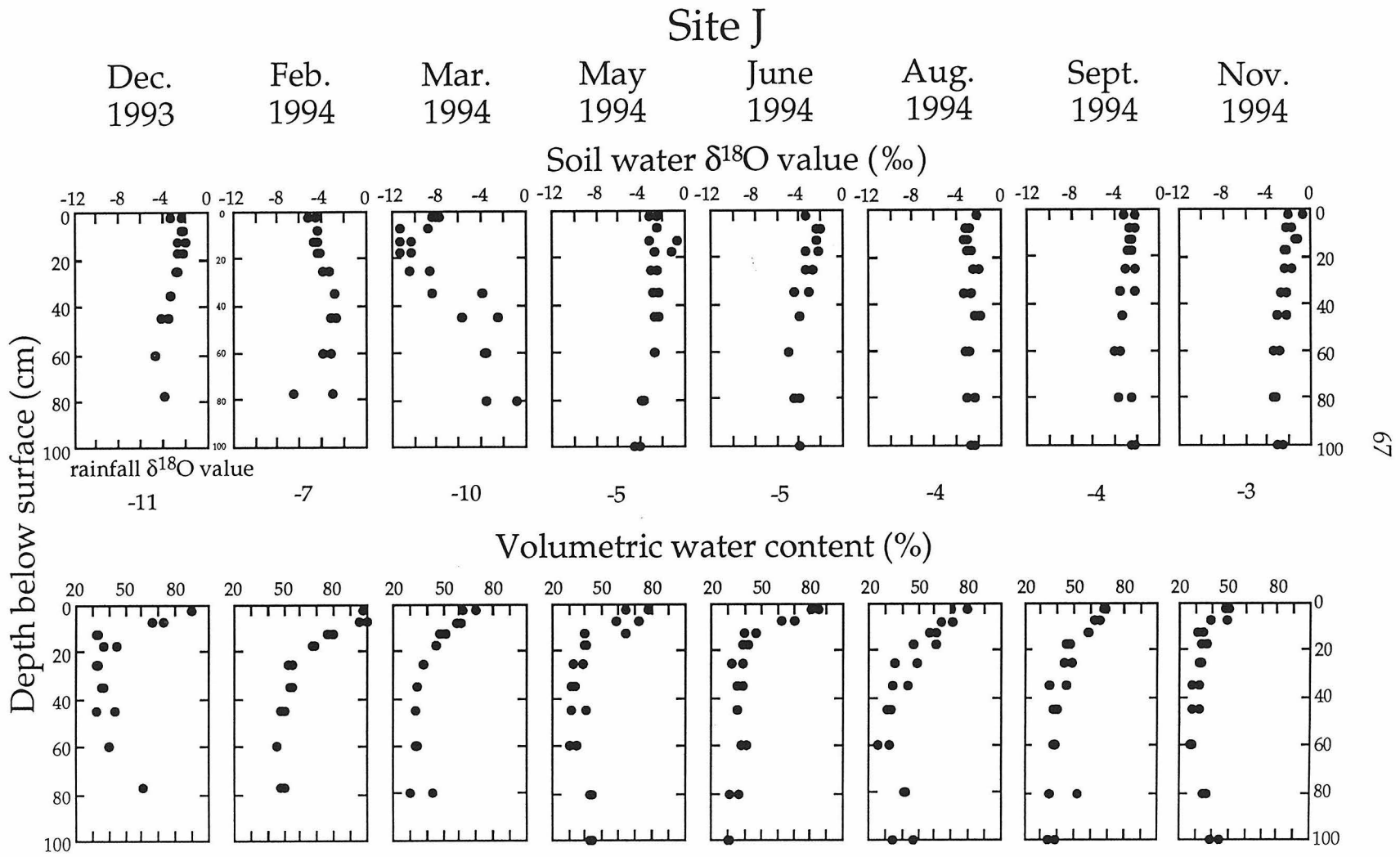
Site J
Dec. 1993
Feb. 1994
Mar. 1994
May 1994
June 1994
Aug. 1994
Sept. 1994
Nov. 1994
Soil water δ18O value (‰)
-12 -8 -4 0
0 20 40 60 80 100
rainfall δ18O value
-11
-7
-10
-5
-5
-4
-4
-3
Volumetric water content (%)
20 50 80
Depth below surface (cm)

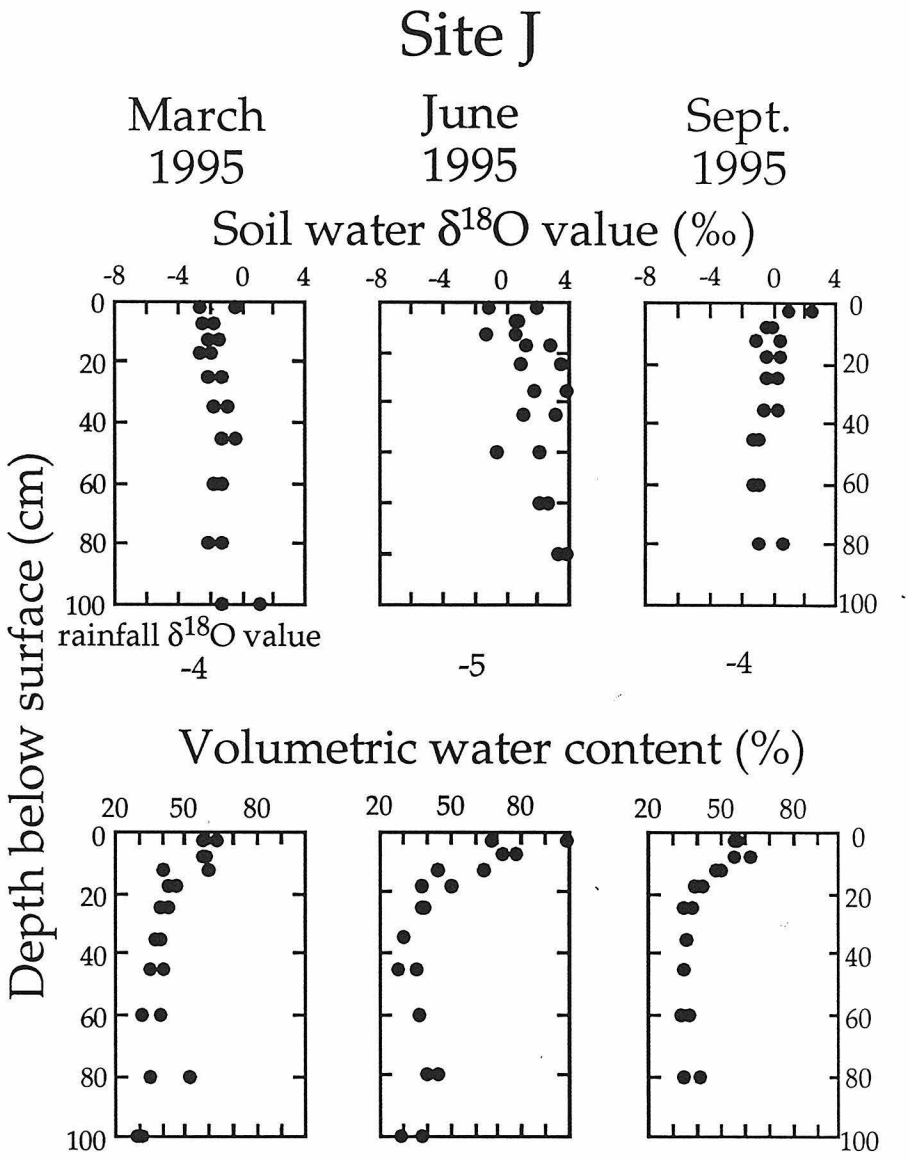

Figure 3.5. Site J results presented as y-axis depth plots with either soil water $\delta^{18}O$ values or volumetric water content on the x-axis. The $\delta^{18}O$ value of the rainfall during the measurement interval is reported below the graph of soil water $\delta^{18}O$ values. The date of sample collection is presented above each pair of graphs. Note scale change for soil water $\delta^{18}O$ values in 1995.

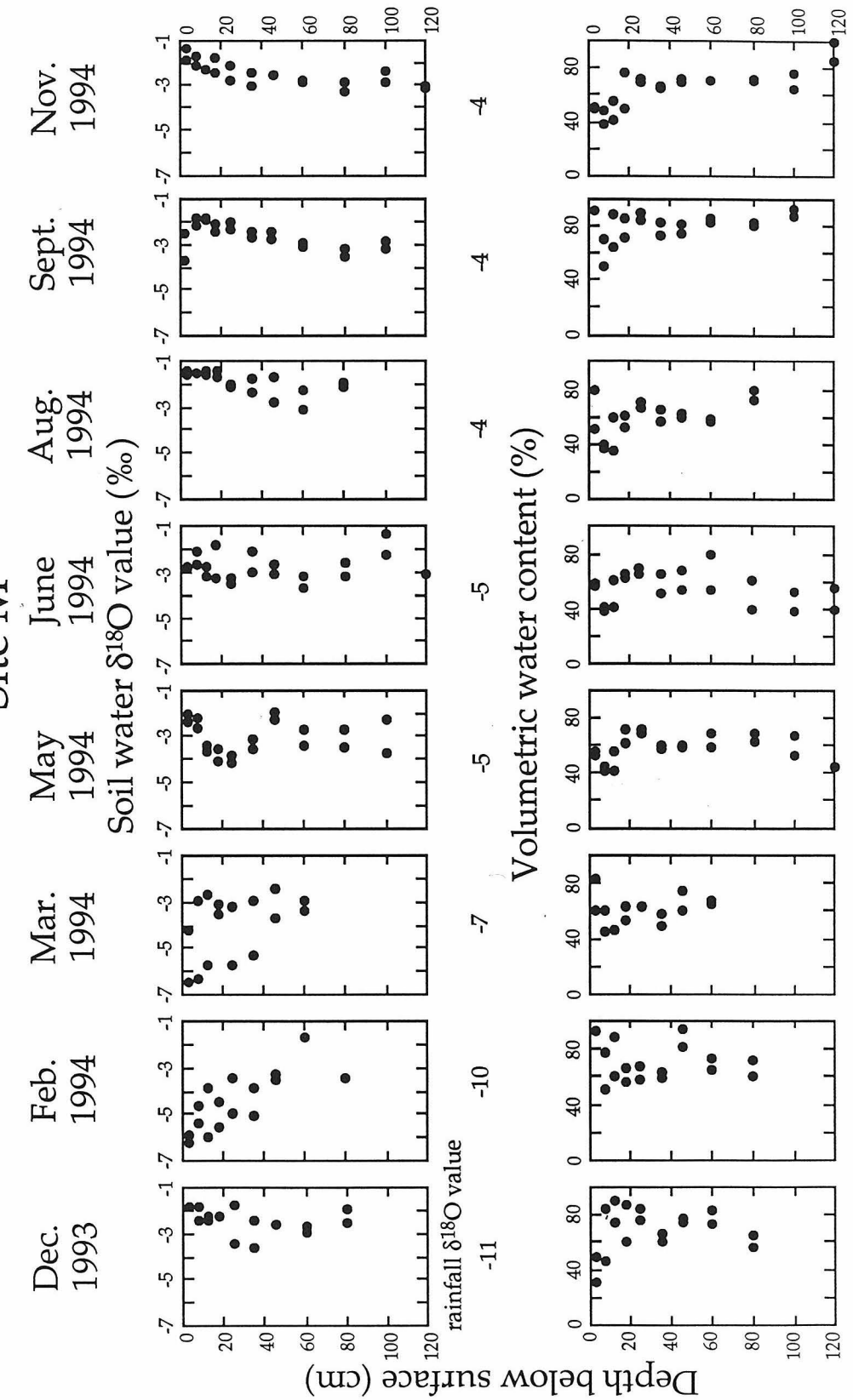
Site M
Dec. 1993
Feb. 1994
Mar. 1994
May 1994
June 1994
Aug. 1994
Sept. 1994
Nov. 1994
Soil water δ18O value (‰)
Volumetric water content (%)
Depth below surface (cm)
rainfall δ18O value
-11
-10
-7
-5
-5
-4
-4
-4

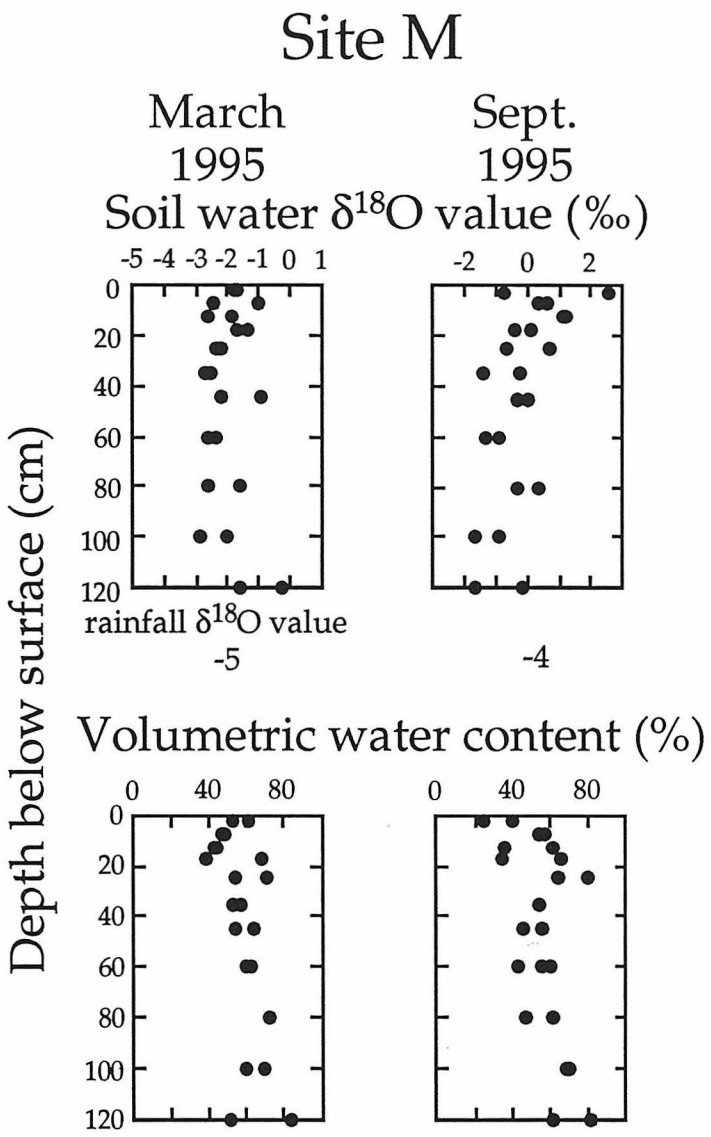

Figure 3.6. Site M results presented as y-axis depth plots with either soil water $\delta^{18}O$ values or volumetric water content on the x-axis. The $\delta^{18}O$ value of the rainfall during the measurement interval is reported below the graph of soil water $\delta^{18}O$ values. The date of sample collection is presented above each pair of graphs. Note scale changes for soil water $\delta^{18}O$ values in 1995.

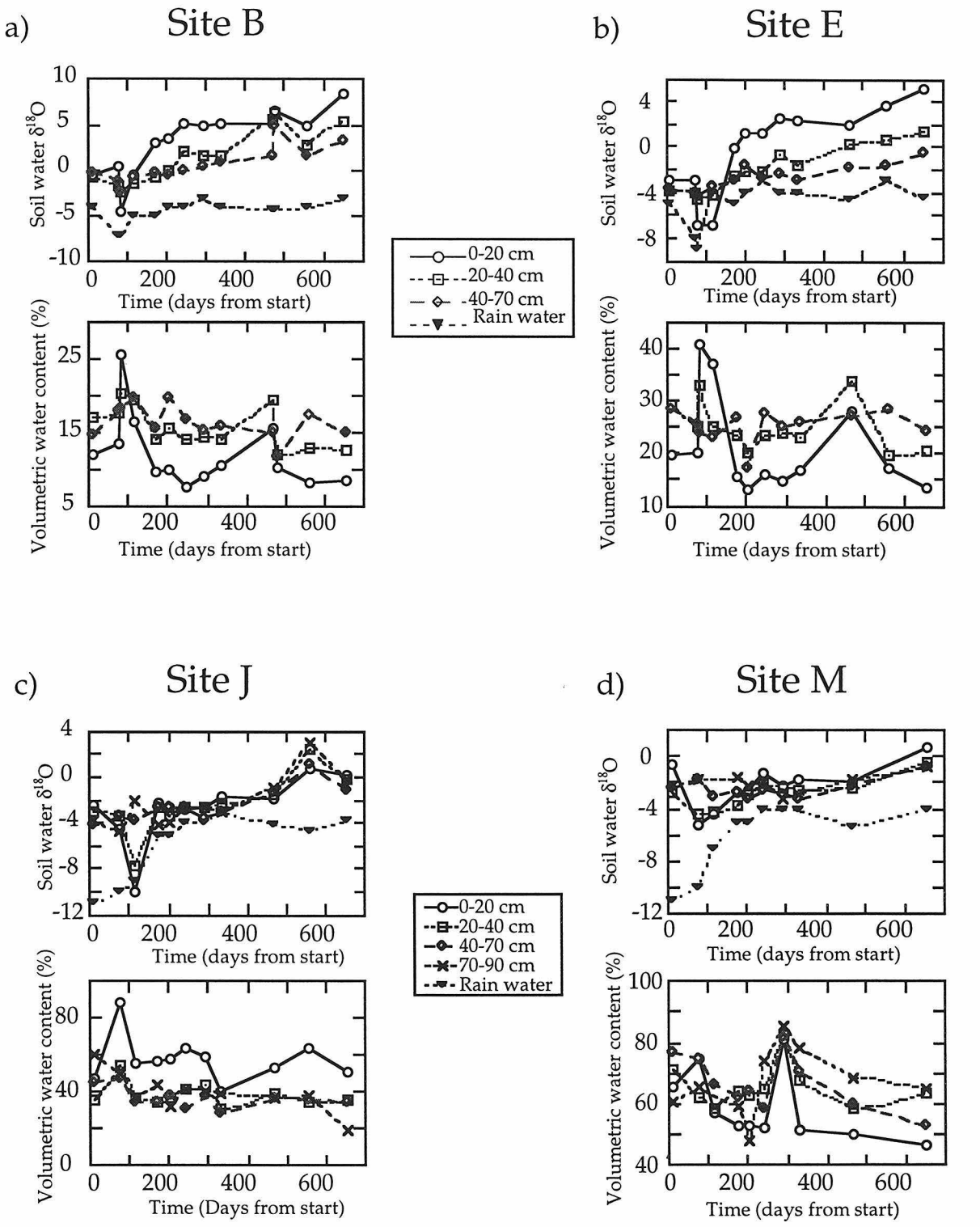

Figure 3.7 a-d. Depth-weighted averages for selected depth zones are plotted as a time-series for Site B (a), Site E (b), Site J (c), and Site M (d). The starting date is December 1, 1993. Soil-water $\delta^{18}O$ values are shown in the upper plot and volumetric water content values are shown in the lower plot.

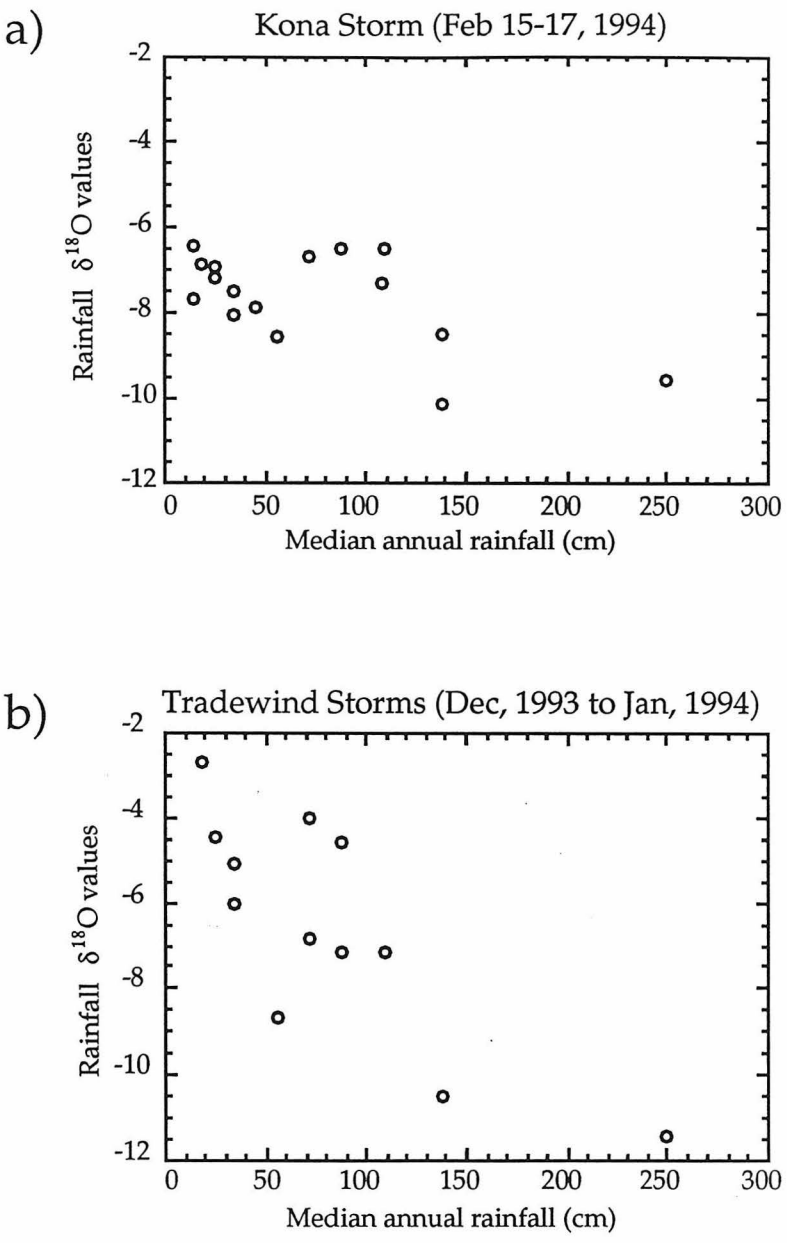

Figure 3.8. Rainfall $\delta^{18}O$ values plotted as a function of median annual rainfall for: (a) a single cyclonic Kona storm and (b) a series of Tradewind storms. Since the Tradewind storms are a result of orographic rise of water vapor masses arising from the prevailing Tradewinds, the series is comparable to the single cyclonic Kona storm.

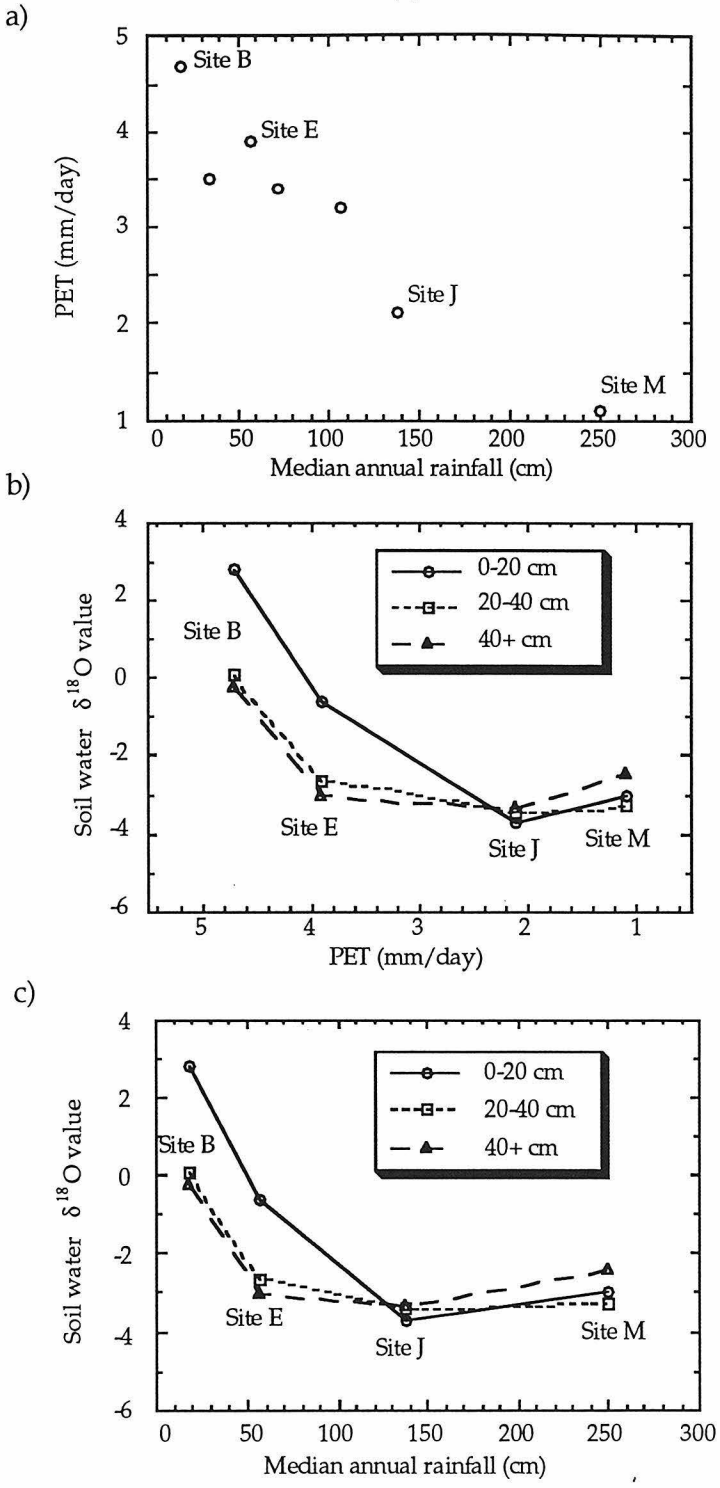

Figure 3.9 a) PET measured using E-TGauge™ Model A evaporimeters plotted as a function of median annual rainfall. PET is presented as mm of water loss/day. b) Time-weighted averages of soil-water $\delta^{18}O$ values for 0-20 cm, 20-40 cm and 40+ cm zones plotted as a function of median annual rainfall. c) Time-weighted averages of soil-water $\delta^{18}O$ values for 0-20 cm, 20-40 cm and 40+ cm zones plotted as a function of measured PET.

Chapter 4. Review of Stable Isotopic Studies of Clay Minerals.

The $\delta^{18}O$ value of precipitation is controlled by several climatic parameters, especially temperature, amount of rain in the precipitation event and the rainout history of the air mass (Dansgaard, 1964). Soils form as precipitation interacts with rock surfaces and infiltrates into the shallow subsurface. The $\delta^{18}O$ value of a pedogenic mineral (i.e., a mineral formed in a soil) should reflect the $\delta^{18}O$ value of soil water and the temperature of mineral formation. The $\delta^{18}O$ value of soil water differs from that of precipitation primarily because water is lost by evaporation from the soil surface. Chapter 3 was an investigation of the $\delta^{18}O$ values of rainfall and soil water. If we can determine the relationship between the $\delta^{18}O$ value of pedogenic minerals and soil waters in which they formed, the $\delta^{18}O$ values of the minerals could be used as indicators of continental climate. The final part of this thesis (Chapters 4 through 6) is an investigation into the relationship between $\delta^{18}O$ values of soil water and pedogenic minerals.

The $^{18}O/^{16}O$ ratio of pedogenic carbonate has been used to reconstruct climate histories in arid environments (Cerling, 1992; Smith et al., 1993; Amundson et al., 1996, and others). However, the occurrence of pedogenic carbonate is largely limited to deserts and some semi-arid grasslands. The formation of pedogenic clays is not restricted to low rainfall environments. Thus, their $^{18}O/^{16}O$ ratios may yield information about a wider range of climates than is possible for pedogenic carbonates. In this study, we isolate

and measure the $\delta^{18}O$ values of halloysite from soils along an arid to humid transect in Hawaii. The relationship between the $\delta^{18}O$ values of soil water and precipitation along the same transect was discussed in Chapter 3.

4.1. Previous stable isotopic studies of clays.

Savin and Esptein (1970) performed the first comprehensive survey of $\delta^{18}O$ and δD values of clay minerals in weathering, sedimentary, and diagenetic environments. They concluded that clays form in isotopic equilibrium with ambient conditions. Furthermore, in the absence of subsequent chemical or mineralogical alteration, the stable isotopic composition of a clay mineral does not change once it has formed. They also determined that interlayer water exchanges with water vapor under ambient laboratory atmosphere in a matter of hours. It is therefore removed from clays prior to isotopic analysis of the aluminosilicate framework. From their oxygen and hydrogen isotopic analyses of kaolinite, a relationship between the δD and $\delta^{18}O$ values was determined. On a δD vs $\delta^{18}O$ graph, this relationship was later termed the kaolinite line.

Lawrence and Taylor (1971, 1972) measured the $\delta^{18}O$ and δD values of clay minerals in several weathering profiles. Consistent with the results of Savin and Epstein (1970), they concluded that clay minerals formed in oxygen and hydrogen isotopic equilibrium with "weathering conditions." Based on a rather coarse sampling of several profiles, they recognized only small variations in the $\delta^{18}O$ values with depth in the profile.

Later studies focused on the preservation of the oxygen and hydrogen isotopic composition of clays in sedimentary, diagenetic, weathering environments (Yeh and Savin, 1976, 1977; Yeh, 1980; Eslinger and Yeh, 1981, and others). Laboratory exchange experiments using a variety of clays have also addressed this issue (James and Baker, 1976; O'Neil and Kharaka, 1976). Results of both laboratory and field studies indicate that hydrogen is much more susceptible to post-formational isotopic exchange than oxygen. O'Neil and Kharaka (1976) observed significant hydrogen isotopic exchange between water and kaolinite, smectite, and illite at temperatures of 100°C and higher on laboratory timescales. On geological timescales, Yeh (1980) found significant D/H changes in montmorillonites and illites from Gulf Coast sediments that had been heated in the geothermal gradient to 120°C. However, most of the change in the D/H ratio may have been due to the transformation of smectite to illite. Bird and Chivas (1988, 1989) reported that the δD and $\delta^{18}O$ values of a suite of kaolinites from the regolith of Australia plotted above the kaolinite line (i.e., to the low $\delta^{18}O$ and/or high δD side). They concluded that the hydrogen of the kaolinites exchanged with diagenetic water at temperatures of up to 80°C, the estimated maximum temperature from burial. Lawrence and Rashkes-Meaux (1993) analyzed kaolinites from weathering profiles from a large number of localities in North America. Their results suggested that hydrogen isotopic compositions of kaolinites were only partially preserved. Although evidence exists for preservation of the δD value of clay minerals in some cases (Bird et al., 1989; Eslinger and Yeh,

1981), the conditions under which δD values of clay minerals are or are not preserved in weathering environments are not yet well known.

On geological timescales, there is little evidence of exchange of oxygen isotopes in clays formed in weathering environments. The $\delta^{18}O$ values of pedogenic minerals have been analyzed as proxies for climatic information in a number of studies (Yapp, 1987, 1993; Bird et al., 1993; Lawrence and Raskes Meaux, 1993; Giral, 1994; Elliot et al., in prep.; Giral et al., in prep.; Stern et al., 1995, 1996, and others).

Yapp (1987, 1993) examined goethite from the Upper Ordovician Neda Formation of the north-central United States, an oolitic sandstone. The formation was subaerially weathered during Late Ordovician time (Paull, 1977). The measured $\delta^{18}O$ and δD values for goethite are -1.0 and -139‰, respectively, from which Yapp calculated water $\delta^{18}O$ and δD values of -7.3 and -49‰, respectively. Measured $\delta^{18}O$ and δD values for modern water at that locale are about -9 and -60‰, respectively. Based on this difference, Yapp speculated that, during the late Ordovician, a low-latitude, low-altitude contintental site was receiving precipitation which originated with a highly seasonal character to it.

Bird and Chivas (1988, 1989) reported no evidence of oxygen isotopic exchange of kaolinite samples from Australia. They suggested that changes in the observed $\delta^{18}O$ value of kaolinite over time reflected local increases in the $\delta^{18}O$ value of meteoric water over time consistent with northwest migration of the Australian continent.

Lawrence and Rashkes-Meaux (1993) analyzed kaolinites from weathering profiles sampled at a large number of localities in North America. Ages of the samples range from Carboniferous to Quaternary. Using variations of the $\delta^{18}O$ value of kaolinite through time, Lawrence and Rashkes-Meaux showed that North America had experienced an overall trend of cooling since Cretaceous time, consistent with evidence from deep sea drill cores (Savin, 1977). Lawrence and Rashkes-Meaux also concluded from the similarities between Pennsylvanian and modern kaolinite data that the isotopic composition of the ocean in the Pennsylvanian was not radically different from that of today.

Several studies of modern soils (Bird et al., 1993; Giral, 1994; Giral et al., in prep.) have focused on Brazilian laterites. Bird and others (1993) were able to isolate separates of kaolinite, goethite/hematite, gibbsite, cryptomelane and anatase from deep weathering profiles in the vicinity of bauxite deposits. The $\delta^{18}O$ values of water calculated using mineral $\delta^{18}O$ values were in good agreement with measured $\delta^{18}O$ values of meteoric water for all minerals except gibbsite. The $\delta^{18}O$ value of water calculated using the $\delta^{18}O$ value of gibbsite is about 2‰ lower than the $\delta^{18}O$ values of modern meteoric water. They concluded that gibbsite probably formed when low ^{18}O monsoonal precipitation was more abundant.

Giral (1994) and Giral et al. (in prep.) examined two deep weathering profiles in Brazil, one in the vicinity of Pitinga and one in the vicinity of Manaus. Their study included a detailed field description and petrologic and

mineralogic examination of samples as well as measurements of $\delta^{18}O$ values of kaolinites. Crystallinity as determined by Hinckley index values increased with depth in the weathering profile. Particle size analyses of the purified kaolinite samples indicated that all samples had polymodal size distributions. The abundance of the coarser modes decreased from the base to the top of the profile. The larger size fraction of kaolinite had greater crystallinity than the smaller size fraction from the same horizon. The $\delta^{18}O$ values of kaolinite (between 18 and 22‰) are compatible with oxygen isotopic equilibrium with modern meteoric water. However, the $\delta^{18}O$ value of the smaller size fraction was consistently more positive than the larger size fraction. Giral et al. suggested that the different sizes were a result of kaolinite growth from soil water that infiltrated through the soil surface during different seasons of the year. The larger grains grew while rainy season precipitation (with low $\delta^{18}O$ values) was infiltrating the crystal growth site, and the smaller grains grew while the dry season precipitation with higher $\delta^{18}O$ values was in contact with the growing grains.

Elliot et al. (in prep.) separated kaolinite with only minor impurities from a saprolite developed on granite in the Piedmont Province of Virginia. They concluded from the $\delta^{18}O$ values that the kaolinites are not in oxygen isotopic equilibrium with modern meteoric water, nor, probably with soil water, at this site. Instead, they suggest that the kaolinite had formed in contact with waters that were more depleted in ^{18}O, perhaps shortly after, or

during, the last Pleistocene glacial stage in North America when that area was receiving ^{18}O-depleted precipitation.

Stern et al. (1995, 1996) measured the $\delta^{18}O$ values of pedogenic smectites isolated from a sequence of paleosols developed on the Himalayan molasse sequence in Pakistan. They found an increase with age of 3 to 4‰ in the $\delta^{18}O$ value of smectites that was synchronous with a 3.5‰ increase in the $\delta^{18}O$ value of pedogenic nodular calcite isolated from the same soils (Quade et al., 1989) at 8.5 to 6.5 Ma. The co-variation suggested that smectite was pedogenic rather than detrital. The measured oxygen isotope fractionation between calcite and smectite within individual paleosols was about +6.4‰ whereas equilibrium fractionations between these phases at soil-forming temperatures are known to be between +3.0 and +3.5‰ (Savin and Lee, 1988; Tarutani et al., 1969). Stern et al. suggested that this isotopic disequilibrium reflected growth of smectite predominantly during the wet summer season and calcite growth predominantly during the drier winter season. Summer monsoonal precipitation has lower $\delta^{18}O$ values than winter precipitation. Highly evaporative winter conditions probably cause the $\delta^{18}O$ of soil water to increase.

4.2. Equilibrium fractionation factors.

Most of the studies described above made use of estimates of equilibraium fractionation factors in clay–water systems. Estimation of these, however, is not without problems. This section is a critical review of the state

of knowledge of equilibrium oxygen isotope fractionations between kaolinite and water. Henceforth, the term fractionation factor will be used to mean equilibrium oxygen isotope fractionation factor.

Fractionation factors can be estimated using four different approaches. The first involves laboratory equilibration experiments, some of which have been done at elevated temperatures and pressures. At temperatures below about 200°C, rates of isotopic exchange are generally too slow to attain a measurable amount of exchange. Instead, fractionation factors of clay minerals are often estimated from the isotopic composition of naturally occurring samples. This empirical approach, however, requires that the conditions of formation be well understood. Often, precise information is not known and estimates of temperature and/or the $\delta^{18}O$ value of water are used instead of actual measurements. Statistical mechanical methods, a third way of calculating isotopic fractionation factors, were described by Urey (1947) and Bigeleisen and Mayer (1947). An excellent summary of the basic techniques was presented by O'Neil (1987). This method is useful for obtaining fractionation factors for low temperatures (Kieffer, 1982), but there have been few published calculations for clay–water systems. Finally, several semi-empirical methods have been used to estimate fractionation factors between clays and water at low temperatures. In one approach, the bond-type method, it is assumed that the oxygen in a chemical bond has similar isotopic behaviour regardless of the mineral in which the bond is located. Another approach, the increment method, is less simplistic than the bond-type

method and may prove to be more accurate. However, because it is arduous to apply, its use for clay minerals has been limited.

Fractionations for the kaolinite–water system are compared in Figure 4.1 for temperatures ranging from 0°C to about 400°C. The fractionation of Kulla and Anderson (1978) was based on synthesis reactions from gels, the fractionation of Land and Dutton (1978) was based on empirical data from Eslinger (1971) and Savin and Epstein (1970), and the fractionation of Sheppard and Gilg (1996) was based on the synthesis of all empirical data to date. The fractionation of Savin and Lee (1988) was calculated using the bond-type method and the fractionation of Zheng (1993) was calculated using the modified increment method.

With the exception of the fractionation estimated by Zheng and Kulla and Anderson, all of the kaolinite–water fractionations agree within 0.5‰ at 20°C and 1.1‰ at 30°C. For this study, we will use the fractionation factors estimated by Savin and Lee (1988) and Sheppard and Gilg (1996), both of which are based heavily on the isotopic compositions of naturally occurring pedogenic kaolinites in the 0°C to 30°C range.

A shortcoming of these fractionation equations derived from the isotopic composition of pedogenic clays is that, in all cases, the fluid with which that clay was assumed in equilibrium was mean annual local precipitation or local stream water (which in many environments is an average of local precipitation). This may be a valid assumption in many pedogenic environments. However, the work presented in Chapter 3 of this

thesis and that of Giral et al. (in prep.) shows that it may introduce errors in some pedogenic environments. At this time, it is not possible to quantify the magnitude of the errors introduced into the kaolinite–water fractionation as a result of this.

4.3. References.

Amundson, R.G., Chadwick, O.A., Kendall, C., Yang, W., DeNiro, M., 1996. Isotopic evidence for shifts in atmospheric circulation patterns during the Late Quaternary in mid-North America. Geology, 24: 23-26.

Bigeleisen, J., and Mayer, M.G., 1947. Calculation of equilibrium constants for isotopic exchange reactions. Journal of Chemical Physics, 23: 2264-2269.

Bird, M.I., and Chivas, A.R., 1988. Stable-isotope evidence for low-temperature kaolinitic weathering and post-formational hydrogen-isotope exchange in Permian kaolinites. Chemical Geology, 72: 249-265.

Bird, M.I., and Chivas, A.R., 1989. Stable isotope geochronology of the Australian regolith. Geochimica et Cosmochimica Acta, 53: 3239-3256.

Bird, M.I., Chivas, A.R., and Andrew, A.S., 1989. A stable-isotope study of lateritic bauxites. Geochimica et Cosmochimica Acta, 53: 1411-1420.

Bird, M.I., Longstaffe, F.J., Fyfe, W.S., Kronber, B.I., and Kishida, A., 1993. An oxygen-isotope study of weathering in the eastern Amazon Basin, Brazil. In: P.K. Swart, K.C. Lohman, J. McKenzie, and S. Savin (editors), Climate Change in Continental Isotopic Records. A.G.U. Geophysical Monograph 78: 295-307.

Cerling, T.E., 1992. Development of grasslands and savannas in East Africa during the Neogene. Palaeogeography, Palaeoclimatology, Palaeoecology (Global Planetary Change Section), 97: 241-247.

Dansgaard, W., 1964. Stable isotopies in precipitation. Tellus, 16: 436-468.

Elliot, W.C., Savin, S.M., Dong, H., and Peacor, D.R., in preparation. Paleoclimate implications of the mineralogy and the oxygen isotope geochemistry of clay minerals formed in a saprolite from the Piedmont province, Virginia.

Eslinger, E.V., 1971. Mineralogy and oxygen isotope ratios of hydrothermal and low-grade metamorphic argillaceous rocks. PhD thesis. Case Western Reserve University.

Eslinger, E.V. and Yeh, H.W., 1981. Mineralogy, O^{18}/O^{16}, and D/H ratios of clay-rich sediments from Deep Sea Drilling Project Site 180, Aleutian trench. Clays and Clay Minerals, 29: 309-315.

Giral, S., 1994. Variations des rapports isotopiques $^{18}O/^{16}O$ des kaolinites de deux profils latéritiques amazoniens: signification pour la pédologie et la paléoclimatologie. Ph.D. Thesis, Université de Droit, D'Économie et des Sciences d'Aix-Marseille.

Giral, S., Savin, S.M., Nahon, D.B., Girard, J.P., Lucas, Y., and Abel, L.J., in preparation. Oxygen isotope geochimistry of kaolinite in laterite-forming processes, Manaus, Amazonas, Brazil.

James, A.T., and Baker, D.R., 1976. Oxygen isotope exchange between illite and water at 22°C. Geochimica et Cosmochimica Acta, 40: 235-239.

Kieffer, S.W., 1982. Thermodynamics and lattice vibrations of minerals: 5. Applications to phase equilibria, isotopic fractionation, and high pressure thermodynamic properties. Reviews of Geophysics and Space Physics, 20: 827-849.

Kulla, J.B., and Anderson, T.F., 1978. Experimental oxygen isotope fractionation between kaolinite and water. In: R.E. Zartman (editor), Short papers of the 4th International Congress, Geochronology, Cosmochronology, Isotope Geology. USGS, Open File Report, 78-70: 234-235.

Land, L.S., and Dutton, S.P., 1978. Cementation of a Pennsylvanian deltaic sandstone: isotopic data. Journal of Sedimentary Petrology, 48: 1167-1176.

Lawrence, J.R., and Raskes Meaux, J., 1993. The stable isotopic composition of ancient kaolinites of North America. In: P.K. Swart, K.C. Lohman, J. McKenzie, and S. Savin (editors), Climate Change in Continental Isotopic Records. A.G.U. Geophysical Monograph 78: 249-261.

Lawrence, J.R., and Taylor, H.P., Jr., 1971. Deuterium and oxygen-18 correlation: Clay minerals and hydroxides in Quaternary soils compared to meteoric waters. Geochimica et Cosmochimica Acta, 35: 993-1003.

Lawrence, J.R., and Taylor, H.P., Jr., 1972. Hydrogen and oxygen isotope systematics in weathering profiles. Geochimica et Cosmochimica Acta, 36: 1377-1393.

O'Neil, J.R., 1987. Theoretical and experimantal aspects of isotopic fractionation. In: J.W. Valley, H.P. Taylor, Jr., and J.R. O'Neil (editors), Stable isotopes in high temperature processes. Reviews in Mineralogy, v16, 1-40.

O'Neil, J.R., and Kharaka, Y.K., 1976. Hydrogen and oxygen isotope exchange reactions between clay minerals and water. Geochimica et Cosmochimica Acta, 40: 241-246.

Paull, R.A., 1977. The Upper Ordovician Neda Formation of eastern Wisconsin, in: K.G. Nelson (editor), Geology of southeastern Wisconsin, A guidebook for the 41st annual Tri-state field conference, C-1 to C-18, Wisconsin Geological and Natural History Survey.

Quade, J., Cerling, T.E., and Bowman, J.R., 1989. Development of Asian monsoon revealed by marked ecological shift during the late Miocene in northern Pakistan, Nature, 342: 163-166.

Savin, S.M., 1977. The history of the earth's surface temperature during the past 100 million years. Annual Reviews of Earth and Planetary Science, 5: 319-355.

Savin, S.M., and Epstein, S., 1970. The oxygen and hydrogen isotope geochemistry of clay minerals. Geochimica et Cosmochimica Acta, 34: 25-42.

Savin, S.M., and Lee, M., 1988. Isotopic studies of phyllosilicates. In: S.W. Bailey (editor) Hydrous phyllosilicates (exclusive of micas). Reviews in Mineralogy, v19, pp. 189-219.

Sheppard, S.M.F. and Gilg, H.A., 1996. Stable-isotope geochemistry of clay-minerals. Clay Minerals, 31(1); 1-24.

Smith, G.A., Wang, Y., and Geissman, J.W., 1993. Comparison of a paleosol-carbonate isotope record to other records of Pliocene-early Pleistocene climate in the western United States. Geology, 21: 691-649.

Stern, L.A., Chamberlin, C.P., and Johnson, G.D., 1995. Record of climate change preserved in oxygen isotope systematics of pedogenic clay minerals in Himalayan molasse. Geological Society of America Abstracts with Programs, 27(6): A-206.

Stern, L.A., Chamberlain, C.P., Reynolds, R.C., and Johnson, G.D., 1996. Oxygen isotope evidence of climate change from pedogenic clay minerals in the Himalayan Molasse. In press, Geochimica et Cosmochimica Acta.

Tarutani, T., Clayton, R.N., and Mayeda, T.K., 1969. The effect of polymorphism and magnesium substitution of oxygen isotope fractionation between calcium carbonate and water. Geochimica et Cosmochimica Acta, 33: 987-996.

Urey, H.C., 1947. The thermodynamic properties of isotopic substances. Journal of the Chemical Society (London), 562-581.

Yapp, C.J., 1993. The stable isotope geochemistry of low temperature Fe(III) and Al oxides with implications for continental paleoclimates. In: P.K. Swart, K.C. Lohman, J. McKenzie, and S. Savin (editors), Climate

Change in Continental Isotopic Records. A.G.U. Geophysical Monograph 78: 285-294.

Yeh, H.W., 1980. D/H/ ratios and late-stage dehydration of shales during burial. Geochimica et Cosmochimica Acta, 44: 341-352.

Yeh, H.W., and Savin, S.M., 1976. The extent of oxygen isotope exchange between clay minerals and sea water. Geochimica et Cosmochimica Acta, 40(7): 743-748.

Yeh, H.W., and Savin, S.M., 1977. Mechanism of burial metamorphism of argillaceous sediments: 3. O-isotope evidence. Geological Society of America Bulletin, 88: 1321-1330.

Zheng, Y.F., 1993. Calculation of oxygen isotope fractionation in hydroxyl-bearing silicates. Earth and Planetary Science Letters, 120: 247-263.

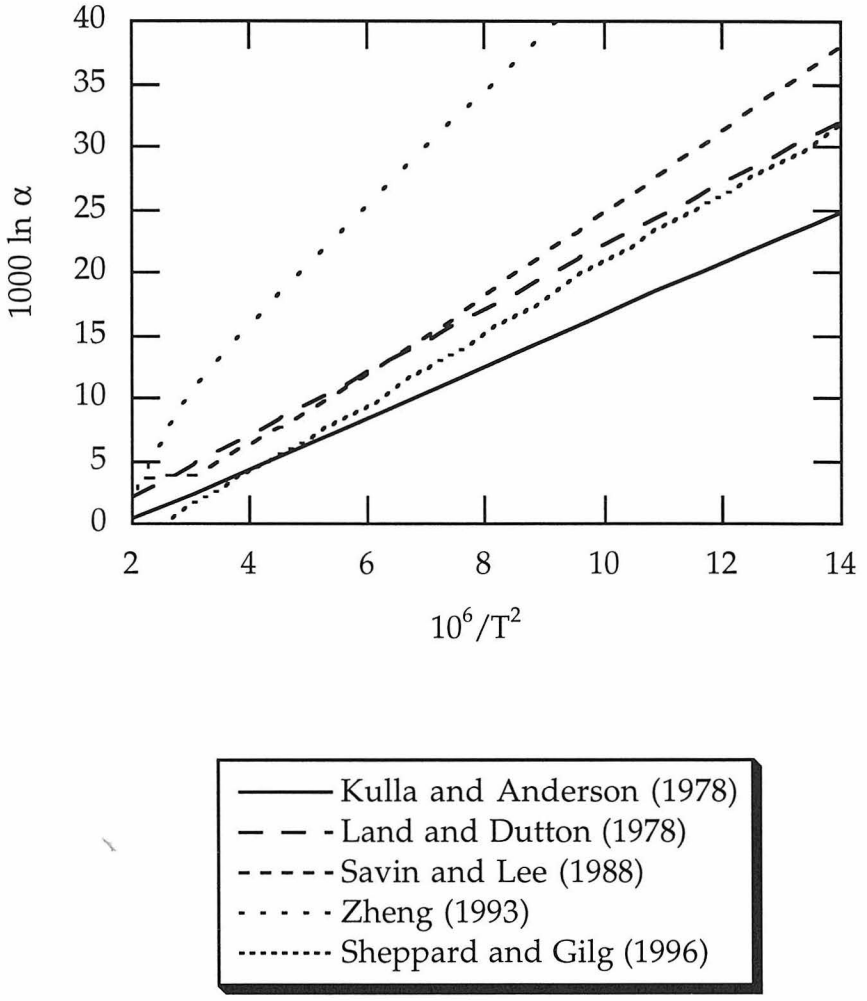

Figure 4.1. A comparison of kaolinite–water fractionations. The equations used are:
Kulla and Anderson (1978) : $1000 \ln \alpha = 2.05 \times 10^6 / T^2 - 3.85$
Land and Dutton (1978) : $1000 \ln \alpha = 2.50 \times 10^6 / T^2 - 2.87$
Savin and Lee (1988) : $1000 \ln \alpha = 0.42 \times 10^6 / T^2 + 10.6 \times 10^3 / T - 15.337$
Zheng (1993) : $1000 \ln \alpha = 4.29 \times 10^6 / T^2 - 6.44 \times 10^3 / T + 2.03$
Sheppard and Gilg (1996) : $1000 \ln \alpha = 2.76 \times 10^6 / T^2 - 6.75$

Chapter 5. Sample Preparation.

Soil is a heterogeneous mix of organic matter and primary and secondary minerals. Isolating monomineralic samples of halloysite, the predominant crystalline clay mineral on Kohala, from soil involves chemical dissolution of coatings followed by physical size separations, which are described in this chapter. Because the $\delta^{18}O$ value of halloysite could be affected during chemical dissolution treatments, we also tested its resistance to isotopic exchange during chemical treatments.

5.1. Methods.

Air-dried samples were processed from soil at Sites B, E, and a soil developed on the Pololu lava flow. For soil from Site J, irreversible dehydration of non-crystalline material produces coatings that are resistant to chemical treatments (Shoji et al., 1993) and thus, field moist samples were processed. The first step in the treatment of all samples is the removal of organic matter by oxidation with 30% H_2O_2 (Jackson, 1979). Non-crystalline (amorphous) iron and aluminum components are removed next using an acid ammonium oxalate (AAO) solution (Sheldrick, 1984; McKeague and Day, 1966) and crystalline iron oxides such as hematite and goethite are removed using a sodium citrate-bicarbonate-dithionite (CBD) extraction (Jackson, 1979). Each sample was treated alternately with the AAO and CBD treatments until there was enough clean clay material (white colored material) for physical

size separation (about 2 to 3 grams). Every sample required at least two repetitions of each treatment, while some required more. A detailed record of treatment by sample is located in Appendix C.

After the chemical treatments, the < 5 μm fraction was isolated by gravitational settling (Black, 1965). Minerals were identified by x-ray diffraction. For all samples, the diffraction pattern was dominated by the peaks of feldspar, magnetite, and mica. The < 2 μm fraction was then isolated by centrifugation (Jackson, 1979). The diffraction patterns of that fraction of many samples indicated the presence of halloysite, mica and gibbsite. Further size separations were required to concentrate halloysite in these samples.

These size separations were guided by measurements of the particle size distribution of the < 2 μm fraction done using a Nicomp Model 370 Submicron Particle Sizer. A typical record of the particle size distribution is shown in Figure 5.1. Many samples exhibited polymodal size distributions. Additional separations were made to isolate individual particle size modes for x-ray diffractometry. Table 5.1 summarizes the average size of each mode, the upper and lower size limits of the separated fraction, and the mineralogy of each fraction. When halloysite was the only mineral identified in a size fraction, it was prepared for isotopic analysis. Fractions that contained more than one mineral identifiable by x-ray diffraction were not used further.

Each halloysite separate was cleaned of soluble ions by dialysis. This treatment minimizes the possibility of contamination by hydrated species that might affect the stable isotopic analysis. The suspension of halloysite were

dialyzed for a minimum of three days. After dialysis, the samples were dried in air at 50°C.

Oxygen is liberated from halloysite, for isotopic analysis, using bromine pentafluoride as described by Clayton and Mayeda (1963) and subsequently converted to CO_2. Isotopic analyses of CO_2 were made by conventional isotope ration mass spectrometry. The reproducibility of the $\delta^{18}O$ values for kaolinite clays on the extraction line at Case Western Reserve University is ±0.2‰ (2 σ). All results are reported using δ-notation in permil (‰) relative to SMOW (Standard Mean Ocean Water). Values are related to SMOW by repeated analyses of National Bureau of Standards (now National Institute of Standards and Technology) isotopic reference material NBS 28 for which we assume a $\delta^{18}O$ value of +9.64‰ SMOW.

5.2. Preservation of $\delta^{18}O$ values of halloysite during chemical treatments.

The chemical treatments used to clean halloysite dissolves other minerals. It is possible that the $\delta^{18}O$ values of clays are affected by these treatments as well. Tests of these treatments have not shown any detectable isotopic exchange with kaolinite (Yeh, 1980; McMurtry et al., 1983). We tested the effects of these treatments on halloysite which, because of its expandable, hydrated nature, might be more susceptible than kaolinite to exchange.

A sample of halloysite with an average size of 0.5 μm was separated as previously described and then treated with solutions made from normal lab distilled water ($\delta^{18}O$= -10‰) and isotopically labelled water ($\delta^{18}O$= +300‰). A

subsample of this material was removed for isotopic analysis and the remainder of the material was split into two aliquots. One aliquot was subjected to a sequential series of AAO and CBD treatments (Figure 5.2) with solutions made using water with a $\delta^{18}O$ value of about -10‰. The other aliquot was subjected to two sequential sets of H_2O_2, AAO and CBD treatments (Figure 5.2) with solutions made using water with a $\delta^{18}O$ value of about +300‰ (made by mixing 2 g of pure $H_2{}^{18}O$ and 2500 ml of distilled water). After each treatment, a subsample of halloysite was removed for isotopic analysis.

Figure 5.2 shows the $\delta^{18}O$ values of the subsample of halloysite at each stage of this test. The initial value of halloysite was +20.7‰. After the treatments with -10‰ solutions, the $\delta^{18}O$ values were within analytical error of the initial value. After the first set of treatments with +300‰ solutions, the $\delta^{18}O$ value of halloysite increased by 2.7‰. A second set of treatments with the same solution caused the $\delta^{18}O$ value of halloysite to increase by an additional 0.6‰.

These tests indicate that the chemical treatements cause only a small amount of isotopic exchange of halloysite. The total amount of exchange can be calculated to be about 1% of the total oxygen in the clay:

$$\%exchanged \approx \left(\frac{\delta_{final} - \delta_{initial}}{\delta_{water} - \delta_{initial}} \right) \times 100$$

where δ_{final} and $\delta_{initial}$ refer to the final and initial clay $\delta^{18}O$ values and δ_{water} refers to the $\delta^{18}O$ value of the water. The calculation is approximate because the fractionation between halloysite and the solutions was neglected.

We can estimate the thickness of the zone of exchange from these results. In one endmember geometry, a sphere with a diameter of 0.5 μm, the volume 6.54×10^{-2} μm^3 and the surface area is 7.85×10^{-1} μm^2. If a shell equivalent to 1% of the sphere exchanges, then that shell would be 6.54×10^{-4} $\mu m^3/7.85 \times 10^{-1}$ μm^2 or 8.3 Å. This is equivalent to exchange of about one unit cell on the surface of a spherical grain with a diameter of 0.5 μm. In the other endmember geometry, we assume a disk-shaped grain with a diameter of 0.5 μm and a thickness of one unit cell, 7Å = 7×10^{-4} μm. The volume of this disk is $\pi r^2 h$ or 1.37×10^{-4} μm^3 and the surface area is $2\pi r^2 + \pi rh$ or 3.93×10^{-1} μm^2. One percent of the volume of this disk corresponds to a thickness of 1.37×10^{-6} $\mu m^3/3.93 \times 10^{-1}$ μm^2 or 0.035 Å. This is equivalent to a very small part of a unit cell.

In nature, halloysite grains have a variety of shapes between these two extremes. At most, only one unit cell of halloysite has exchanged during the chemical purification treatments and a more realistic particle geometry would imply that exchange must be occurring primarily at the edges and corners of the crystal lattice where there are incomplete or broken bonds. We conclude that the chemical purification of halloysite using solutions made with laboratory distilled water does not measurably affect its isotopic composition.

5.3. References.

Black, C.A. (ed.), 1965. Methods of soil analysis, Part 1. Agronomy, 9, pp. 770.

Clayton, R.N., and Mayeda, T.K., 1963. The use of bromine pentafluoride in the extraction of oxygen from oxides and silicates for isotopic analysis. Geochimica et Cosmochimica Acta, 27: 43-52.

Jackson, M.L., 1979. Soil Chemical Analysis- Advanced course. 2nd edition, 11th printing. Published by the author, Madison, WI. 53705.

McKeague, J.A., and Day, J.H., 1966. Dithionite- and oxalate-extractable Fe and Al as aids in differentiating various classes of soils. Canadian Journal of Soil Science, 46: 13-22.

McMurtry, G.M., Wang, C.H., and Yeh, H.W., 1983. Chemical and isotopic investigation into the origin of clay minerals from the Galapagos hydrothermal mounds field. Geochimica et Cosmochimica Acta, 47: 475-489.

Sheldrick, B.H., 1984. Acid Ammonium Oxalate extractable Fe and Al. In: B.H. Sheldrick (editor), Analytical methods manual. Land Resource Research Institute contribution No. 84-30.

Shoji, S., Nanzyo, M., and Dahlgren, R., 1993. Volcanic ash soils: genesis, properties and utilization. Developments in Sóil Science, 21. Elsevier, pp. 288.

Yeh, H.W., 1980. D/H/ ratios and late-stage dehydration of shales during burial. Geochimica et Cosmochimica Acta, 44: 341-352.

Table 5.1 Particle size modes and x-ray mineralogy.

Site	Depth (cm)	Size (μ) mode 1	XRD mode 1	Size (μ) mode 2	XRD mode 2	Size (μ) mode 3	Size cut (μ)
B	0-10	0.6	H, M, G(tr)	0.1	H		0.25
	10-37	0.5	H, M, G	0.5	H		0.25
	37-65	< 2	H				2
	65-100	0.4	H	0.09	H		0.25
E	0-13	0.4	H, M	0.1	H		0.25
	13-30	0.4	H, M	0.1	H		0.25
	30-44	1.6	H, M	0.3	H	0.03	0.5
	44-62	< 2	H				2
	62-85	< 2	H				2
J	0-5	1.3	M, H*	0.25	n.d.*		0.5
	5-10	0.95		0.2			0.5
	10-15	1.1	M, H	0.2	H(?)		0.5
	15-20	0.7	M, H	0.1	M, H		0.25
	20-30	1.8	M, H	0.3	M, H	0.2	0.5
	30-40	0.4	M, H	0.1	n.d.		0.25
	40-50	< 2	H				2
	50-70	< 2	H				2
Pololu	5-26	0.5	H, G, M(tr)	0.1	H		0.25
	26-43	1.2	G,H,M	0.25	G, H(tr)		0.5
	43-60	1.1	G, H, M(tr)	0.2	G, H	0.02	0.5
	60-96	1.7	G, H, M(tr)	0.3	G, H	0.04	0.5
	90-102	1.8	H, G(tr)	0.4	H	0.03	
	102-115	1.1	H, G(tr)	0.2	H		0.65

H- halloysite, G- gibbsite, M- mica, tr- trace, n.d. not detectable, ?- questionable
Minerals are listed in order of abundance.
* Samples 0-5 and 5-10 were mixed because individual samples were too small for analyses.

JH-3-3 < 2 microns

VOLUME-Weighted NICOMP DISTRIBUTION Analysis (Solid Particles)

NICOMP SUMMARY:
Peak Number 1: Mean Diameter = 70.1 nm Volume: 16.72 %
Peak Number 2: Mean Diameter = 521.2 nm Volume: 83.28 %

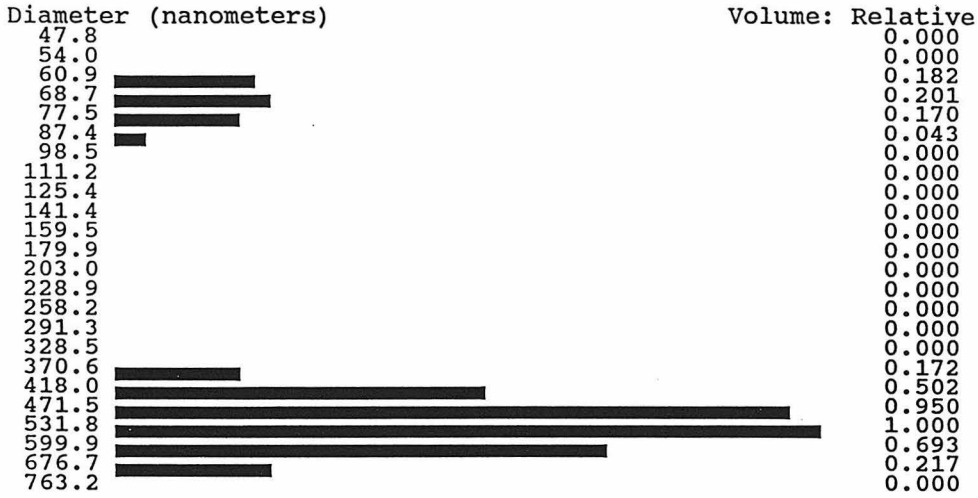

Mean Diameter = 449.9 nm Fit Error = 2.466 Residual = 33.033

NICOMP SCALE PARAMETERS:
Min. Diam. = 10.0 nm Plot Size = 45
Smoothing = 3 Plot Range = 200

Run Time = 0 Hr 22 Min 14 Sec
Count Rate = 210 Khz Temperature = 23 deg C
Channel #1 = 1574.4 K Viscosity = 0.933 cp
Channel Width = 75.0 uSec Index of Ref. = 1.333

GAUSSIAN SUMMARY:
Mean Diameter = 721.4 nm Chi Squared = 2.141
Stnd. Deviation = 389.0 nm (53.9 %) Baseline Adj. = 0.000 %
Coeff. of Var'n = 0.539 Mean Diff. Coeff. = 6.44E-09 cm2/s

Figure 5.1. An example of the result from a Nicomp Particle Size analyzer for sample 3-3 (Site B, 37-65 cm). There is a bimodal distribution. To isolate the modes, a size separation at 0.25 μm was chosen.

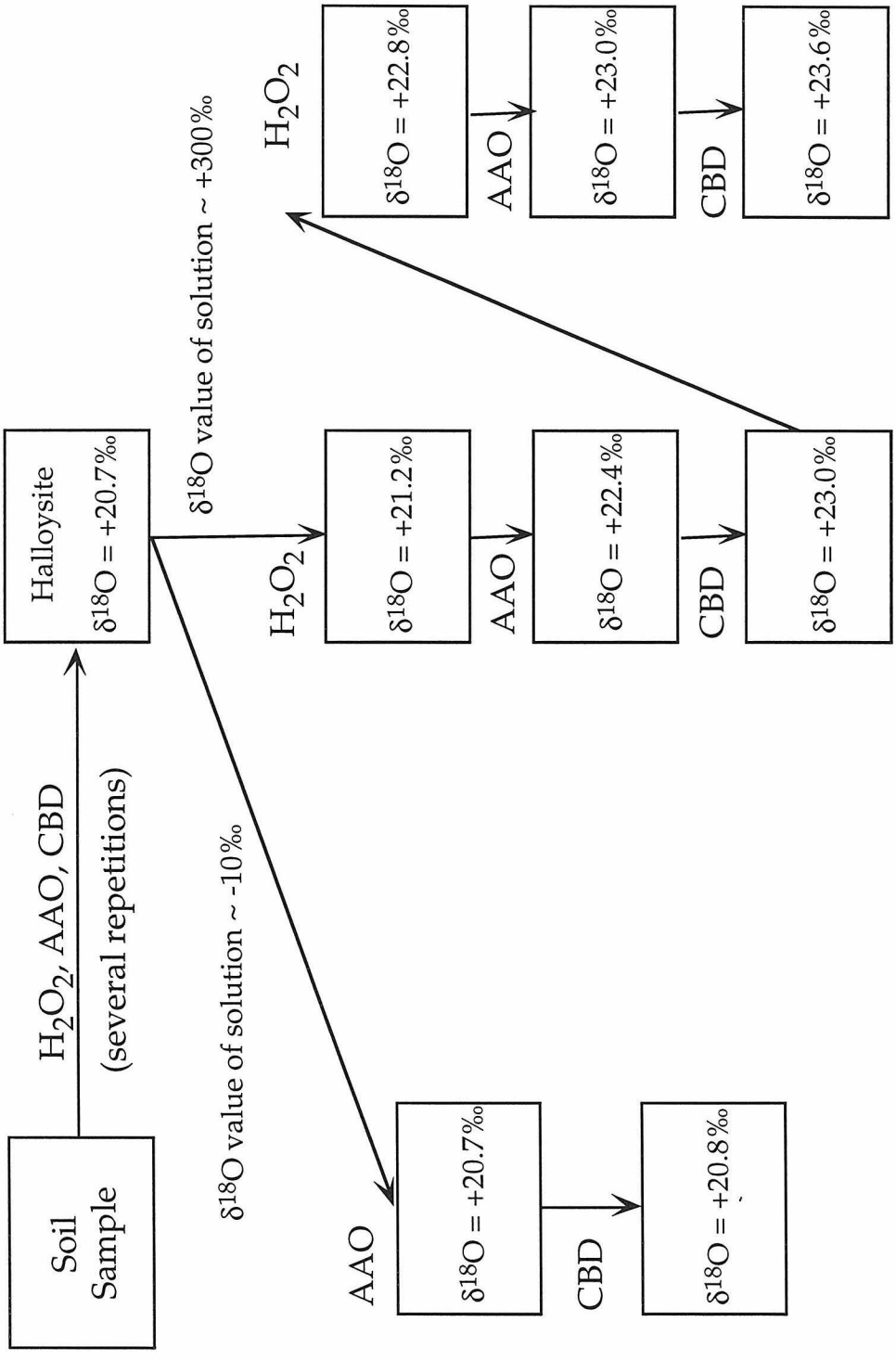

Figure 5.2. A schematic flow chart of the tests performed to check for exchange of oxygen in halloysite during chemical treatments. The $\delta^{18}O$ value of halloysite at each stage of the test is shown in the box.

Chapter 6. The Oxygen Isotope Geochemistry of Pedogenic Halloysite in Kohala Soils.

The $^{18}O/^{16}O$ ratios of pedogenic clays have the potential to provide information about the climate during the time of their formation. In Chapter 3, we examined the $\delta^{18}O$ values of soil waters and their variation over the course of a year along a transect where climate is the dominant variable. In this chapter, we examine the $\delta^{18}O$ values of halloysite separated from soils along the same transect. These soils are old enough to have formed crystalline clays, but young enough to minimize the number of climatic changes that influenced their formation. We relate the $\delta^{18}O$ values of clays to those of the soil waters and of the climates. We know of only one other study (Giral et al., in prep.) in which the isotopic compositions of pedogenic clays have been related to those of soil waters in the same profile.

6.1. Results from Kohala.

Four soil profiles were sampled for isotopic analysis of halloysite. Three of the profiles, at Site B, E, and J, are developed on 0.17 Ma Hawi lava flows (Figure 3.1). The fourth profile is in the same rainfall zone as Site B, but is developed on a 0.35 Ma Pololu lava flow. The $\delta^{18}O$ value of a sample of pedogenic carbonate from 60 cm depth at Site B was also measured by reaction with 100% phosphoric acid as described by Wang et al. (1993). The isotopic results are listed in Table 6.1 and are plotted as a function of depth at each site

in Figure 6.1. Time-weighted annual average soil-water $\delta^{18}O$ values (closed circles) as well as individual measured $\delta^{18}O$ values (small crosses) from Chapter 3 are plotted as a function of depth in Figure 6.2 for comparison with halloysite and carbonate $\delta^{18}O$ values.

At Site B, the $\delta^{18}O$ values of halloysite decrease by 3‰ (Table 6.1) from the surface horizon to the bottom of the soil (Figure 6.1a). The average $\delta^{18}O$ values of soil water at this site parallel the trend of the halloysite, decreasing by a corresponding amount, from about +2.5‰ at the surface to -0.5‰ at 70 cm depth (Figure 6.2a). The $\delta^{18}O$ value of the pedogenic carbonate at 60 cm depth is +27.7‰.

At Site E, the $\delta^{18}O$ values of halloysite lie between 21.6‰ to 22.1‰ (Table 6.1) and do not vary systematically with depth (Figure 6.1c); a pattern which is not parallel to the trend observed for the isotopic compositions of soil water at that site. The average $\delta^{18}O$ values of soil water decrease by 4 ‰ from +1‰ at the surface to about -3‰ at 85 cm depth (Figure 6.2b).

At Site J, the $\delta^{18}O$ values of halloysite from only two levels were measured because of difficulties in obtaining high quality mineral separates. The values, 18.7‰ and 18.0‰, are approximately equal and are lower than those Sites B and E (Table 6.1, Figure 6.1d). The pattern with depth parallels the trend of soil-water $\delta^{18}O$ values in the sense that, below about 40 cm, $\delta^{18}O$ values of halloysite and soil water do not vary systematically with depth. The average soil-water $\delta^{18}O$ values range between -2‰ at the surface to about -4 ‰ at 100 cm depth (Figure 6.2c).

For the Pololu soil, the $\delta^{18}O$ value of halloysite decreases by about 2 ‰ from the surface to the bottom of the soil (Table 6.1, Figure 6.1b). These halloysite $\delta^{18}O$ values are nearly indistinguishable from those at Site B. The soil-water $\delta^{18}O$ values in this profile were not measured. However, the average soil-water $\delta^{18}O$ values from Site B (Figure 6.2a) serve as a reasonable approximation because they are located in the same rainfall/temperature zone. The shape of the halloysite $\delta^{18}O$ profile generally parallels the shape of the soil-water $\delta^{18}O$ values.

For each sample, the $\delta^{18}O$ value of halloysite is related to the $\delta^{18}O$ value of soil water at the same depth interval. The results are plotted on a graph of soil-water $\delta^{18}O$ vs halloysite $\delta^{18}O$ (Figure 6.3). All the points, except for the data from the lower horizons at Site E, form a linear array. The trend of this array is roughly parallel to the trend of the kaolinite-water relationship of Savin and Lee (1988). The relationship of Savin and Lee is roughly parallel to that of Sheppard and Gilg (1996) on this graph; for the sake of clarity, only the Savin and Lee isotherms were plotted. The data lie between the 50°C and 60°C isotherms of this fractionation relationship.

The values for Δ, calculated from the soil-water and halloysite $\delta^{18}O$ values, (Table 6.2) are plotted against $1/T^2$ (Figure 6.4). All the data fall below the kaolinite-water fractionation factor curves of Savin and Lee (1988) and Sheppard and Gilg (1996). The values calculated for all except the surface horizon at Site E lie closer to the curves while the rest lie along a horizontal trend below them.

6.2. Interpretation.

The $\delta^{18}O$ vs depth profiles of soil waters (Chapter 3) were indicative of evaporation of ^{18}O-depleted water from the soil surface. While profiles of individual sampling were more variable, reflecting infiltration of rain from isotopically distinct storms, average annual profiles consistently showed decreasing soil-water $\delta^{18}O$ values with depth until about 40 cm where the values were relatively constant. The halloysite $\delta^{18}O$ curves for all soils are also relatively constant below about 40 cm (Figure 6.5). At Sites B and Pololu, the parallelism between the two curves is especially noticeable, even though the sampling interval is smaller for the soil-water $\delta^{18}O$ curve than for the halloysite $\delta^{18}O$ curve (Figure 6.5a). This resemblance is clearly absent at Site E and we cannot evaluate the shape of the curve from the two halloysite $\delta^{18}O$ measurements at Site J.

As noted in Chapter 3, the average $\delta^{18}O$ values of soil water and precipitation decrease with increasing amount of rainfall (see Figures 3.9 and 6.2). A similar relationship exists between halloysite $\delta^{18}O$ values and median annual rainfall at the sites (Figure 6.1). The halloysite $\delta^{18}O$ values at the low rainfall sites (B, Pololu, and E) are between 1.7‰ to 5.6‰ more positive (Table 6.1) than at Site J, which is located in a highér annual rainfall zone. The $\delta^{18}O$ values of halloysite among the lower rainfall sites all fall within 3.2‰ of one another, but the values below 30 cm at Site E are up to 1.5‰ more positive than the values below 30 cm at Sites B and Pololu.

The relationships between halloysite and soil-water $\delta^{18}O$ values in Figure 6.3 suggests that halloysite formed in oxygen isotopic equilibrium with soil water (although not necessarily modern soil water). However, the data in Figure 6.3 other than those from Site E are bound by 50°C and 60°C isotherms, temperatures unreasonable for a weathering profile. The fractionation between soil water and halloysite for our data is much smaller than estimates given by the kaolinite-water fractionation curves of Savin and Lee (1988) or Sheppard and Gilg (1996) (Figure 6.4). The fractionations between soil water and halloysite at Site E, however, are nearly the same as the estimated fractionations. At Site E, the $\delta^{18}O$ values of halloysite do not vary systematically with depth, can be more positive than at Site B, and the fractionations between soil water and halloysite are larger than those at other sites. Explanations for these anomalies include the possibility that Site E is located in a zone in which climatic regimes have fluctuated over a long time, resulting in a soil that has been affected by a range of climatic conditions. It is also possible that the profile at Site E initially resembled that at Site B, but that the top part of the soil profile was subsequently eroded, leaving only the section with a relatively invariant halloysite $\delta^{18}O$-depth curve. Another possibility is that the orignal halloysite $\delta^{18}O$ values of the lower horizons have been altered. For this soil profile, samples were collected from a road cut that has been exposed for approximately 10 years. Dehydration and movement of mineral bound water from the non-crystalline material could have influenced the $\delta^{18}O$ value of halloysite. In any case, soil-water curves

would be unaffected because evaporation is controlled by the current climate and the soil-water $\delta^{18}O$ values are measured on the liquid water component of soil water. Further investigation of these samples is underway, and for the remainder of the discussion, these results will not be considered.

6.3. Reliability of fractionation factors.

The measured isotopic fractionation between the pedogenic carbonate samples and soil water is only 0.6‰ more negative than the fractionation calculated from the fractionation factor between calcite and water (Tarutani et al., 1969). This behaviour lends support to the use of the isotopic composition of pedogenic carbonate as a climatic indicator.

The measured isotopic fractionation between halloysite and soil water is smaller than those estimated for equilibrium fractionations for kaolinite and water (Figure 6.4). No halloysite–water fractionation factor has been established. By analogy with other polymorphic systems, it is likely that the difference between kaolinite–water and halloysite–water fractionations is small. For example, the difference between the calcite–water and aragonite–water fractionations is only about 0.1‰ at 25°C (Friedman and O'Neil, 1977). Sheppard and Gilg (1996) suggest that the halloysite–water fractionation is slightly smaller than the kaolinite–water fractionation and a study of coexisting halloysite and kaolinite from hydrothermal deposits in Japan (F.J. Longstaffe, personal communication) suggests that halloysite is depleted in ^{18}O by about a 1‰ relative to kaolinite. The difference between the

fractionation calculated from our results and the equilibrium fractionations is between 4‰ and 5‰. The substitution of a kaolinite–water fractionation factor for halloysite–water only accounts for about 1‰ of the difference.

The problems that arise from straightforward interpretations of our data using published fractionation factors for kaolinite-water imply that either the climatic conditions were different when our halloysite formed or that the kaolinite–water equilibrium fractionation factor differs markedly from that for halloysite–water. With the data available from this study, we cannot differentiate between the two possibilities. Below, we discuss the implications if one or the other is true.

If we assume that the kaolinite–water fractionation factor is appropriate to use for halloysite–water systems, then the results suggest that either the formation temperature of the halloysite was unrealistically high, 50°C to 60°C, or that soil-water $\delta^{18}O$ values were more negative in the past when halloysite formed. If we assume that soil temperatures have always remained between 20°C and 30°C at these sites, then the $\delta^{18}O$ value of soil water must have been 4 to 5‰ more negative when the halloysite formed than today. Larger rainstorms or lower evaporative demand regimes are possible ways to have more negative soil-water $\delta^{18}O$ values (see Chapter 3). At least 1.5 complete glacial/interglacial cycles have occurred since the lava beneath the soils was erupted (Porter, 1979). Glacial storm tracks could have been very different from today, bringing much more rain to Kohala. Evidence from other soils (Gavenda, 1992), glacial deposits on Mauna Kea

(Porter, 1979), and pollen from bogs on Kohala (Hotchkiss, 1996a, b) suggests that climate during the glacial periods was cooler and drier. Broecker (1996) also suggests that glacial climate in the tropics could have been up to 5°C cooler than in the interglacials and thus, there is less evaporation, and consequently less subsequent precipitation. However, from the available information, we cannot assess the stability of climate on Kohala over the past 0.35 Ma.

If we assume that the $\delta^{18}O$ value of soil water has not changed over the last 0.35 Ma, that implies that the kaolinite–water fractionation factor is inappropriate to use in dealing with the halloysite–water system. As discussed in Chapter 4, it is also possible that the kaolinite–water fractionation factor itself is in error because it is based heavily on the $\delta^{18}O$ values of pedogenic kaolinites and the $\delta^{18}O$ values of precipitation at locations where the kaolinite formed. As seen in Chapter 3, the $\delta^{18}O$ value of precipitation may differ by as much as a few permil from that of soil water at these same locations. While we are confident that the Savin and Lee and Sheppard and Gilg kaolinite–water fractionation factors are not grossly inaccurate, we are unable to assess their accuracy quantitatively.

6.4. Comparison with other studies.

Some similarities exist between the results of this study and previous studies. Lawrence and Taylor (1971, 1972) found no significant variation in the $\delta^{18}O$ values of kaolinite with depth in soil profiles from North America

and Bird and Chivas (1988, 1989) and Bird et al. (1993) found similar results for profiles from Australia and Brazil. Giral et al. (in prep.), however, collected samples at a finer resolution and found significant variations in both soil-water and kaolinite $\delta^{18}O$ values. The soil-water and halloysite $\delta^{18}O$ depth profiles from Hawaii also suggest that a significant difference exists between the surface horizons and those at depth. The coarser sampling interval used in previous studies may have been responsible for the lack of variations observed.

Several studies indicate that each mineral or mineral population within the same soil may be formed under a different set of conditions and that these conditions may be determined by seasonal changes or longer term changes in climate. Stern et al. (1995, 1996) found that the smectite–calcite fractionation, 6.4‰, was larger than equilibrium fractionations, 3.0 to 3.5‰, using smectite–water fractionstion factors of Savin and Lee (1988) and the calcite–water fractionation factor of Tarutani et al. (1969). Because summer monsoonal precipitation has a more negative $\delta^{18}O$ value than winter precipitation, they interpreted this as indicating that each mineral formed during a different season. Giral (1994), Giral et al. (in prep.) found that two different size populations of kaolinite were formed from precipitation of difference sources. In this case, winter precipitation has a more negative $\delta^{18}O$ value than summer precipitation. For Hawaii, the fractionation between calcite and halloysite from the same horizon is 7‰, larger than equilibrium kaolinite–calcite fractionation of about 4.5‰ based on the kaolinite–water

fractionation of Savin and Lee (1988) and the calcite–water fractionation of Tarutani et al. (1969). These minerals probably formed from water of markedly different isotopic compositions. Seasonal differences in the $\delta^{18}O$ value of precipitation in Hawaii are not great enough to account for the calcite and halloysite results. Rather, differences in seasonal evaporation produce the large effects on the $\delta^{18}O$ value of water (Chapter 3).

In a follow-up to the study of a lateritic profile by Giral (1994), Giral et al. (in prep.) found a correlation between the degree of crystallinity and the $\delta^{18}O$ value of kaolinite. Coarser-grained kaolinites generally had a higher crystallinity, as determined by the Hinckley index, and more negative $\delta^{18}O$ values than the finer fractions. In our study, the average grain size of samples from Site J is larger than that of samples from Site B or E (< 2 μm vs < 0.25 μm) (Table 6.1). The Hinckley Index, which is an indicator of crystallinity of kaolinite is not normally measured for halloysite because the inherent structure is not known. However, qualitatively the x-ray diffraction peaks of the samples from Site J are generally larger and sharper than the ones from Site B or E (See Appendix C) and the $\delta^{18}O$ values are also more negative. The soil at Site J remains moist throughout the year, while Sites B and E are dry most of the year. Thus, continuous mineral growth at Site J could have resulted in the formation of larger grains. The $\delta^{18}O$ values of halloysites from Site J are probably more negative than those at Site B or E because the $\delta^{18}O$ value of soil water is also more negative at Site J.

6.5. Conclusions.

A series of samples along a bioclimatic transect in Hawaii was collected for analysis of the $\delta^{18}O$ value of halloysite, and the $\delta^{18}O$ values were compared with the soil water $\delta^{18}O$ values presented in Chapter 3. Halloysite was isolated from bulk soil material through a series of chemical treatments and then physical size separations. The results were interpreted in terms of uncertainties in the calculation of equilibrium fractionation factors and in the external climate controls on clay mineral synthesis.

The depth profiles of the $\delta^{18}O$ values of halloysite are relatively invariant below about 40 cm, which parallels the soil-water $\delta^{18}O$ results presented in Chapter 3. At Site B and Pòlolu, the halloysite $\delta^{18}O$ values also parallel the gradual decrease with depth of soil-water $\delta^{18}O$ values. These trends are consistent with the formation of halloysite from soil water which is enriched in ^{18}O near the surface as a result of evaporation. The $\delta^{18}O$ values of halloysite at the lower rainfall sites are more positive than the $\delta^{18}O$ values at the high rainfall site, a pattern also found in the soil-water $\delta^{18}O$ values.

The interpretations of the halloysite and water isotopic data imply one of two conclusions. One possibility is that the isotopic behaviour of the halloysite–soil-water system resembles that of the kaolinite–water system, and the other possibility is that the soil-water $\delta^{18}O$ values have not changed over the past 0.35 Ma. If the isotopic behaviour of kaolinite and halloysite are similar, soil-water $\delta^{18}O$ values must have been about 4 to 5‰ more negative

when the halloysite formed than today, implying that climate may have been different. If the isotopic behaviour of halloysite differs significantly from that of kaolinite (or what is generally assumed to be the behaviour of kaolinite) in weathering environments, then halloysite and kaolinite may be sufficiently different to account for the observed isotopic relationships. In addition, the generally accepted kaolinite–water fractionation may be in error, because this curve is based on the isotopic composition of precipitation rather that soil water. At present, these two possibilities are equally valid, and it is even possible that a combination of the two may apply to the halloysite–soil-water system.

6.6. References.

Bird, M.I., and Chivas, A.R., 1988. Stable-isotope evidence for low-temperature kaolinitic weathering and post-formational hydrogen-isotope exchange in Permian kaolinites. Chemical Geology, 72: 249-265.

Bird, M.I., and Chivas, A.R., 1989. Stable isotope geochronology of the Australian regolith. Geochimica et Cosmochimica Acta, 53: 3239-3256.

Bird, M.I., Longstaffe, F.J., Fyfe, W.S., Kronber, B.I., and Kishida, A., 1993. An oxygen-isotope study of weathering in the eastern Amazon Basin, Brazil. In: P.K. Swart, K.C. Lohman, J. McKenzié, and S. Savin (editors), Climate Change in Continental Isotopic Records. A.G.U. Geophysical Monograph 78: 295-307.

Broecker, W., 1996. Glacial Climates in the Tropics. Science, 272: 1902-1904.

Friedman, I. and O'Neil, J.T., 1977. Compilation of stable isotope fractionation factors of geochemical interest. USGS Professional Paper, 440-KK.

Gavenda, R.T., 1992. Hawaiian Quaternary paleoenvironments: A review of geological, pedological, and botanical evidence. Pacific Science, 46: 295-307.

Giral, S., 1994. Variations des rapports isotopiques $^{18}O/^{16}O$ des kaolinites de deux profils latéritiques amazoniens: signification pour la pédologie et la paléoclimatologie. Ph.D. Thesis, Université de Droit, D'Économie et des Sciences d'Aix-Marseille.

Giral, S., Savin, S.M., Nahon, D.B., Girard, J.P., Lucas, Y., and Abel, L.J., in prep. Oxygen isotope geochemistry of kaolinite in laterite-forming processes, Manaus, Amazonas, Brazil.

Hotchkiss, S. C., 1996a. A 29,000-year record of vegetation and fire history from Kohala Mountain, Hawai'i. (Abstract) Bulletin of the Ecological Society of America, 77(3): 203.

Hotchkiss, S.C., 1996b. Last Glacial and Holocene pollen records from Oahu and North Kohala, Hawai'i. (Abstract) IX International Palynological Congress Meeting, Houston, Texas, USA, Juné 23-28, 1996. Abstracts Volume: 68.

Lawrence, J.R., and Taylor, H.P., Jr., 1972. Hydrogen and oxygen isotope systematics in weathering profiles. Geochimica et Cosmochimica Acta, 36: 1377-1393.

Lawrence, J.R., and Taylor, H.P., Jr., 1971. Deuterium and oxygen-18 correlation: Clay minerals and hydroxides in Quaternary soils compared to meteoric waters. Geochimica et Cosmochimica Acta, 35: 993-1003.

Nullet, D., Ikawa, H., and Kilham, P., 1990. Local differences in soil temperature and soil moisture regimes on a mountain slope, Hawaii. Geoderma, 47: 171-184.

Porter, S.C., 1979. Hawaiian glacial ages. Quaternary Research, 12: 161-187.

Savin, S.M., and Lee, M., 1988. Isotopic studies of phyllosilicates. In: S.W. Bailey (editor) Hydrous phyllosilicates (exclusive of micas). Reviews in Mineralogy, v19, pp. 189-219.

Sheppard, S.M.F. and Gilg, H.A., 1996. Stable-isotope geochemistry of clay-minerals. Clay Minerals, 31(1); 1-24.

Stern, L.A., Chamberlin, C.P., and Johnson, G.D., 1995. Record of climate change preserved in oxygen isotope systematics of pedogenic clay minerals in Himalayan molasse. Geological Society of America Abstracts with Programs, 27(6): A-206.

Stern, L.A., Chamberlain, C.P., Reynolds, R.C., and Johnson, G.D., 1996. Oxygen isotope evidence of climate change from pedogenic clay

minerals in the Himalayan Molasse. In press, Geochimica et Cosmochimica Acta.

Tarutani, T., Clayton, R.N., and Mayeda, T.K., 1969. The effect of polymorphism and magnesium substitution of oxygen isotope fractionation between calcium carbonate and water. Geochimica et Cosmochimica Acta, 33: 987-996.

Table 6.1. Mineral $\delta^{18}O$ values and soil temperatures.

	Depth (cm)	Mineral size (μ)	Mineral measured	$\delta^{18}O$ of mineral	Soil T* (°C)
Site B	0-10	< 0.25	halloysite	23.6	29
	10-37	< 0.25	halloysite	22.1	27
	37-65	< 2	halloysite	20.7	25
	65-100	< 0.25	halloysite	20.4	23
	60-62		(Ca,Mg) CO_3	27.7	23
Site E	0-13	< 0.25	halloysite	21.6	26
	13-30	< 0.25	halloysite	22.1	25
	30-44	< 0.5	halloysite	21.8	23
	44-62	< 2	halloysite	21.8	22
	62-85	< 2	halloysite	21.7	21
Site J	40-50	< 2	halloysite	18.0	18
	50-70	< 2	halloysite	18.7	18
Pololu	5-26	< 0.25	halloysite	22.9	28
	90-102	< 0.65	halloysite	21.7	25
	102-115	< 0.65	halloysite	21.0	24

* Temperatures calculated using the regression of Nullet et al. (1990)

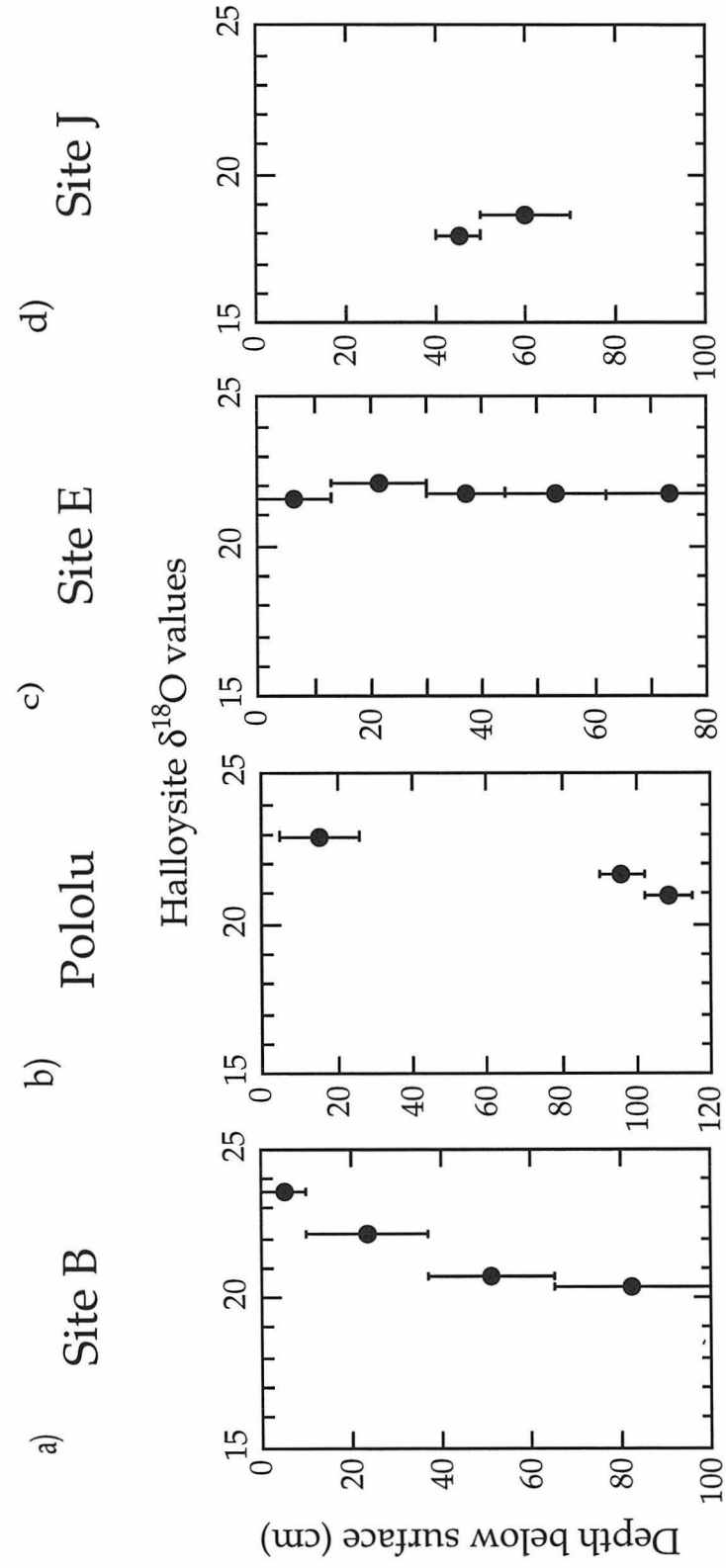

Figure 6.1 Plots of the depth distribution of the $\delta^{18}O$ values of halloysite from a) Site B, b) Site E, c) Site J, and d) the Pololu soil which is in the same rainfall zone as Site B. The bars represent the range of depth over which the bulk sample was collected.

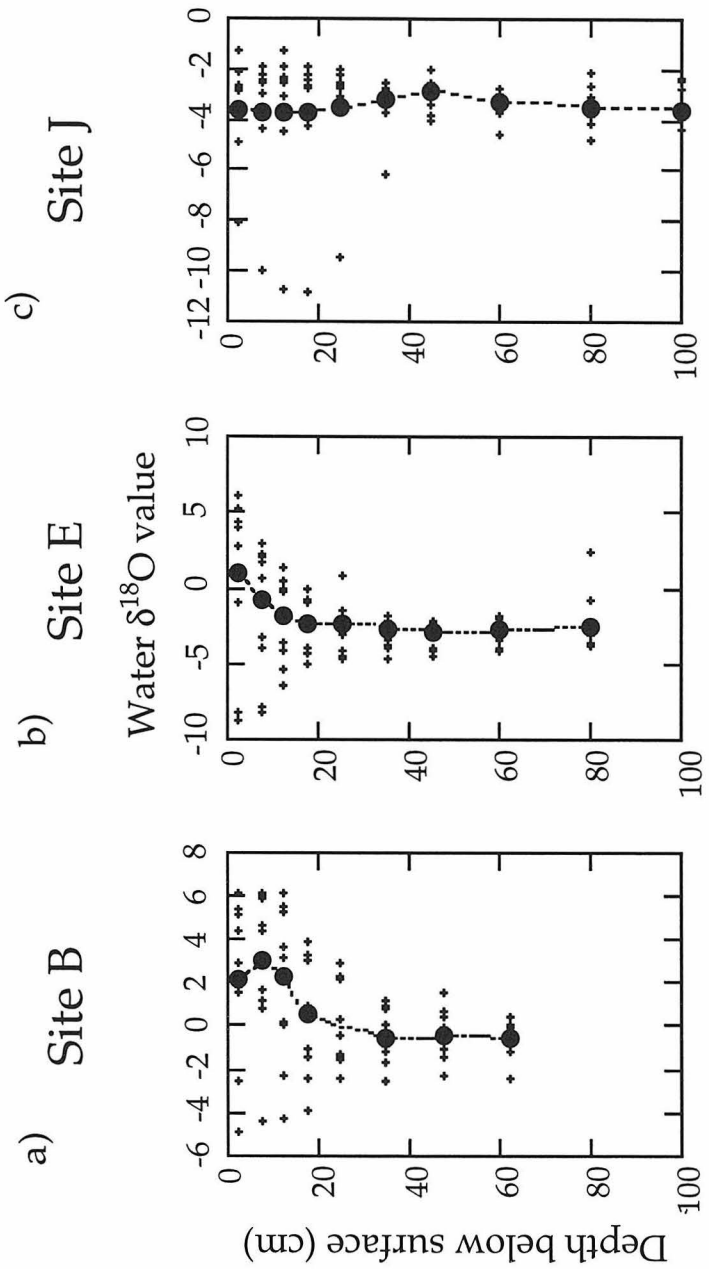

Figure 6.2. Depth profiles for the time-weighted average soil water $\delta^{18}O$ values (shown as closed circles) for a) Site B, b) Site E, and c) Site J. Individual data points are represented by the small crosses (the soil water data were discussed in Chapter 3).

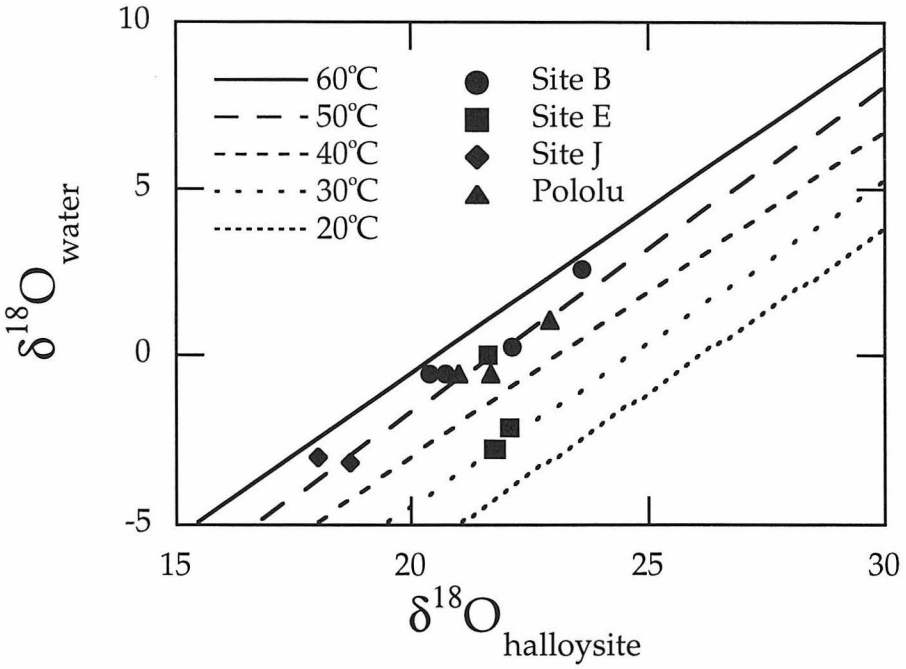

Figure 6.3. A plot of the measured $\delta^{18}O$ value of soil water against the measured $\delta^{18}O$ value of halloysite from Sites B, E, J, and the Pololu soil. Most of the data lie in an array bound by the 50°C and 60°C isotherms calculated from the kaolinite–water fractionation factor equation of Savin and Lee (1988).

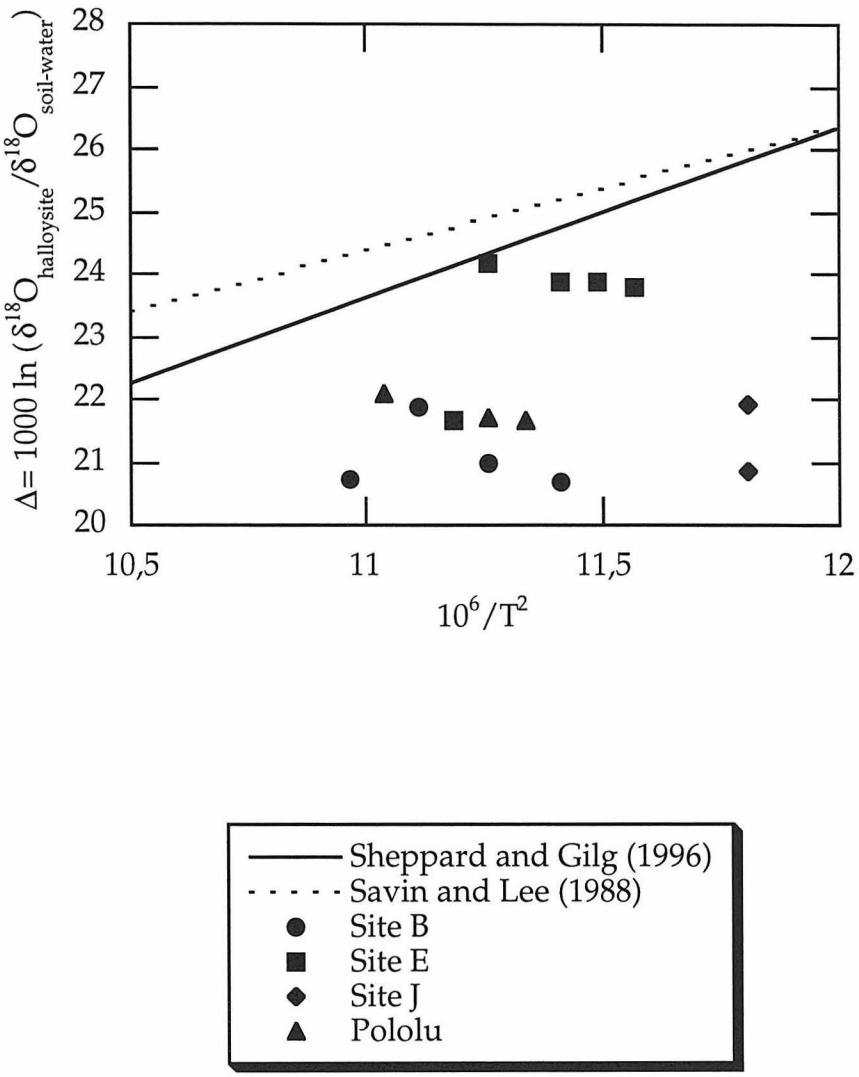

Figure 6.4. A plot of Δ against $1/T^2$ for the data from Hawaiian soils. Also included on the graph are the estimates from Sheppard and Gilg (1996) and Savin and Lee (1988) for the kaolinite-water fractionation factor.

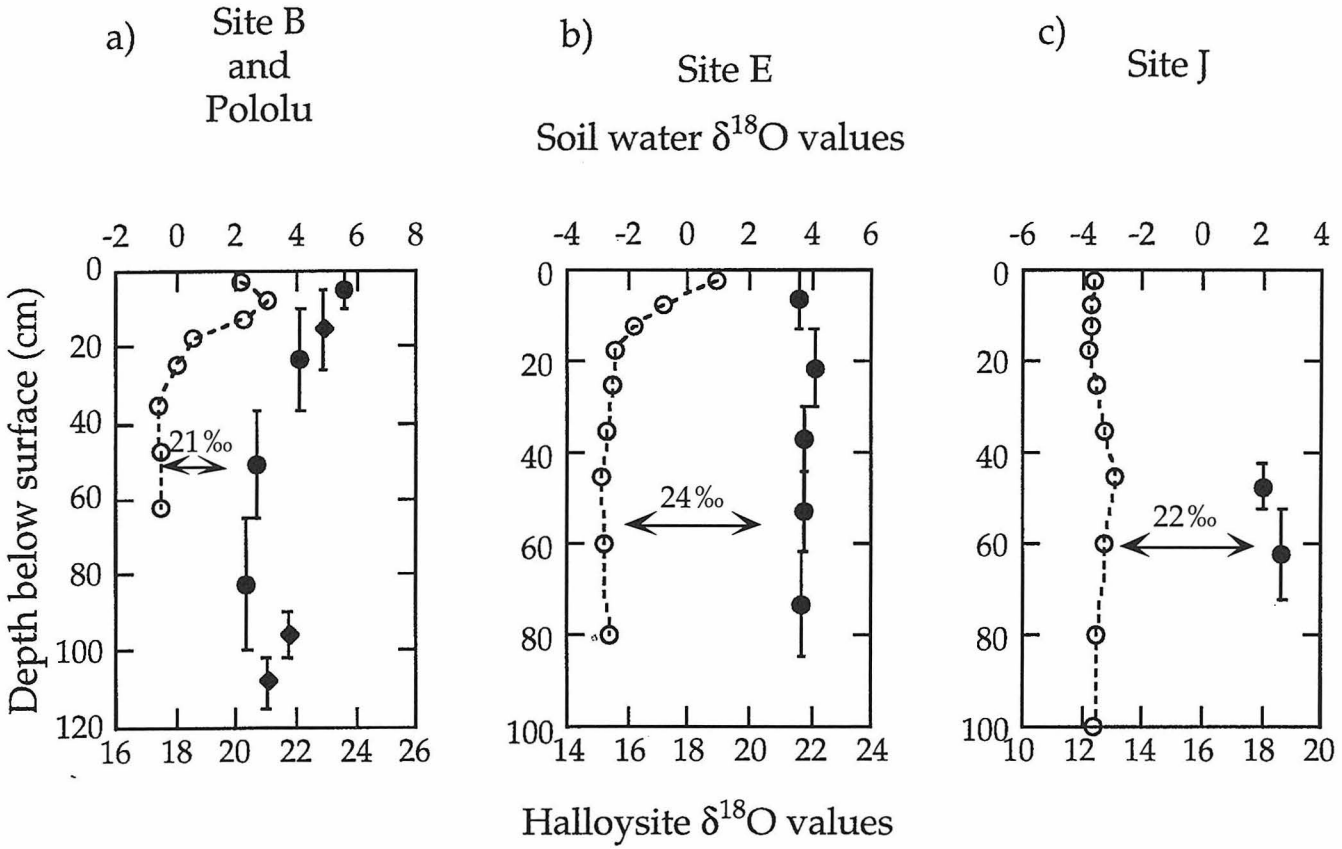

Figure 6.5. Depth profiles of time-weighted average soil-water $\delta^{18}O$ values and halloysite $\delta^{18}O$ values at a) Sites B and Pololu, b) Site E, and c) Site J. Soil water values are plotted as open circles. Halloysite values are plotted as closed points. Circles represent results from Site B, E, and J and diamonds represent results for Pololu. Bars indicate the depths from which the samples were taken for halloysite. The difference between halloysite and soil-water $\delta^{18}O$ values is indicated on the plot.

Chapter 7 Conclusions.

For my thesis research, I have investigated the behaviour of oxygen isotopes in soil water and the variability of soil-water and halloysite $\delta^{18}O$ values in a natural soil system in Hawaii. The results of this thesis project have significant new findings. Each part of the project brought forth conclusions that have implications for other areas of research. The important conclusions will be outlined below and some suggestions for future studies are described.

7.1. CO_2 equilibration method.

This study was the first to specifically test the use of an equilibration method on soil material and the effect of biological respiration, water content, and soil type on equilibration. There are three main conclusions from this study: 1) This method is viable for measurements of soil-water $\delta^{18}O$ values; 2) Biological activity can influence the equilibration process; and 3) The $\delta^{18}O$ value of soil water changes as function of soil type and water content. Each will be discussed separately below.

The reproducibility of measurements of the $\delta^{18}O$value of soil H_2O ranged from 0.3‰ to 0.4‰, approximately the same as for azeotropic and vacuum distillation methods. Thus, the reproducibility of analyses by the direct equilibration method is just as good as existing methods for measurement of the $\delta^{18}O$ value of soil water. The former, however, has the

advantage of requiring only one step and not requiring the use of carcinogenic substances such as toluene (for azeotropic distillation).

The $\delta^{18}O$ values of soil water measured on sets of sterilized and non-sterilized samples differed by 0.3‰ to 1.2‰. In another test, the $\delta^{13}C$ and $\delta^{18}O$ values of CO_2 changed by 5‰ and 1‰ respectively when a sample of soil was allowed to equilibrate for over 5 months. These results suggest degradation of organic material has influenced the isotopic composition of CO_2 as it equilibrated with the soil sample. Radiation treatment is recommended for soil samples regardless of the method by which the $\delta^{18}O$ value is analyzed, and our results show that radiation is crucial in applying the equilibration method.

CO_2 equilibration of samples prepared by adding water with a known isotopic composition to dry soil exhibited a $\delta^{18}O$ value of soil water which varied as a function of the amount of water added. Furthermore, the measured soil-water $\delta^{18}O$ values were not the same as the $\delta^{18}O$ value of the added water except at high water contents (~30% or more by weight). These results suggest that water in soils can be partitioned into different "compartments" or "pools" such as bulk liquid water and chemically adsorbed water of various types, each of which likely have different thermodynamic properties. Each "compartment"' thus would have a different isotopic composition, even at equilibrium, and changing the proportions of the different "compartments" of water can change the measured $\delta^{18}O$ value. When liquid water dominates by mass (i.e., wet soils),

the $\delta^{18}O$ value of soil water is the same as the $\delta^{18}O$ value of the water that was added.

If the "compartments" of soil water are in isotopic equilibrium and have different isotopic compositions, then there are important implications for other studies. For instance, hydrological studies that use the $\delta^{18}O$ value of water in soils to trace water movement would need to determine which "compartments" of water are being measured, and how fast isotopic equilibrium is attained. If the residence time of water in different "compartments" is variable, then the relative amounts of water in each "compartment" and the degree of mixing between "compartments" become important when determining pathways of water flow.

Another example of the implication of soil-water "compartments" is the comparison of mineral $\delta^{18}O$ values to soil-water $\delta^{18}O$ values. From the limited amount of data in this study, we have determined that $\delta^{18}O$ measurements of an operationally defined liquid component of water are possible. This $\delta^{18}O$ value may be more appropriate for comparisons with mineral $\delta^{18}O$ values through the use of mineral–liquid water isotopic fractionation factors.

7.2. Additional studies of the equilibration method.

These conclusions point to the need to determine the nature of the different "compartments" and the degree of isotopic fractionation between the "compartments". Several questions that can be asked include: Are there

discrete "compartments" of water or is there a gradational boundary between them? Is it possible to define these pools using measurable parameters? Is it possible to determine the isotopic fractionations between these "pools" and if so, what are they? Is there isotopic exchange between the "pools" of water after the addition of new water to the system? At what timescale does that occur?

One of the studies that could answer some of these questions is a well controlled comparison of the direct equilibration method with other methods. Samples have already been collected from two sandy soils for measurement of the $\delta^{18}O$ value of soil water using: 1) the direct equilibration method; 2) the azeotropic distillation method in conjunction with Claudia Mora at the University of Tennessee; and 3) the vacuum distillation method in conjunction with Hope Jahren at Georgia Tech. Differences in the measured $\delta^{18}O$ values should determine whether different forms of water are being removed and/or measured for each method.

An additional study which has been discussed with Claudia Mora is to look at the relationship between the $\delta^{18}O$ value of water and the matric potential at which it was removed. Possible results include a smoothly varying relationship between water $\delta^{18}O$ values and the matric potential under which the water was removed. This could indicate that the influence of mineral surfaces on water molecules extends to great distances. A relationship with distinct breaks would define "compartments" in terms of absolute values of matric potential.

Equilibration experiments with CO_2 could be used to determine rates of isotopic exchange and reveal more about the ease of isotopic exchange between "compartments" of water after the addition of new water to the system. If all "compartments" are in isotopic equilibrium with one another, we could determine the timescale for re-equilibration. If they exchange slowly, then the residence time for some "compartments" may be very long and fossil water could be preserved and possibly measured.

7.3. Soil-water monitoring study.

The soil-water monitoring study reported here is the first documentation of the $\delta^{18}O$ value of soil water along an arid-to-humid transect through two seasonal cycles. It was also an opportunity to apply the CO_2 equilibration method for measuring actual soil-water $\delta^{18}O$ values. There are three main conclusions from this part of the study: 1) There are variations with depth that reflect evaporation of water from the soil profile as well as infiltration of water into the soil profile; 2) There is a trend along the arid-to-humid transect that reflects the influence of macroenvironmental parameters; and 3) There is a measurable difference between the $\delta^{18}O$ value of soil water and the incoming rainfall at each site. Each conclusion will be discussed separately below.

At all sites, the volumetric water content increases with depth and the soil-water $\delta^{18}O$ value decreases with depth in the soil profile due to evaporation of water from the surface in the dry season. In the rainy season,

recharge of water from storms results in volumetric water contents that decrease with depth, and soil-water $\delta^{18}O$ values that increase with depth in the soil profile. These depth profiles also resemble the theoretical profiles calculated for soils in arid environments.

The volumetric water contents generally increase and the soil-water $\delta^{18}O$ values generally decrease with increasing annual rainfall. These trends correlate with regimes of decreasing evaporative demand and decreasing rainfall $\delta^{18}O$ values. This conclusion is consistent with our current understanding of the parameters that influence the isotopic composition of rain and soil water.

Soil-water $\delta^{18}O$ values were found to be more positive than incoming rainfall $\delta^{18}O$ values at the same location. The difference at the arid sites was about 5‰ while the difference at the humid sites was smaller, approximately 2‰ to 3‰. This is significant because, previous to this study, the assumption had been that the values were the same.

7.4. Future studies on soil water.

In addition to recording soil-water $\delta^{18}O$ values and understanding the trends, we can ask: How much evaporation occurs to yield the signal we see? Is this a significant amount relative to the amount of water lost by transpiration? How does evaporation in a forest environment compare with these grassland environments? What soil properties are most critical for

determining the amount of water loss? Do these effects show up in other continental areas?

The amount of evaporative loss versus transpirative loss of water is important to land surface hydrological models because it represents the latent heat flux component of the models. This quantity is poorly constrained and is normally estimated with little understanding of its contribution to models. Attempts to use the volumetric water content and $\delta^{18}O$ data from this study for modeling evaporative and transpirative losses of water indicated that these data were not appropriate for that purpose. Better documented rainfall amounts at specific sample locations, and shorter intervals between sample collections are needed. A future attempt to determine the balance between evaporation and transpiration will benefit from the knowledge and experience gained in this study.

7.5. The pedogenic mineral study.

The halloysite $\delta^{18}O$ values comprise the first set of data for which detailed soil-water $\delta^{18}O$ values are available for comparison. The conclusions from this part of the project are more preliminary, but include: 1) Halloysite can (with some difficulty) be physically separated from bulk soil material in quantities sufficient for $^{18}O/^{16}O$ analysis; 2) The $\delta^{18}O$ value of halloysite is preserved during the laboratory separation techniques; 3) The consistency of the $\delta^{18}O$ values suggests that halloysite indeed does form in isotopic equilibrium with its environment; and 4) Equilibrium isotopic fractionation

factors for minerals formed in weathering environments need to be recalibrated. Each conclusion will be discussed separately below.

Separation of halloysite from bulk soil material was possible despite its low abundance in these soils. Standard soil chemical treatments and size separations were employed. But, each sample had to be considered individually to determine the use and sequence of treatments. We determined that standard protocols should be avoided, because each sample has a different mixture of minerals.

An early study suggested that the D/H ratio of halloysite was easily changed (Lawrence and Taylor, 1972), but up to the present, no one has investigated its oxygen isotope exchangeability. We performed tests using isotopically labeled water (+300‰), and found that only about 1% exchange of oxygen isotopes occurred during separation of halloysite. The $^{18}O/^{16}O$ ratio was not easily changed in the laboratory. This result also lends support to the preservation of halloysite $\delta^{18}O$ values in weathering environments. Those environments are more neutral (pH and salinity) and isotopically less extreme than the conditions imposed during the laboratory chemical treatments. Direct evidence of the preservation of $\delta^{18}O$ values of halloysite in natural geological environments will have to await later studies.

Halloysite $\delta^{18}O$ values for Site B and for Pololu in Hawaii are almost identical, ranging from between +20.4‰ to +23.6‰ (decreasing with depth in both profiles). The implication of these data is that the environmental conditions of halloysite formation have been stable for 0.35 Ma, the age of

Pololu lava flows. In addition, it implies that halloysite formation in two different soils from the same general rainfall zone since 0.35 Ma and since 0.17 Ma resulted in the same $\delta^{18}O$ values. It is possible then that the conditions of halloysite formation (temperature and the $\delta^{18}O$ value of the water that is present at formation) are restricted to a small interval. If the conditions varied outside of that interval, halloysite did not form, and those conditions therefore would not be recorded by this mineral.

The results also show an $^{18}O/^{16}O$ inconsistency between independently determined kaolinite–water systems and the halloysite–water system in Hawaii. A straightforward application of the kaolinite–water fractionation curves to the halloysite–water system would imply that the halloysite in Hawaii formed between 50°C and 60°C, obviously an unrealistic circumstance. This brings into question whether mineral–water fractionations for minerals generally in low-temperature weathering environments have been properly calibrated. When comparing $\delta^{18}O$ values of clays from natural systems to water $\delta^{18}O$ values, the water that is often assumed to be present during their formation is local meteoric water collected at the surface, not the actual water in the pores of the soil. In other words, the $\delta^{18}O$ value of rainfall, nearby stream water or springwater is used to calculate fractionations. However, the pedogenic clays clearly must have formed *in situ* from soil water, which we have shown may have a different $\delta^{18}O$ value than that of local surface meteoric water. Obviously, the former $\delta^{18}O$ value should be the one used in calculating the fractionation between pedogenic clays and water. Isotopic

analyses of soil waters and coexisting kaolinites from different kaolinite deposits around the world should be made to estimate a new kaolinite–water fractionation factor.

7.6. Additional pedogenic mineral studies.

Because the soil environment is an open system composed of many different mineral phases, it is possible that each mineral records a specific range of temperature and chemical conditions. Coexisting minerals, do not necessarily imply cogenesis. Furthermore, because different soil minerals can form at different times, the $\delta^{18}O$ value of water that was present during the formation of each mineral may be different from the measured soil-water $\delta^{18}O$ values. Thus, measurements of a variety of other minerals in the soil system may be required in order to constrain the range of environments that the soil has experienced.

A logical extension of the current study would be to measure the $\delta^{18}O$ value of another mineral in these soils. Gibbsite is present in some horizons in the lower rainfall sites and hematite is present in all soils along the transect. Sample separation of both minerals will be critical for these measurements.

7.7. Final comments.

The fact that soils are open systems implies that both the careful documentation of soil properties and well-designed laboratory investigations

are necessary in order to interpret the natural system. This project has attempted to use both types of studies to understand pedogenic processes in Hawaii. The results show that there are significant differences in the oxygen isotopic systematics at arid and humid sites for both soil water and for halloysite, and that annual rainfall can be an important factor in soil formation. The project demonstrates that oxygen isotopic information can be a powerful tool for tracing geochemical transfers in the soil system. However, many details regarding the $^{18}O/^{16}O$ behaviour of clay minerals still need to be determined. In Hawaii, the climatic history of Kohala also needs to be further constrained before a meaningful interpretation of the change in chemical conditions can be made. Consequently, it is not surprising that this project has resulted in many new questions to be answered.

7.8. References.

Jusserand, C. 1980. Extraction de l'eau intersticielle des sediments et des sols. Comparaison des valeurs de l'oxygene 18 par differentes methodes. Premiers resultats. Catena, 7: 87-96.

Lawrence, J.R., and Taylor, H.P., Jr., 1972. Hydrogen and oxygen isotope systematics in weathering profiles. Geochimica et Cosmochimica Acta, 36: 1377-1393.

Scrimgeour, C.M., 1995. Measurement of plant and soil water isotope composition by direct equilibration methods. Journal of Hydrology, 173: 261-274.

Appendix A

A.1. CO_2-soil equilibration procedure.

All equilibrations were performed on the carbonate line at Case Western Reserve University and the water line in Rm 09 North Mudd at Caltech.

1) Place 10-15 g of sample into the vessel, about 2 teaspoons full of sample.

2) Freeze sample on vacuum line with an ethanol-dry ice slush for 5 minutes.

3) Close line to vacuum open valve, record pressure on thermocouple gauge and then pump out vessel.

4) Close valve. Remove dry ice slush and thaw with hot water.

5) Repeat (2) to (4) two more times (a total of three freeze-thaw repetitions).

6) Flush CO_2 through line and pump down to high-vacuum. Record level of Hg on manometer. Add about 30 cm of CO_2 into the line. Open valve on vessel and close quickly. Record level of Hg on manometer.

7) Place sample in water bath at 25°C.

8) Wait appropriate amount of time for equilibration.

9) Remove one aliquot of CO_2 from vessel through septum with 3ml syringe. Inject into vessel and freeze with liquid nitrogen for 3 minutes. Open valve on vessel and pump away non-condensibles. Replace liquid nitrogen with ethanol-dry ice slurry. Freeze CO_2 into sample tube with liquid nitrogen.

10) Take sample tube for analysis on a mass spectrometer.

A.2. Method results.

	Reproducibility test	
Sample	Clay Loam	Coarse Sandy Loam
a	-5.93	-9.12
b	-6.08	-8.97
c	-5.04	-9.23
d	-6.25	-8.43
e	-5.91	-8.63
f	-5.59	-8.67
g	-5.45	-8.95
h	-5.74	
Average:	-5.75	-8.86
Standard deviation:	0.38	0.29

Time of Equilibration - Data for Figure 2.3.

Wet Silt Loam		Dry Silt Loam		Clay Loam	
Time (min)	Water $\delta^{18}O$ value	Time (min)	Water $\delta^{18}O$ value	Time (min)	Water $\delta^{18}O$ value
0	-37.60	0	-37.61	0	-40.00
60	-10.22	105	-9.64	61	-29.50
118	-5.27	225	-6.07	145	-21.70
238	-3.46	477	-5.14	240	-17.50
1011	-3.40	1423	-5.63	326	-14.93
1437	-3.21	1815	-5.43	551	-12.68
1827	-3.26	2896	-4.98	1276	-12.01
2910	-3.30	4304	-5.10	1862	-11.94
4320	-3.29	5440	-5.64	2880	-11.85
7007	-3.30	6993	-4.98	3349	-11.72
				4314	-11.96

Appendix B - Soil water data.

Site B - December, 1993.

Depth (cm)	$\delta^{18}O$ a	$\delta^{18}O$ b	$\delta^{18}O$ c	Avg.	$H_2O\%$ a	$H_2O\%$ b	$H_2O\%$ c	Avg.
0-5	1.45	2.46	1.57	1.83	8.98	7.83	10.98	9.26
5-10	1.86	0.76	-0.22	0.80	8.67	9.58	10.59	9.61
10-15	-1.66	-2.98	-2.29	-2.31	12.72	14.94	13.18	13.62
15-20	-2.14	-2.78	-2.27	-2.40	14.60	16.55	16.01	15.72
20-30	-1.75	-1.96	-0.05	-1.25	17.20	16.45	16.69	16.78
30-40	-0.48	-0.13	0.67	0.02	17.93	16.78	17.49	17.40
40-55	-0.13	-0.18	-0.03	-0.11	17.23	19.25	14.45	16.98
55-70	-0.36	-0.59	-0.65	-0.53	13.19	12.52	12.13	12.61

Site B - February 13, 1994.

Depth (cm)	$\delta^{18}O$ a	$\delta^{18}O$ b	Avg.	$H_2O\%$ a	$H_2O\%$ b	Avg.
0-5	1.91	1.19	1.55	11.02	13.09	12.06
5-10	1.59	0.65	1.12	12.73	12.07	12.40
10-15	0.47	-0.05	0.21	15.04	12.76	13.90
15-20	-0.55	-1.51	-1.03	15.56	14.76	15.16
20-30	-1.08	-2.11	-1.59	14.49	17.85	16.17
30-40	-1.28	-2.15	-1.71	18.12	19.75	18.94
40-55	-1.31	-0.89	-1.10	18.63	15.68	17.22
55-70	-1.38	-0.98	-1.18	20.49	17.19	18.84

Site B - February 17, 1994.

Depth (cm)	$\delta^{18}O$ a	$\delta^{18}O$ b	Avg.	$H_2O\%$ a	$H_2O\%$ b	Avg.
0-5	-5.38	-4.50	-4.94	24.23	23.33	23.78
5-10	-4.67	-4.22	-4.45	28.59	21.53	25.06
10-15	-4.25	-4.39	-4.32	29.96	23.77	26.86
15-20	-3.98	-3.86	-3.92	27.79	26.35	27.07
20-30	-2.66	-2.12	-2.39	24.83	21.73	23.28
30-40	-2.44	-2.56	-2.50	16.67	17.88	17.27
40-55	-2.33	-2.14	-2.24	18.82	17.44	18.13
55-70	-2.54	-2.26	-2.40	20.06	16.67	18.36

Site B - March, 1994.

Depth (cm)	$\delta^{18}O$ a	$\delta^{18}O$ b	Avg.	$H_2O\%$ a	$H_2O\%$ b	Avg.
0-5	-3.86	-1.26	-2.56	20.27	20.74	20.51
5-10	1.53	1.68	1.61	15.51	14.50	15.01
10-15	0.67	-0.45	0.11	12.96	13.39	13.18
15-20	-0.96	-1.80	-1.38	17.29	17.38	17.34
20-30	-1.39	-1.54	-1.46	18.46	18.38	18.42
30-40	-0.99	-1.43	-1.21	20.23	20.59	20.41
40-55	-0.66	-0.34	-0.50	18.82	20.11	19.46
55-70	-0.67	-1.01	-0.84	18.21	21.01	19.61

Site B - May, 1994.

Depth (cm)	$\delta^{18}O$ a	$\delta^{18}O$ b	Avg.	$H_2O\%$ a	$H_2O\%$ b	Avg.
0-5	3.06	2.64	2.85	6.39	5.52	5.95
5-10	3.92	5.36	4.64	5.79	8.81	6.95
10-15	3.19	4.20	3.70	12.41	11.27	11.84
15-20	0.45	1.09	0.77	13.39	13.58	13.48
20-30	-0.77	-0.11	-0.44	12.96	14.37	13.67
30-40	-0.487	-1.36	-0.92	16.23	13.33	14.78
40-55	-1.09	0.41	-0.34	14.75	14.53	14.64
55-70	-1.09	1.04	-0.03	15.37	17.09	16.23

Site B - June, 1994.

Depth (cm)	$\delta^{18}O$ a	$\delta^{18}O$ b	Avg.	$H_2O\%$ a	$H_2O\%$ b	Avg.
0-5	5.05	5.26	5.15	5.30	6.35	5.83
5-10	3.98	4.85	4.41	8.07	11.94	10.00
10-15	3.09	3.31	3.20	9.84	11.36	10.60
15-20	0.91	0.90	0.09	13.90	14.05	13.97
20-30	1.05	-0.40	0.33	16.15	16.89	16.52
30-40	0.31	-0.87	-0.28	15.66	13.99	14.82
40-55	-1.44	-1.34	-1.398	17.90	20.87	19.38
55-70	-1.35	2.11	0.38	21.29	18.62	19.95

Site B - August, 1994.

Depth (cm)	$\delta^{18}O$ a	$\delta^{18}O$ b	Avg.	$H_2O\%$ a	$H_2O\%$ b	Avg.
0-5	3.46	5.29	4.37	5.11	5.98	5.54
5-10	5.64	6.36	6.00	6.29	6.01	6.15
10-15	6.83	5.34	6.08	7.74	8.48	8.11
15-20	4.39	3.47	3.93	12.23	9.38	10.81
20-30	4.09	1.79	2.94	14.41	11.32	12.87
30-40	0.25	2.14	1.20	15.40	15.70	15.55
40-55	0.83	0.10	0.46	16.84	15.47	16.16
55-70	-0.44	-0.36	-0.40	17.10	17.58	17.34

Site B - September, 1994.

Depth (cm)	$\delta^{18}O$ a	$\delta^{18}O$ b	Avg.	$H_2O\%$ a	$H_2O\%$ b	Avg.
0-5	5.30	5.48	5.39	5.14	5.78	5.46
5-10	6.49	5.38	5.93	8.25	10.27	9.26
10-15	5.22	5.91	5.56	8.17	9.67	8.92
15-20	2.98	3.01	2.99	12.68	12.32	12.50
20-30	3.25	1.45	2.35	13.02	13.59	13.30
30-40	0.09	1.56	0.83	15.49	15.51	15.50
40-55	0.30	0.99	0.64	15.96	14.83	15.39
55-70	0.05	0.07	0.06	14.31	16.07	15.19

Site B - November, 1994.

Depth (cm)	$\delta^{18}O$ a	$\delta^{18}O$ b	Avg.	$H_2O\%$ a	$H_2O\%$ b	Avg.
0-5	7.86	4.47	6.16	7.17	5.87	6.52
5-10	6.57	5.68	6.13	10.87	8.40	9.63
10-15	4.71	5.89	5.30	12.60	12.73	12.66
15-20	3.64	3.02	3.33	13.38	12.61	12.99
20-30	2.52	1.92	2.22	14.19	13.17	13.68
30-40	1.22	0.56	0.89	15.36	13.07	14.22
40-55	1.82	1.28	1.55	16.72	12.56	14.64
55-70	-0.10	0.35	0.12	16.93	17.37	17.15

Site B - March, 1995.

Depth (cm)	$\delta^{18}O$ a	$\delta^{18}O$ b	Avg.	$H_2O\%$ a	$H_2O\%$ b	Avg.
0-5	6.35	5.95	6.15	13.01	12.99	13.00
5-10	5.47	3.27	4.37	13.78	14.87	14.33
10-15	1.93	7.97	4.95	20.72	13.19	16.96
15-20	3.54	7.52	5.53	19.06	16.46	17.76
20-30	6.36	5.89	6.13	19.67	20.18	19.93
30-40	3.19	6.69	4.94	21.45	16.15	18.80
40-55	3.91	–	–	16.42	14.83	15.62
55-70	0.57	0.76	0.67	15.20	13.28	14.24

Site B - June, 1995.

Depth (cm)	$\delta^{18}O$ a	$\delta^{18}O$ b	Avg.	$H_2O\%$ a	$H_2O\%$ b	Avg.
0-5	3.95	2.75	3.35	4.40	4.29	4.35
5-10	6.83	7.65	7.24	8.21	9.08	8.65
10-15	3.53	6.83	5.18	12.48	10.34	11.41
15-20	3.24	5.41	4.33	11.41	9.99	10.70
20-30	2.19	4.67	3.43	12.39	9.82	11.10
30-40	1.56	2.89	2.22	15.42	13.52	14.47
40-55	2.06	2.60	2.33	16.62	15.02	15.82
55-70	1.32	0.40	0.86	20.10	18.13	19.11

Site B - September, 1995.

Depth (cm)	$\delta^{18}O$ a	$\delta^{18}O$ b	Avg.	$H_2O\%$ a	$H_2O\%$ b	Avg.
0-5	9.07	7.70	8.38	4.95	4.98	4.96
5-10	8.25	9.72	8.98	9.97	8.40	9.18
10-15	9.32	11.03	10.18	8.87	9.34	9.11
15-20	6.29	6.20	6.25	11.49	12.68	12.09
20-30	7.79	4.68	6.23	11.62	13.60	12.61
30-40	4.50	4.19	4.34	13.41	11.46	12.44
40-55	3.46	3.98	3.72	14.77	13.69	14.23
55-70	2.65	3.15	2.90	15.29	16.45	15.87

Site E - December, 1993.

Depth (cm)	$\delta^{18}O$ a	$\delta^{18}O$ b	Avg.	$H_2O\%$ a	$H_2O\%$ b	Avg.
0-5	0.97	0.40	0.68	15.09	12.91	14.00
5-10	-3.68	-4.36	-4.02	22.31	20.09	21.20
10-15	-4.89	-3.31	-4.10	24.17	14.32	19.25
15-20	-3.13	-5.04	-4.08	24.79	23.67	24.23
20-30	-4.07	-4.18	-4.12	25.71	28.56	27.13
30-40	-3.43	-3.54	-3.48	32.56	29.11	30.83
40-50	-2.93	-3.42	-3.17	31.15	28.26	29.70
50-65	-3.36	-3.74	-3.55	26.88	28.06	27.47
65-90	-3.67	-3.89	-3.78	27.60	29.23	28.41

Site E - February 13, 1994.

Depth (cm)	$\delta^{18}O$ a	$\delta^{18}O$ b	Avg.	$H_2O\%$ a	$H_2O\%$ b	Avg.
0-5	-0.32	-1.59	-0.95	16.77	20.90	18.83
5-10	-3.30	–	–	16.72	16.04	16.38
10-15	-3.77	-3.53	-3.65	18.23	24.76	21.19
15-20	-4.82	-3.74	-4.28	22.97	24.57	23.77
20-30	-4.36	-4.16	-4.26	22.59	24.84	23.71
30-40	-3.96	-3.78	-3.87	25.58	27.52	26.55
40-50	-4.07	-4.21	-4.14	24.87	34.13	29.50
50-65	-4.07	-4.29	-4.18	29.45	29.08	29.27
65-90	-3.64	-4.18	-3.91	24.48	18.38	21.43

Site E -February 18, 1994.

Depth (cm)	$\delta^{18}O$ a	$\delta^{18}O$ b	Avg.	$H_2O\%$ a	$H_2O\%$ b	Avg.
0-5	-8.89	-7.62	-8.25	54.44	46.29	50.36
5-10	-8.04	-7.64	-7.84	33.54	31.90	32.72
10-15	-7.01	-6.05	-6.53	39.95	38.79	39.37
15-20	-5.97	-4.24	-5.10	39.83	39.84	39.83
20-30	-5.22	-3.75	-4.49	36.77	35.70	36.23
30-40	-4.97	-4.33	-4.65	30.61	28.43	29.52
40-50	-4.76	-4.12	-4.44	27.11	25.30	26.20
50-70	-4.57	-3.68	-4.12	27.44	15.04	21.24

Site E - March, 1994.

Depth (cm)	$\delta^{18}O$ a	$\delta^{18}O$ b	Avg.	$H_2O\%$ a	$H_2O\%$ b	Avg.
0-5	-9.46	-8.09	-8.77	44.18	41.81	42.99
5-10	-8.89	-7.74	-8.32	38.11	39.16	38.63
10-15	-4.96	-5.99	-5.48	37.67	36.27	36.97
15-20	-5.56	-4.61	-5.08	25.26	34.54	29.90
20-30	-4.69	-4.55	-4.62	23.76	24.97	24.37
30-40	-4.16	-3.91	-4.04	25.08	26.82	25.95
40-50	-3.74	-4.35	-4.05	27.98	29.84	28.91
50-65	-3.85	-4.51	-4.18	23.51	29.04	26.28
65-90	-3.72	-2.31	-3.02	19.65	17.48	18.56

Site E - May, 1994.

Depth (cm)	$\delta^{18}O$ a	$\delta^{18}O$ b	Avg.	$H_2O\%$ a	$H_2O\%$ b	Avg.
0-5	2.89	2.80	2.84	10.19	9.22	9.70
5-10	2.52	0.71	1.61	11.08	13.93	12.50
10-15	-1.41	-2.83	-2.12	18.11	21.22	19.66
15-20	-1.82	-3.69	-2.75	19.00	22.53	20.76
20-30	-3.00	-3.37	-3.18	20.67	25.00	22.84
30-40	-2.12	-1.68	-1.90	20.13	27.35	23.74
40-50	-2.15	-3.65	-2.90	26.18	30.00	28.09
50-65	-2.79	-2.76	-2.78	23.79	28.17	25.98
65-90	-3.08	-2.94	-3.01	24.20	28.16	26.18

Site E - June, 1994.

Depth (cm)	$\delta^{18}O$ a	$\delta^{18}O$ b	Avg.	$H_2O\%$ a	$H_2O\%$ b	Avg.
0-5	2.44	8.06	5.25	11.10	6.13	8.61
5-10	-0.16	1.53	0.68	13.03	12.99	13.01
10-15	-0.47	-0.01	-0.24	13.84	13.47	13.65
15-20	-1.62	-0.47	-1.04	18.34	16.43	17.39
20-30	-2.09	-0.99	-1.54	19.33	18.16	18.75
30-40	-2.44	-3.32	-2.88	18.16	24.90	21.53
40-50	-3.11	-1.58	-2.34	23.09	27.77	25.43
50-70	-1.68	-2.46	-2.07	12.00	18.22	15.11
70-90	-1.49	–	–	13.21	–	–

Site E - August, 1994.

Depth (cm)	$\delta^{18}O$ a	$\delta^{18}O$ b	Avg.	$H_2O\%$ a	$H_2O\%$ b	Avg.
0-5	2.90	4.97	3.94	9.59	11.13	10.36
5-10	1.71	2.76	2.24	16.64	14.78	15.71
10-15	-0.98	0.87	-0.05	19.65	16.85	18.25
15-20	-1.46	-0.45	-0.96	20.52	18.70	19.61
20-30	-2.22	-1.99	-2.10	22.30	19.82	21.06
30-40	-3.10	-1.61	-2.36	25.36	26.13	25.75
40-50	-1.65	-2.93	-2.29	26.49	26.16	26.32
50-70	-3.03	-2.43	-2.73	27.33	27.01	27.17
70-85	-2.97	-2.81	-2.89	29.08	27.63	28.35

Site E - September, 1994.

Depth (cm)	$\delta^{18}O$ a	$\delta^{18}O$ b	Avg.	$H_2O\%$ a	$H_2O\%$ b	Avg.
0-5	5.67	6.60	6.14	10.98	8.48	9.73
5-10	3.56	2.44	3.00	14.40	17.78	16.09
10-15	1.84	0.99	1.41	12.30	14.31	13.30
15-20	-0.33	0.03	-0.15	18.05	20.51	19.28
20-30	-0.98	2.76	0.89	21.50	18.42	19.96
30-40	-2.19	-2.27	-2.23	23.61	32.08	27.84
40-50	-2.33	-2.88	-2.61	30.89	27.27	29.08
50-70	-2.94	-0.92	-1.93	34.11	14.84	24.48
70-90	-2.86	-2.34	-2.60	29.17	18.74	23.96

Site E - November, 1994.

Depth (cm)	$\delta^{18}O$ a	$\delta^{18}O$ b	Avg.	$H_2O\%$ a	$H_2O\%$ b	Avg.
0-5	4.99	4.81	4.90	13.76	14.26	14.01
5-10	2.84	3.68	3.26	17.74	15.29	16.52
10-15	0.91	1.13	1.02	19.93	14.67	17.30
15-20	0.15	0.10	0.13	20.17	18.80	19.48
20-30	-1.26	-1.90	-1.58	22.61	21.84	22.23
30-40	-1.57	-1.70	-1.64	22.59	24.10	23.34
40-50	-1.97	-2.83	-2.40	24.65	21.22	22.93
50-70	-3.43	-3.26	-3.34	28.79	28.53	28.66
70-90	–	-2.59	–	–	22.54	–

Site E - March, 1995.

Depth (cm)	$\delta^{18}O$ a	$\delta^{18}O$ b	Avg.	$H_2O\%$ a	$H_2O\%$ b	Avg.
0-5	3.15	4.37	3.76	24.20	28.52	26.36
5-10	1.41	2.02	1.72	24.97	24.13	24.55
10-15	2.07	1.49	1.78	27.68	30.14	28.91
15-20	0.12	0.74	0.43	30.41	32.40	31.41
20-30	-0.09	0.38	0.15	32.70	30.26	31.48
30-40	0.06	1.05	0.56	36.46	34.71	35.58
40-50	-1.50	-1.38	-1.44	33.23	35.87	34.55
50-70	-2.25	–	–	29.35	–	–
70-90	-1.75	–	–	19.55	–	–

Site E - June, 1995.

Depth (cm)	$\delta^{18}O$ a	$\delta^{18}O$ b	Avg.	$H_2O\%$ a	$H_2O\%$ b	Avg.
0-5	5.04	5.73	5.38	14.39	12.16	13.27
5-10	4.19	2.84	4.02	16.64	14.89	15.77
10-15	5.00	2.03	3.51	20.16	19.24	19.70
15-20	1.81	1.61	1.71	20.04	20.22	20.13
20-30	1.40	-0.01	0.70	20.19	21.09	20.64
30-40	0.39	0.47	0.43	17.51	20.10	18.80
40-50	-0.32	-0.60	-0.46	27.99	19.61	23.80
50-70	-1.81	-1.69	-1.75	28.08	28.32	28.20
70-90	-2.40	-1.36	-1.88	26.19	35.15	30.67

Site E - September, 1995.

Depth (cm)	$\delta^{18}O$ a	$\delta^{18}O$ b	Avg.	$H_2O\%$ a	$H_2O\%$ b	Avg.
0-5	7.57	6.20	6.89	9.98	8.48	9.23'
5-10	5.06	7.79	6.42	12.97	9.98	11.48
10-15	3.83	3.18	3.51	14.86	16.59	15.73
15-20	3.71	4.57	4.14	16.08	17.88	16.98
20-30	3.30	1.86	2.58	15.34	22.55	18.94
30-40	2.27	-1.78	0.24	16.75	28.07	22.41
40-50	-0.30	–	–	19.38	27.47	23.43
50-70	-1.92	0.62	-0.30	25.82	22.95	24.38
70-80	0.12	–	–	25.84	–	–

Site J - December, 1993.

Depth (cm)	$\delta^{18}O$ a	$\delta^{18}O$ b	Avg.	$H_2O\%$ a	$H_2O\%$ b	Avg.
0-5	-3.34	-2.28	-2.81	–	89.81	–
5-10	-2.09	-2.34	-2.22	72.99	66.52	69.76
10-15	-1.93	-2.69	-2.31	32.81	34.33	33.57
15-20	-2.71	-2.12	-2.41	44.67	37.38	41.02
20-30	-2.56	-2.74	--2.65	33.82	33.08	33.45
30-40	-3.37	-3.36	-3.36	35.62	37.21	36.42
40-50	-4.16	-3.52	-3.84	32.73	43.28	38.01
50-70	-4.58	–	–	40.17	–	–
70-85	-3.80	–	–	60.13	–	–

Site J - February, 1994.

Depth (cm)	$\delta^{18}O$ a	$\delta^{18}O$ b	Avg.	$H_2O\%$ a	$H_2O\%$ b	Avg.
0-5	-4.56	-5.21	-4.88	97.95	115.95	106.95
5-10	-4.32	-4.38	-4.35	96.11	99.84	97.98
10-15	-4.61	-4.39	-4.50	79.51	76.80	78.16
15-20	-4.37	-4.09	-4.23	67.64	68.79	68.21
20-30	-3.91	-3.28	-3.59	54.48	53.03	53.75
30-40	-2.83	–	–	54.34	54.70	54.52
40-50	-2.67	-3.17	-2.92	47.79	50.41	49.10
50-70	-3.84	-3.20	-3.52	45.35	45.84	45.60
70-85	-6.57	-3.02	-4.80	47.97	50.38	49.18

Site J - March, 1994.

Depth (cm)	$\delta^{18}O$ a	$\delta^{18}O$ b	Avg.	$H_2O\%$ a	$H_2O\%$ b	Avg.
0-5	-8.43	-7.66	-8.05	69.06	61.70	65.38
5-10	-11.33	-8.69	-10.01	57.98	61.10	59.54
10-15	-11.22	-10.31	-10.77	51.26	48.22	49.74
15-20	-11.35	-10.27	-10.81	46.61	45.91	46.26
20-30	-10.38	-8.60	-9.49	38.36	38.46	38.41
30-40	-8.37	-3.87	-6.12	35.11	34.37	34.74
40-50	-5.74	-2.43	-4.09	33.79	33.46	33.63
50-70	-3.42	-3.70	-3.56	33.42	34.83	34.13
70-90	-3.52	-0.81	-2.16	43.33	30.29	36.81

Site J - May, 1994.

Depth (cm)	$\delta^{18}O$ a	$\delta^{18}O$ b	Avg.	$H_2O\%$ a	$H_2O\%$ b	Avg.
0-5	-2.55	-3.13	-2.84	64.23	77.54	70.88
5-10	-2.54	-2.54	-2.54	58.57	72.37	65.47
10-15	-0.69	-3.22	-1.95	39.06	64.33	51.70
15-20	-2.61	-1.21	-1.91	39.53	40.88	40.21
20-30	-2.45	-3.10	-2.77	38.68	33.04	35.86
30-40	-2.87	-2.34	-2.60	33.87	31.21	32.54
40-50	-2.71	-2.42	-2.56	40.21	31.67	35.94
50-70	-2.71	-2.75	-2.73	35.10	30.83	32.97
70-90	-3.77	-3.87	-3.82	43.22	43.50	43.36
90-110	-4.05	-4.60	-4.32	43.19	43.81	43.50

Site J - June, 1994.

Depth (cm)	$\delta^{18}O$ a	$\delta^{18}O$ b	Avg.	$H_2O\%$ a	$H_2O\%$ b	Avg.
0-5	-3.39	-3.37	-3.38	80.18	84.73	82.46
5-10	-2.40	-2.14	-2.27	70.17	62.65	66.41
10-15	-2.44	-2.43	-2.43	47.16	40.36	43.76
15-20	-3.38	-2.21	-2.79	42.47	38.55	40.51
20-30	-3.44	-2.75	-3.10	31.66	39.27	35.47
30-40	-4.34	-3.03	-3.68	39.43	35.67	37.55
40-50	-3.92	-1.21	-2.56	35.10	35.16	35.13
50-70	-0.63	-4.93	-2.78	37.25	41.69	39.47
70-90	-3.85	-4.37	-4.11	37.07	30.63	33.85
90-110	-3.87	-3.92	-3.89	31.14	30.32	30.73

Site J - August, 1994.

Depth (cm)	$\delta^{18}O$ a	$\delta^{18}O$ b	Avg.	$H_2O\%$ a	$H_2O\%$ b	Avg.
0-5	-2.11	-2.16	-2.14	79.30	69.97	74.64
5-10	-3.15	-2.78	-2.97	70.64	64.34	67.48
10-15	-2.99	-3.28	-3.13	61.04	57.74	59.39
15-20	-3.01	-2.63	-2.82	60.70	47.01	53.86
20-30	-2.47	-2.01	-2.24	49.95	35.35	42.65
30-40	-2.72	-3.28	-3.00	43.91	34.48	39.19
40-50	-2.35	-1.76	-2.05	34.00	31.27	32.64
50-70	-3.14	-2.82	-2.98	32.67	25.27	28.97
70-90	-2.92	-2.35	-2.63	41.71	42.42	42.06
90-110	-2.37	-2.59	-2.48	47.32	34.93	41.13

Site J - September, 1994.

Depth (cm)	$\delta^{18}O$ a	$\delta^{18}O$ b	Avg.	$H_2O\%$ a	$H_2O\%$ b	Avg.
0-5	-3.23	-2.12	-2.68	67.63	69.37	68.50
5-10	-2.26	-2.63	-2.45	62.46	65.65	64.05
10-15	-2.68	-2.49	-2.59	58.59	58.42	58.50
15-20	-2.83	-2.54	-2.68	44.93	47.26	46.10
20-30	-3.02	-2.17	-2.59	48.06	44.49	46.27
30-40	-2.10	-3.49	-2.80	35.08	45.75	40.42
40-50	-3.33	-3.41	-3.37	37.66	39.67	38.66
50-70	-4.08	-3.49	-3.78	38.81	37.05	37.93
70-90	-3.63	-2.45	-3.04	51.80	35.33	43.56
90-110	-2.46	-2.15	-2.31	38.43	34.54	36.48

Site J - November, 1994.

Depth (cm)	$\delta^{18}O$ a	$\delta^{18}O$ b	Avg.	$H_2O\%$ a	$H_2O\%$ b	Avg.
0-5	-2.00	-0.69	-1.34	49.94	47.45	48.69
5-10	-2.17	-1.63	-1.90	38.57	49.49	44.03
10-15	-1.21	-1.44	-1.33	34.79	31.34	33.11
15-20	-2.44	-2.14	-2.29	36.79	33.66	35.22
20-30	-2.40	-1.71	-2.05	33.10	32.12	32.61
30-40	-2.30	-2.78	-2.54	27.12	32.29	29.70
40-50	-2.17	-3.11	-2.64	32.55	27.99	30.27
50-70	-2.89	-3.34	-3.11	26.77	27.69	27.23
70-90	-3.33	-3.24	-3.28	34.41	36.23	35.32
90-110	-2.54	-3.09	-2.82	39.11	45.07	42.09

Site J - March, 1995.

Depth (cm)	$\delta^{18}O$ a	$\delta^{18}O$ b	Avg.	$H_2O\%$ a	$H_2O\%$ b	Avg.
0-5	-0.45	-2.57	-1.51	57.14	63.26	60.20
5-10	-1.82	-2.50	-2.16	57.75	58.69	58.22
10-15	-1.46	-2.18	-1.82	40.49	59.72	50.11
15-20	-1.89	-2.58	-2.23	42.25	46.34	44.40
20-30	-1.24	-2.08	-1.66	28.75	43.18	40.97
30-40	-1.86	-0.94	-1.40	38.79	36.79	37.79
40-50	-0.43	-1.27	-0.85	39.88	34.89	37.38
50-70	-1.26	-1.81	-1.53	39.25	31.25	35.25
70-90	-2.07	-1.24	-1.65	51.95	34.92	43.44
90-110	-1.33	1.05	-0.14	31.76	28.75	30.25

Site J - June, 1995.

Depth (cm)	$\delta^{18}O$ a	$\delta^{18}O$ b	Avg.	$H_2O\%$ a	$H_2O\%$ b	Avg.
0-5	1.94	-1.12	0.41	67.59	99.32	83.46
5-10	0.83	0.60	0.71	71.67	77.16	74.41
10-15	0.55	-1.25	-0.35	44.38	63.39	53.89
15-20	2.80	1.22	2.01	38.27	50.35	44.31
20-30	0.98	3.44	2.21	39.33	38.22	38.77
30-40	3.77	1.79	2.78	29.73	30.35	30.04
40-50	1.04	3.21	2.12	35.11	27.40	31.25
50-70	2.08	-0.57	0.76	37.24	36.70	36.97
70-90	2.63	2.17	2.40	44.40	39.65	42.03
90-110	3.37	3.75	3.56	38.25	28.59	33.42

Site J - September, 1995.

Depth (cm)	$\delta^{18}O$ a	$\delta^{18}O$ b	Avg.	$H_2O\%$ a	$H_2O\%$ b	Avg.
0-5	2.43	0.89	1.66	57.11	56.10	56.61
5-10	-0.16	-0.52	-0.34	55.20	62.02	58.61
10-15	-1.07	0.40	-0.33	49.39	47.86	48.63
15-20	-0.37	0.47	0.05	42.12	38.50	40.31
20-30	-0.50	0.24	-0.13	37.10	34.57	35.83
30-40	0.17	-0.65	-0.24	34.93	35.51	35.22
40-50	-1.23	-0.96	-1.10	34.10	34.67	34.38
50-70	-1.28	-0.97	-1.12	32.77	36.90	34.84
70-90	-0.99	0.56	-0.22	41.09	34.69	37.89

Site M - December, 1993.

Depth (cm)	$\delta^{18}O$ a	$\delta^{18}O$ b	Avg.	$H_2O\%$ a	$H_2O\%$ b	Avg.
0-5	–	-1.84	–	30.99	48.66	39.82
5-10	-2.46	-1.87	-2.16	47.14	84.54	65.84
10-15	-2.29	-2.45	-2.37	74.94	89.98	82.46
15-20	0.91	-2.31	-0.70	60.56	86.78	73.67
20-30	-3.45	-1.74	-2.60	84.31	75.31	79.81
30-40	-3.66	-2.47	-3.07	66.02	60.58	63.30
40-50	-2.62	-0.80	-1.71	76.99	74.10	75.54
50-70	-2.97	-2.70	-2.84	72.91	83.27	78.09
70-90	-2.52	-1.97	-2.25	56.74	64.68	60.71

Site M - February, 1994.

Depth (cm)	$\delta^{18}O$ a	$\delta^{18}O$ b	Avg.	$H_2O\%$ a	$H_2O\%$ b	Avg.
0-5	-6.27	-5.89	-6.08	108.55	92.34	100.50
5-10	-5.42	-4.66	-5.04	76.84	50.78	63.81
10-15	-6.00	-3.83	-4.91	88.90	60.18	74.54
15-20	-5.58	-4.47	-5.03	65.92	55.69	60.80
20-30	-4.99	-3.43	-4.21	57.27	68.06	62.67
30-40	-5.05	-3.85	-4.45	58.39	63.83	61.11
40-50	-3.57	-3.26	-3.41	81.89	94.40	88.15
50-70	–	-1.63	–	64.46	72.71	68.59
70-90	–	-3.42	–	59.88	71.79	65.83

Site M - March, 1994.

Depth (cm)	$\delta^{18}O$ a	$\delta^{18}O$ b	Avg.	$H_2O\%$ a	$H_2O\%$ b	Avg.
0-5	-6.46	-4.20	-5.33	83.05	60.52	71.78
5-10	-6.30	-2.95	-4.63	60.35	45.04	52.70
10-15	-5.75	-2.69	-4.22	46.76	46.97	46.86
15-20	-3.56	-3.06	-3.31	63.19	53.60	58.40
20-30	-5.76	-3.17	-4.47	63.30	63.12	63.21
30-40	-5.31	-2.90	-4.11	57.69	49.42	53.55
40-50	-3.73	-2.45	-3.09	74.62	61.03	67.82
50-70	-2.93	-3.33	-3.13	64.21	67.00	65.61

Site M - May, 1994.

Depth (cm)	$\delta^{18}O$ a	$\delta^{18}O$ b	Avg.	$H_2O\%$ a	$H_2O\%$ b	Avg.
0-5	-2.04	-2.36	-2.20	55.51	52.96	54.23
5-10	-2.66	-2.23	-2.44	41.45	45.02	43.24
10-15	-3.63	-3.43	-3.53	56.41	41.94	49.18
15-20	-4.10	-3.58	-3.84	71.75	61.10	66.43
20-30	-4.17	-3.82	-4.00	71.43	68.26	69.85
30-40	-3.56	-3.10	-3.33	59.45	56.84	58.15
40-50	-1.92	-2.31	-2.11	59.25	59.57	59.41
50-70	-3.40	-2.71	-3.05	68.47	58.03	63.25
70-90	-3.49	-2.69	-3.09	62.99	68.94	65.97
90-110	-3.70	-2.30	-3.00	66.77	53.74	60.26

Site M - June, 1994.

Depth (cm)	$\delta^{18}O$ a	$\delta^{18}O$ b	Avg.	$H_2O\%$ a	$H_2O\%$ b	Avg.
0-5	-2.77	-2.85	-2.81	56.62	58.34	57.48
5-10	-2.64	-2.08	-2.36	41.45	38.16	39.80
10-15	-3.21	-2.72	-2.96	40.67	60.42	50.54
15-20	-3.28	-1.85	-2.56	65.82	62.84	64.33
20-30	-3.55	-3.25	-3.40	64.59	69.97	67.28
30-40	-2.11	-2.98	-2.55	51.07	65.11	58.09
40-50	-2.65	-3.05	-2.85	53.99	68.75	61.37
50-70	-3.67	-3.15	-3.41	53.30	78.72	66.01
70-90	-3.18	-2.59	-2.89	39.30	61.54	50.42
90-110	-2.23	-1.31	-1.77	52.57	38.38	45.48
110-130	-3.05	-0.97	-2.01	55.05	39.52	47.29

Site M - August, 1994.

Depth (cm)	$\delta^{18}O$ a	$\delta^{18}O$ b	Avg.	$H_2O\%$ a	$H_2O\%$ b	Avg.
0-5	-1.59	-1.41	-1.50	51.44	79.14	65.29
5-10	-1.50	-0.30	-0.90	37.84	40.61	39.22
10-15	-1.44	-1.56	-1.50	36.06	60.17	48.11
15-20	-1.69	-1.44	-1.57	52.47	60.72	56.59
20-30	-2.03	-2.12	-2.08	66.50	71.69	69.10
30-40	-2.38	-1.75	-2.07	65.07	56.44	60.75
40-50	-1.72	-2.82	-2.27	63.18	59.98	61.58
50-70	-3.12	-2.23	-2.68	56.86	58.13	57.49
70-90	-2.08	-1.91	-1.99	72.42	76.14	74.28

Site M - September, 1994.

Depth (cm)	$\delta^{18}O$ a	$\delta^{18}O$ b	Avg.	$H_2O\%$ a	$H_2O\%$ b	Avg.
0-5	-2.48	-3.74	-3.11	91.12	128.39	109.75
5-10	-2.20	-1.80	-2.00	70.49	50.35	60.42
10-15	-1.88	-1.92	-1.90	65.00	87.57	76.28
15-20	-2.43	-2.11	-2.27	70.69	85.69	78.19
20-30	-2.31	-1.99	-2.15	83.95	89.60	86.78
30-40	-2.40	-2.70	-2.55	82.24	73.52	77.88
40-50	-2.43	-2.76	-2.60	81.27	74.85	78.06
50-70	-2.95	-3.13	-3.04	84.95	82.42	83.69
70-90	-3.57	-3.21	-3.39	79.89	83.16	81.53
90-110	-2.84	-3.21	-3.03	93.09	86.27	89.68

Site M - November, 1994.

Depth (cm)	$\delta^{18}O$ a	$\delta^{18}O$ b	Avg.	$H_2O\%$ a	$H_2O\%$ b	Avg.
0-5	-1.33	-1.85	-1.59	51.46	50.12	50.79
5-10	-2.14	-1.70	-1.92	48.12	37.95	43.04
10-15	-2.32	-0.62	-1.47	41.51	55.05	48.28
15-20	-2.46	-1.75	-2.10	49.39	76.26	62.82
20-30	-2.83	-2.16	-2.49	71.96	69.50	70.73
30-40	-3.04	-2.50	-2.77	66.12	64.74	65.43
40-50	-2.54	-5.95	-4.25	71.88	69.26	70.57
50-70	-2.87	-2.78	-2.83	70.60	71.08	70.84
70-90	-3.30	-2.85	-3.08	72.28	70.01	71.15
90-110	-2.37	-2.91	-2.64	65.51	76.60	71.06
110-130	-3.04	-3.10	-3.07	86.51	99.67	93.09

Site M - March, 1995.

Depth (cm)	$\delta^{18}O$ a	$\delta^{18}O$ b	Avg.	$H_2O\%$ a	$H_2O\%$ b	Avg.
0-5	-1.75	-1.65	-1.70	60.42	52.63	56.53
5-10	-2.47	-1.00	-1.74	47.85	47.44	47.64
10-15	-1.84	-2.58	-2.21	42.71	44.51	43.61
15-20	-1.34	-1.66	-1.50	67.66	38.49	53.07
20-30	-2.39	-2.16	-2.28	70.91	54.04	62.47
30-40	-2.51	-2.72	-2.62	56.57	52.36	54.47
40-50	-2.18	-0.94	-1.56	64.48	53.69	59.09
50-70	-2.66	-2.41	-2.53	62.85	58.85	60.85
70-90	-2.59	-1.62	-2.10	72.80	72.77	72.78
90-110	-2.86	-2.00	-2.43	69.33	60.17	64.75
110-130	-1.62	-0.29	-0.95	83.38	51.84	67.61

Site M - March, 1995.

Depth (cm)	$\delta^{18}O$ a	$\delta^{18}O$ b	Avg.	$H_2O\%$ a	$H_2O\%$ b	Avg.
0-5	-1.33	-0.70	-1.02	40.66	51.46	46.06
5-10	0.60	0.36	0.48	57.60	54.35	55.97
10-15	1.24	1.13	1.18	61.12	35.86	48.49
15-20	-0.44	0.11	-0.16	65.58	35.26	50.42
20-30	-0.67	0.69	0.01	65.00	79.40	72.20
30-40	-1.42	-0.21	-0.82	55.02	54.78	54.90
40-50	-0.28	-0.01	-0.14	46.06	56.22	51.15
50-70	-0.95	-1.32	-1.14	43.73	55.74	49.73
70-90	-0.31	0.40	0.05	61.39	46.84	54.12
90-110	-0.88	-1.71	-1.30	69.26	69.21	69.23
110-130	-1.66	-0.18	-0.92	81.30	61.95	71.62

Appendix C - Clay mineral methods and data.

The details of chemical and physical treatments are described in this appendix. Following these methods are a series of tables which document the sequence of treatments and include the isotopic results. Finally, the Nicomp results and final x-ray diffraction patterns are included.

C.1. Sample preparation.

C.1.1 Chemical treatments.

Organic matter was removed from soil samples by oxidation with 30% H_2O_2. About 20-30 g of soil was mixed with a solution of approximately 25 ml of 30% H_2O_2 and 25 ml of deionized water in a 250 ml glass centrifuge bottle. The bottle was placed in a New Brunswick Scientific gyratory water bath-shaker at 40°C and ~60 rpm. The mixture was allowed to react for about 24 hours. After the reaction, it was spun in an IEC HN-SII centrifuge for 15 min at 1500 rpm. All of the sample flocculated except for some root material which floated in the supernatant and was discarded.

An acid ammonium oxalate solution (AAO solution) removes non-crystalline (amorphous) iron and aluminum components. The AAO solution is made by mixing 700 ml of 0.2 M ammonium oxalate $[(NH_4)_2C_2O_4 \bullet H_2O]$ with 535 ml of 0.2 M oxalic acid $[H_2C_2O_4 \bullet 2H_2O]$. Following the H_2O_2 treatment, the sample was mixed with about 50 ml of AAO solution. The mixture was allowed to react for 12 hours at 40°C and ~60 rpm in the

shaker-bath. After the reaction, the mixture was centrifuged for 15 minutes at 1500 rpm. All of the sample flocclated and the supernatant, a brownish green color, was discarded.

A sodium citrate-sodium bicarbonate solution (CB solution) to which solid sodium dithionite has been added (together known as CBD treatment) removes crystalline iron oxides such as hematite and goethite. The CB solution is made by mixing 8 parts of 0.3 M sodium citrate with 1 part 1 M sodium bicarbonate. Following an AAO treatment, the sample was mixed with about 50 ml of CB solution. The mixture was allowed to react for 15 minutes at 40°C and ~60 rpm in the shaker-bath. After 15 minutes, 1 g of sodium dithionite was added. The mixture was allowed to react for another 15 minutes. This was repeated until a total of three 1 g aliquots had been added. The mixture was then allowed to react for at least 6 hours. After the reaction, the mixture was centrifuged at 1500 rpm for 15 minutes. All of the sample flocclated and the supernatant, a reddish brown color, was discarded.

C.1.2. Physical treatments.

All phases were identified by x-ray diffraction after each size separation. At Caltech, analyses were made using a Scintag PadV x-ray diffractometer (CuKα radiation, 35kV, 30mA). At Case Western Reserve University, analyses were made using a Phillips XRG 30 x-ray diffractometer (CuKα radiation, 40 kV, 20mA).

An initial size separation was made at 5 μm. The < 5 μm fraction was collected by gravitational setting. Each sample was mixed with approximately 200 ml of deionized water in a 250 ml glass centrifuge bottle. After 35 minutes and 47 seconds, the top 5 cm of the suspension was decanted into a separate beaker. The sample was then resuspended and allowed to settle again. After two repetitions, the decanted material was spun in a centrifuge at 1500 rpm to recover the < 5 μm material. If the sample did not flocculate after 20 minutes, a drop of 6 N HCl was added to the suspension to promote flocculation.

A further size separation was made at 2 μm by centrifugation. The < 5 μm fraction was suspended in deionized water in a 250 ml glass centrifuge bottle and spun for 2 minutes and 47 seconds at 1100 rpm on an IEC International Centrifuge. The supernatant containing the < 2 μm fraction was decanted into a separate beaker. The sample was resuspended and spun for a second time. After two repetitions, the decanted material was spun in a centrifuge at 1500 rpm for 20 minutes to recover the < 2 μm fraction. Flocculation was promoted by adding a drop of 6 N HCl to the suspension. The particle size distribution of the < 2 μm fraction was analyzed on a Nicomp Model 370 Submicron Particle Sizer, an instrument based on scattering of laser light by different size particles. The next size of separation was guided by this analysis and was done by centrifugation.

C.2. Treatment of samples.

Sample: Site B, 0-10 cm

	Treatments:			Size separations:					$\delta^{18}O$	
Date	H_2O_2	AAO	CBD	< 5 μ	< 2 μ	size	XRD	Nicomp	Analysis	result
11/27/95	X									
11/29/95		X								
11/30/95		X	X							
12/1/95			X	X						
12/8/95					X					
12/13/95							X	X		
12/14/95						< 0.25 μ	X			
1/11/96									X	23.66‰ yield= 94%
2/7/96									X	23.50‰ yield= 95%

Sample: Site B, 10-37 cm

	Treatments:			Size separations:					$\delta^{18}O$	
Date	H_2O_2	AAO	CBD	< 5 μ	< 2 μ	size	XRD	Nicomp	Analysis	result
11/27/95	X									
11/29/95		X								
11/30/95		X	X							
12/1/95			X	X						
12/8/95					X					
12/13/95							X	X		
12/14/95						< 0.25 μ	X			
1/11/96									X	22.14‰ yield=103%

Samples: Site B, 37-65 cn					All samples < 2 μ	
	Treatments			Isotopic analysis		
Aliquot	H_2O_2	AAO	CBD	$\delta^{18}O$	yield	date
HI-3-3-A				20.7‰	90%	Oct. 4, 1995
HI-3-3-A				20.7‰	85%	Aug. 1, 1995
HI-3-3-B	X			21.2‰	103%	Aug. 1, 1995
HI-3-3-C		X		22.4‰	99%	Aug. 1, 1995
HI-3-3-D			X	23.0‰	100%	Aug. 3, 1995
HI-3-3-E		#		20.7‰	102%	Oct. 4, 1995
HI-3-3-F			#	20.8‰	103%	Oct. 4, 1995
HI-3-3-F			#	20.7‰	103%	Oct. 4, 1995
HI-3-3-G	X			22.6‰	97%	Oct. 27, 1995
HI-3-3-G	X			23.0‰	100%	Oct. 25, 1995
HI-3-3-H		X		23.0‰	100%	Oct. 25, 1995
HI-3-3-I			X	23.6‰	100%	Nov. 1, 1995
HI-3-3-I			X	23.6‰	100%	Nov. 1, 1995

X- with +300‰ water, #- with -10‰ water

Sample: Site B, 65-100 cm

	Treatments:			Size separations:					$\delta^{18}O$	
Date	H_2O_2	AAO	CBD	< 5 μ	< 2 μ	size	XRD	Nicomp	Analysis	result
11/27/95	X									
11/29/95		X								
11/30/95		X	X							
12/1/95			X	X						
12/8/95					X					
12/13/95							X	X		
12/14/95						< 0.25 μ	X			
1/11/96									X	20.36‰
										yield=100%

Sample: Site E, 0-13 cm

	Treatments:			Size separations:					$\delta^{18}O$	
Date	H_2O_2	AAO	CBD	< 5 μ	< 2 μ	size	XRD	Nicomp	Analysis	result
11/27/95	X									
11/29/95		X								
11/30/95		X	X							
12/1/95			X	X						
12/8/95					X					
12/13/95							X	X		
12/14/95						< 0.25 μ	X			
1/18/96									X	23.66‰
										yield= 94%
4/10/96									X	23.50‰
										yield= 95%
2/23-25/96	X									
2/26/96		X								
2/27/96		X	X							
2/28/96		X	X							
2/29/96			2X	X						
3/8/96						< 0.25 μ	X			
4/10/96									X	21.38‰
										yield=92%

Sample: Site E, 13-30 cm

	Treatments:			Size separations:					$\delta^{18}O$	
Date	H_2O_2	AAO	CBD	< 5 μ	< 2 μ	size	XRD	Nicomp	Analysis	result
11/27/95	X									
11/29/95		X								
11/30/95		X	X							
12/1/95			X	X						
12/8/95					X					
12/13/95							X	X		
12/14/95						< 0.25 μ	X			
1/23/96									X	22.14‰ yield= 96%
2/7/96									X	22.43‰ yield= 99%
2/23-25/96	X									
2/26/96		X								
2/27/96		X	X							
2/28/96		X	X							
2/29/96			2X	X						
3/8/96						< 0.25 μ	X			
4/18/96									X	21.69‰ yield=100%

Sample: Site E, 30-44 cm

	Treatments:			Size separations:					$\delta^{18}O$	
Date	H_2O_2	AAO	CBD	< 5 μ	< 2 μ	size	XRD	Nicomp	Analysis	result
11/27/95	X									
11/29/95		X								
11/30/95		X	X							
12/1/95			X	X						
12/8/95					X					
12/13/95							X	X		
12/14/95						< 0.5 μ	X			
1/11/96									X	21.79‰ yield=95%

Sample: Site E, 44-62 cm

	Treatments:			Size separations:					$\delta^{18}O$	
Date	H_2O_2	AAO	CBD	< 5 μ	< 2 μ	size	XRD	Nicomp	Analysis	result
7/20-21/95	X									
7/22/95		X								
7/23/95		X	X							
7/24/95			X	X						
7/25/95					X					
9/5/95							X			
10/4/95									X	21.75‰ yield=100%

Sample: Site E, 62-85 cm

	Treatments:			Size separations:					$\delta^{18}O$	
Date	H_2O_2	AAO	CBD	< 5 μ	< 2 μ	size	XRD	Nicomp	Analysis	result
7/20-21/95	X									
7/22/95		X								
7/23/95		X	X							
7/24/95			X	X						
7/25/95					X					
9/5/95							X			
10/4/95									X	21.71‰
										yield=103%

Sample: Site J, 0-5 cm

	Treatments:			Size separations:					$\delta^{18}O$	
Date	H_2O_2	AAO	CBD	< 5 μ	< 2 μ	size	XRD	Nicomp	Analysis	result
11/27/95	X									
11/29/95		X								
11/30/95		X	X							
12/1/95			X	X						
12/8/95					X					
12/13/95							X	X		
										NONE

Sample: Site J, 5-10 cm

	Treatments:			Size separations:					$\delta^{18}O$	
Date	H_2O_2	AAO	CBD	< 5 μ	< 2 μ	size	XRD	Nicomp	Analysis	result
11/27/95	X									
11/29/95		X								
11/30/95		X	X							
12/1/95			X	X						
12/8/95					X					
12/13/95							X	X		
										NONE

Sample: Site J, 10-15 cm

	Treatments:			Size separations:					$\delta^{18}O$	
Date	H_2O_2	AAO	CBD	< 5 μ	< 2 μ	size	XRD	Nicomp	Analysis	result
11/27/95	X									
11/29/95		X								
11/30/95		X	X							
12/1/95			X	X						
12/8/95					X					
12/13/95							X	X		
										NONE

Sample: Site J, 15-20 cm

	Treatments:			Size separations:					$\delta^{18}O$	
Date	H_2O_2	AAO	CBD	< 5 μ	< 2 μ	size	XRD	Nicomp	Analysis	result
11/27/95	X									
11/29/95		X								
11/30/95		X	X							
12/1/95			X	X						
12/8/95					X					
12/13/95							X	X		
										NONE

Sample: Site J, 20-30 cm

	Treatments:			Size separations:					$\delta^{18}O$	
Date	H_2O_2	AAO	CBD	< 5 μ	< 2 μ	size	XRD	Nicomp	Analysis	result
11/27/95	X									
11/29/95		X								
11/30/95		X	X							
12/1/95			X	X						
12/8/95					X					
12/13/95							X	X		
										NONE

Sample: Site J, 30-40 cm

	Treatments:			Size separations:					$\delta^{18}O$	
Date	H_2O_2	AAO	CBD	< 5 μ	< 2 μ	size	XRD	Nicomp	Analysis	result
11/27/95	X									
11/29/95		X								
11/30/95		X	X							
12/1/95			X	X						
12/8/95					X					
12/13/95							X	X		
										NONE

Sample: Site J, 40-50 cm

	Treatments:			Size separations:					$\delta^{18}O$	
Date	H_2O_2	AAO	CBD	< 5 μ	< 2 μ	size	XRD	Nicomp	Analysis	result
11/27/95	X									
11/29/95		X								
11/30/95		X	X							
12/1/95			X	X						
12/8/95					X					
12/13/95								X		
12/14/95							X			
1/18/96									X	17.98‰
										yield=87%

Sample: Site J, 50-70 cm

	Treatments:			Size separations:					$\delta^{18}O$	
Date	H_2O_2	AAO	CBD	< 5 μ	< 2 μ	size	XRD	Nicomp	Analysis	result
11/27/95	X									
11/29/95		X								
11/30/95		X	X							
12/1/95			X	X						
12/8/95					X					
12/13/95							X	X		
12/14/95						< 0.25 μ	X			
1/18/96									X	18.67‰ yield=88%

Sample: Pololu, 5-26 cm

	Treatments:			Size separations:					$\delta^{18}O$	
Date	H_2O_2	AAO	CBD	< 5 μ	< 2 μ	size	XRD	Nicomp	Analysis	result
2/29/96	X									
3/1/96		X								
3/4/96			X							
3/5/96			2X	X						
3/8/96					X					
3/9/96							X	X		
3/10/96						< 0.25 μ	X			
4/24/96									X	22.93‰ yield=88%

Sample: Pololu, 26-43 cm

	Treatments:			Size separations:					$\delta^{18}O$	
Date	H_2O_2	AAO	CBD	< 5 μ	< 2 μ	size	XRD	Nicomp	Analysis	result
2/29/96	X									
3/1/96		X								
3/4/96			X							
3/5/96			2X	X						
3/8/96					X					
3/9/96							X	X		
										NONE

Sample: Pololu, 43-60 cm

	Treatments:			Size separations:					$\delta^{18}O$	
Date	H_2O_2	AAO	CBD	< 5 μ	< 2 μ	size	XRD	Nicomp	Analysis	result
2/29/96	X									
3/1/96		X								
3/4/96			X							
3/5/96			2X	X						
3/8/96					X					
3/9/96							X	X		
										NONE

Sample: Pololu, 60-90 cm

	Treatments:			Size separations:					$\delta^{18}O$	
Date	H_2O_2	AAO	CBD	< 5 μ	< 2 μ	size	XRD	Nicomp	Analysis	result
2/29/96	X									
3/1/96		X								
3/4/96			X							
3/5/96			2X	X						
3/8/96					X					
3/9/96							X	X		
										NONE

Sample: Pololu, 90-102 cm

	Treatments:			Size separations:					$\delta^{18}O$	
Date	H_2O_2	AAO	CBD	< 5 μ	< 2 μ	size	XRD	Nicomp	Analysis	result
2/29/96	X									
3/1/96		X								
3/4/96			X							
3/5/96			2X	X						
3/8/96					X					
3/9/96							X	X		
3/10/96						< 0.25 μ	X			
4/18/96									X	21.68‰
										yield=99%

Sample: Pololu, 102-115 cm

	Treatments:			Size separations:					$\delta^{18}O$	
Date	H_2O_2	AAO	CBD	< 5 μ	< 2 μ	size	XRD	Nicomp	Analysis	result
2/29/96	X									
3/1/96		X								
3/4/96			X							
3/5/96			2X	X						
3/8/96					X					
3/9/96							X	X		
3/10/96						< 0.25 μ	X			
4/24/96									X	20.98‰
										yield=90%

C.3. Nicomp and x-ray diffraction patterns.

JH-3-1 < 5microns

VOLUME-Weighted NICOMP DISTRIBUTION Analysis (Solid Particles)

NICOMP SUMMARY:
Peak Number 1: Mean Diameter = 121.8 nm Volume: 17.71 %
Peak Number 2: Mean Diameter = 629.5 nm Volume: 82.29 %

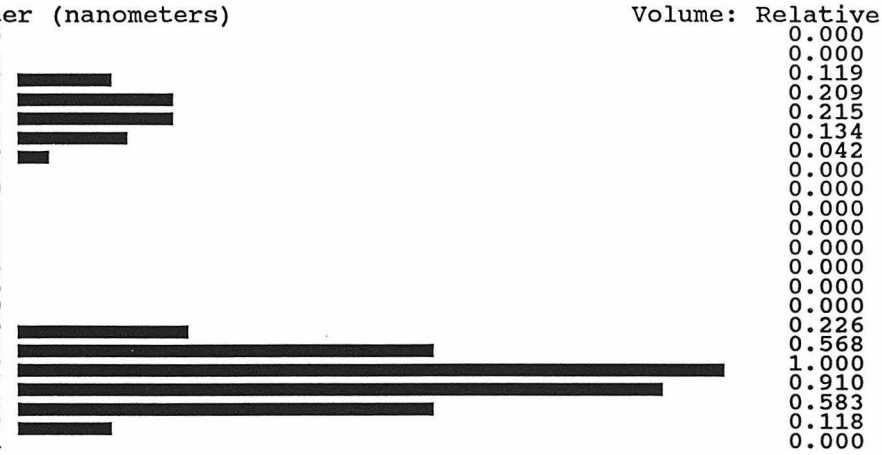

Mean Diameter = 547.6 nm Fit Error = 2.922 Residual = 52.949

NICOMP SCALE PARAMETERS:
Min. Diam. = 10.0 nm Plot Size = 45
Smoothing = 3 Plot Range = 200

Run Time = 0 Hr 11 Min 53 Sec
Count Rate = 335 Khz Temperature = 23 deg C
Channel #1 = 2541.0 K Viscosity = 0.933 cp
Channel Width = 98.0 uSec Index of Ref. = 1.333

GAUSSIAN SUMMARY:
Mean Diameter = 1092.5 nm Chi Squared = 190.468
Stnd. Deviation = 734.0 nm (67.2 %) Baseline Adj. = 0.064 %
Coeff. of Var'n = 0.672 Mean Diff. Coeff. = 6.44E-09 cm2/s

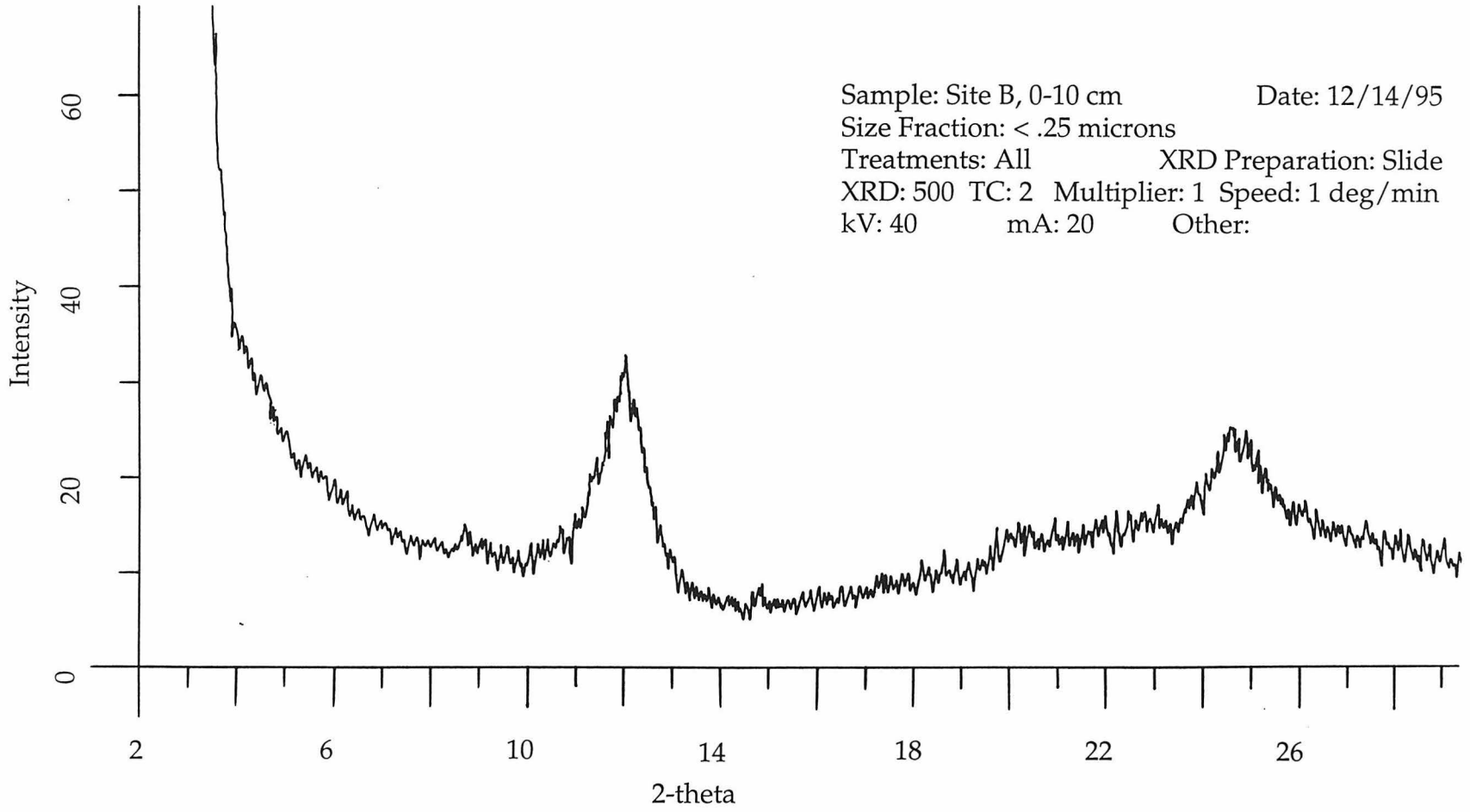
Sample: Site B, 0-10 cm
Date: 12/14/95
Size Fraction: < .25 microns
Treatments: All
XRD Preparation: Slide
XRD: 500 TC: 2 Multiplier: 1 Speed: 1 deg/min
kV: 40
mA: 20
Other:
Intensity
0
20
40
60
2
6
10
14
18
22
26
2-theta

JH-3-2 < 5microns

VOLUME-Weighted NICOMP DISTRIBUTION Analysis (Solid Particles)

NICOMP SUMMARY:
Peak Number 1: Mean Diameter = 126.8 nm Volume: 31.34 %
Peak Number 2: Mean Diameter = 489.8 nm Volume: 68.66 %

Diameter (nanometers)	Volume: Relative
77.5	0.000
87.4	0.000
98.5	0.167
111.2	0.313
125.4	0.456
141.4	0.311
159.5	0.177
179.9	0.000
203.0	0.000
228.9	0.000
258.2	0.000
291.3	0.000
328.5	0.000
370.6	0.289
418.0	0.580
471.5	1.000
531.8	0.823
599.9	0.543
676.7	0.085
763.2	0.000

Mean Diameter = 384.2 nm Fit Error = 4.298 Residual = 53.352

NICOMP SCALE PARAMETERS:
Min. Diam. = 10.0 nm Plot Size = 45
Smoothing = 3 Plot Range = 200

Run Time = 0 Hr 11 Min 10 Sec
Count Rate = 339 Khz Temperature = 23 deg C
Channel #1 = 1822.4 K Viscosity = 0.933 cp
Channel Width = 76.0 uSec Index of Ref. = 1.333

GAUSSIAN SUMMARY:
Mean Diameter = 676.5 nm Chi Squared = 200.804
Stnd. Deviation = 434.3 nm (64.2 %) Baseline Adj. = 0.277 %
Coeff. of Var'n = 0.642 Mean Diff. Coeff. = 6.44E-09 cm2/s

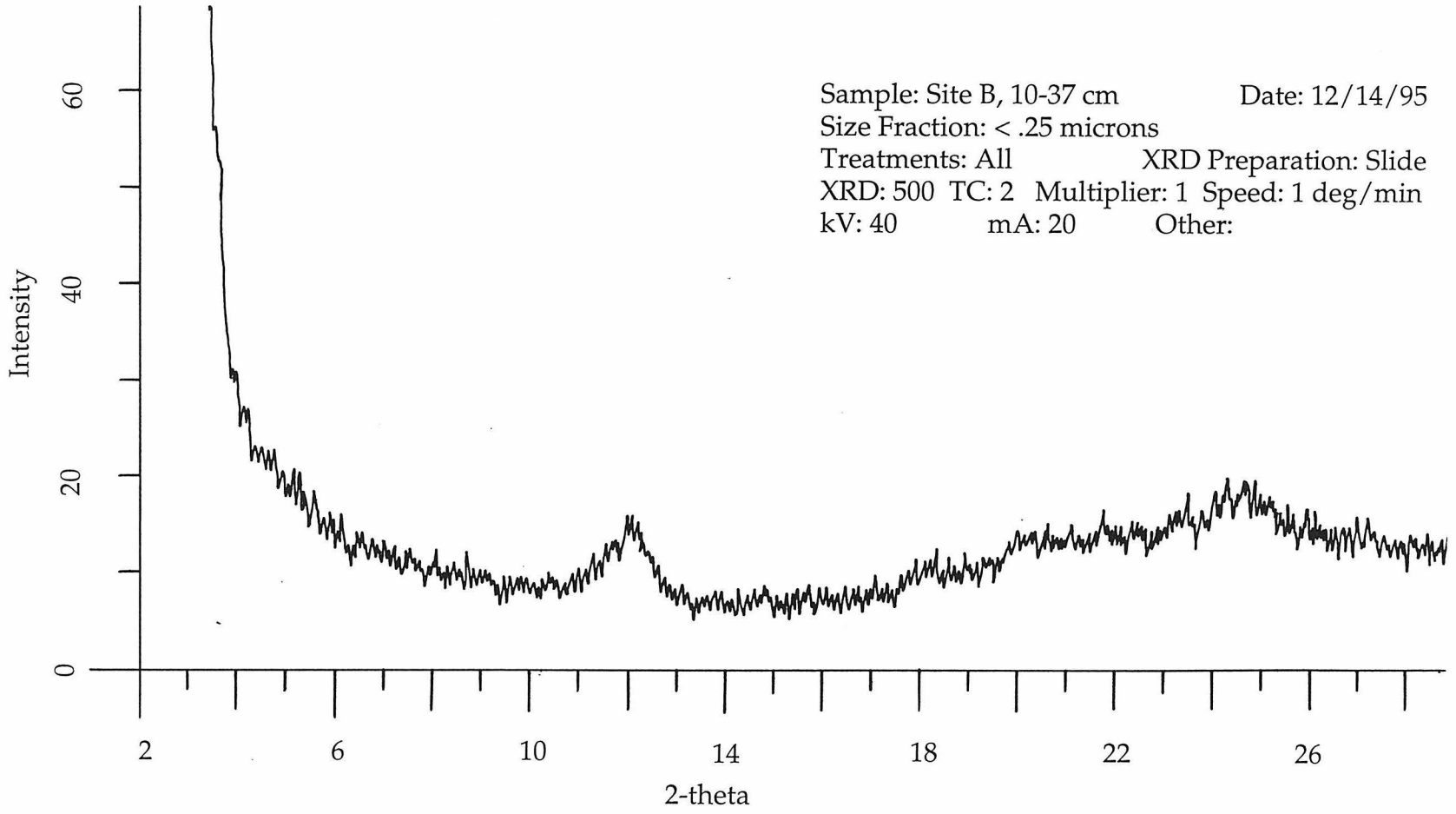
Sample: Site B, 10-37 cm
Date: 12/14/95
Size Fraction: < .25 microns
Treatments: All
XRD Preparation: Slide
XRD: 500 TC: 2 Multiplier: 1 Speed: 1 deg/min
kV: 40
mA: 20
Other:
Intensity
0
20
40
60
2
6
10
14
18
22
26
2-theta

JH-3-3 < 2 microns

VOLUME-Weighted NICOMP DISTRIBUTION Analysis (Solid Particles)

NICOMP SUMMARY:
Peak Number 1: Mean Diameter = 70.1 nm Volume: 16.72 %
Peak Number 2: Mean Diameter = 521.2 nm Volume: 83.28 %

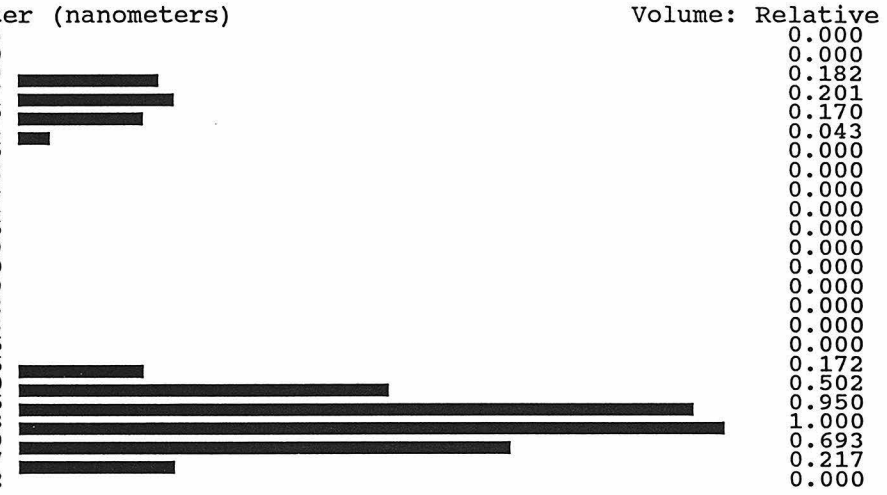

Mean Diameter = 449.9 nm Fit Error = 2.466 Residual = 33.033

NICOMP SCALE PARAMETERS:
Min. Diam. = 10.0 nm Plot Size = 45
Smoothing = 3 Plot Range = 200

Run Time = 0 Hr 22 Min 14 Sec
Count Rate = 210 Khz Temperature = 23 deg C
Channel #1 = 1574.4 K Viscosity = 0.933 cp
Channel Width = 75.0 uSec Index of Ref. = 1.333

GAUSSIAN SUMMARY:
Mean Diameter = 721.4 nm Chi Squared = 2.141
Stnd. Deviation = 389.0 nm (53.9 %) Baseline Adj. = 0.000 %
Coeff. of Var'n = 0.539 Mean Diff. Coeff. = 6.44E-09 cm2/s

JH-3-4 light colored material

VOLUME-Weighted NICOMP DISTRIBUTION Analysis (Solid Particles)

NICOMP SUMMARY:
Peak Number 1: Mean Diameter = 113.5 nm Volume: 28.75 %
Peak Number 2: Mean Diameter = 427.3 nm Volume: 71.25 %

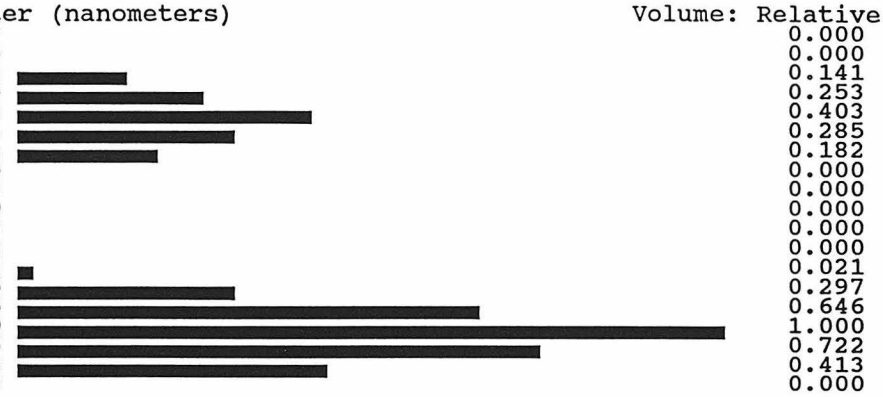

Mean Diameter = 335.7 nm Fit Error = 1.875 Residual = 36.439

NICOMP SCALE PARAMETERS:
Min. Diam. = 10.0 nm Plot Size = 45
Smoothing = 3 Plot Range = 200

Run Time = 0 Hr 12 Min 50 Sec
Count Rate = 314 Khz Temperature = 23 deg C
Channel #1 = 1363.6 K Viscosity = 0.933 cp
Channel Width = 52.0 uSec Index of Ref. = 1.333

GAUSSIAN SUMMARY:
Mean Diameter = 501.8 nm Chi Squared = 33.501
Stnd. Deviation = 307.1 nm (61.2 %) Baseline Adj. = 0.019 %
Coeff. of Var'n = 0.612 Mean Diff. Coeff. = 6.44E-09 cm2/s

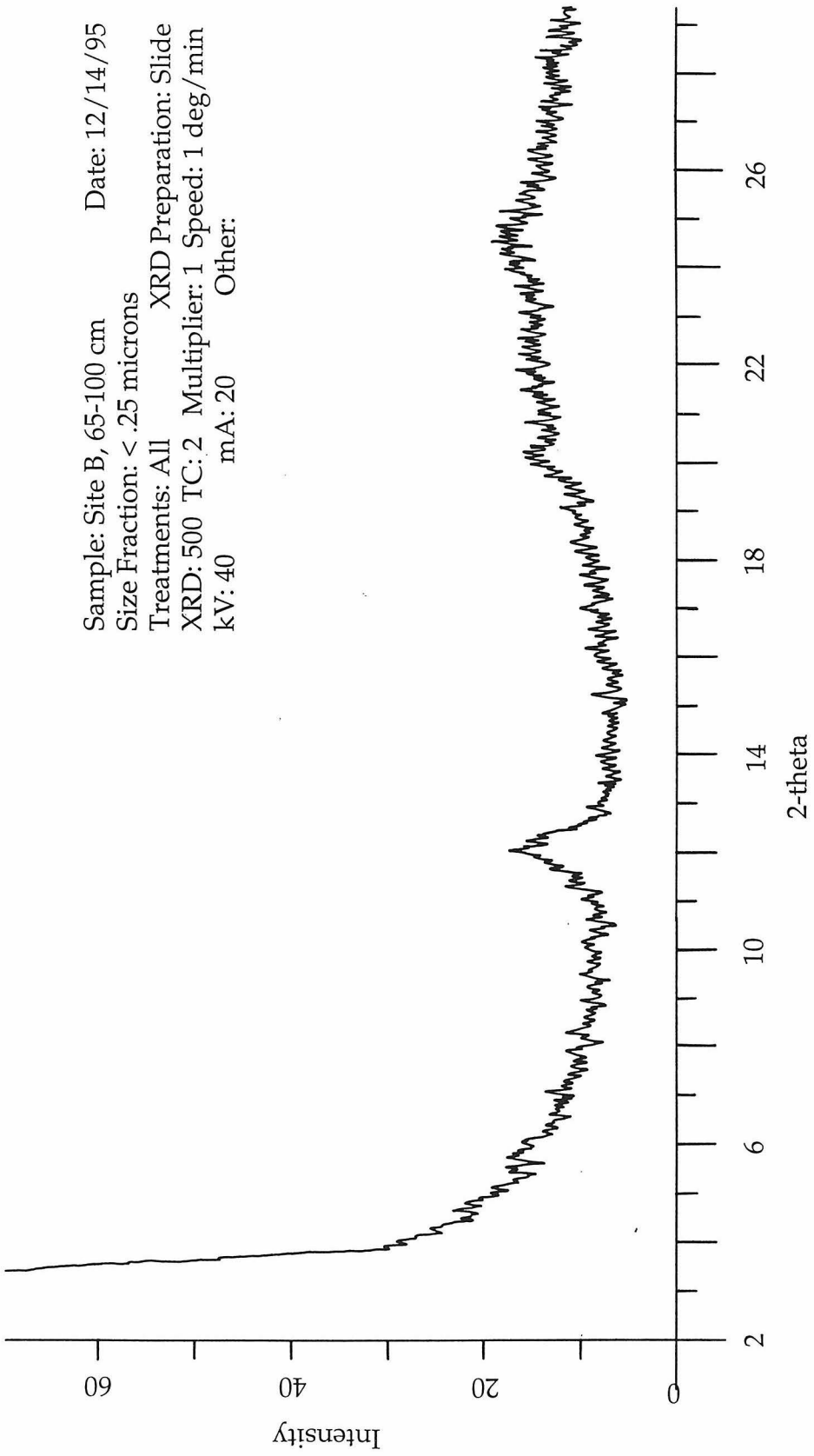
Sample: Site B, 65-100 cm Date: 12/14/95
Size Fraction: < .25 microns
Treatments: All XRD Preparation: Slide
XRD: 500 TC: 2 Multiplier: 1 Speed: 1 deg/min
kV: 40 mA: 20 Other:
Intensity
0
20
40
60
2
6
10
14
18
22
26
2-theta

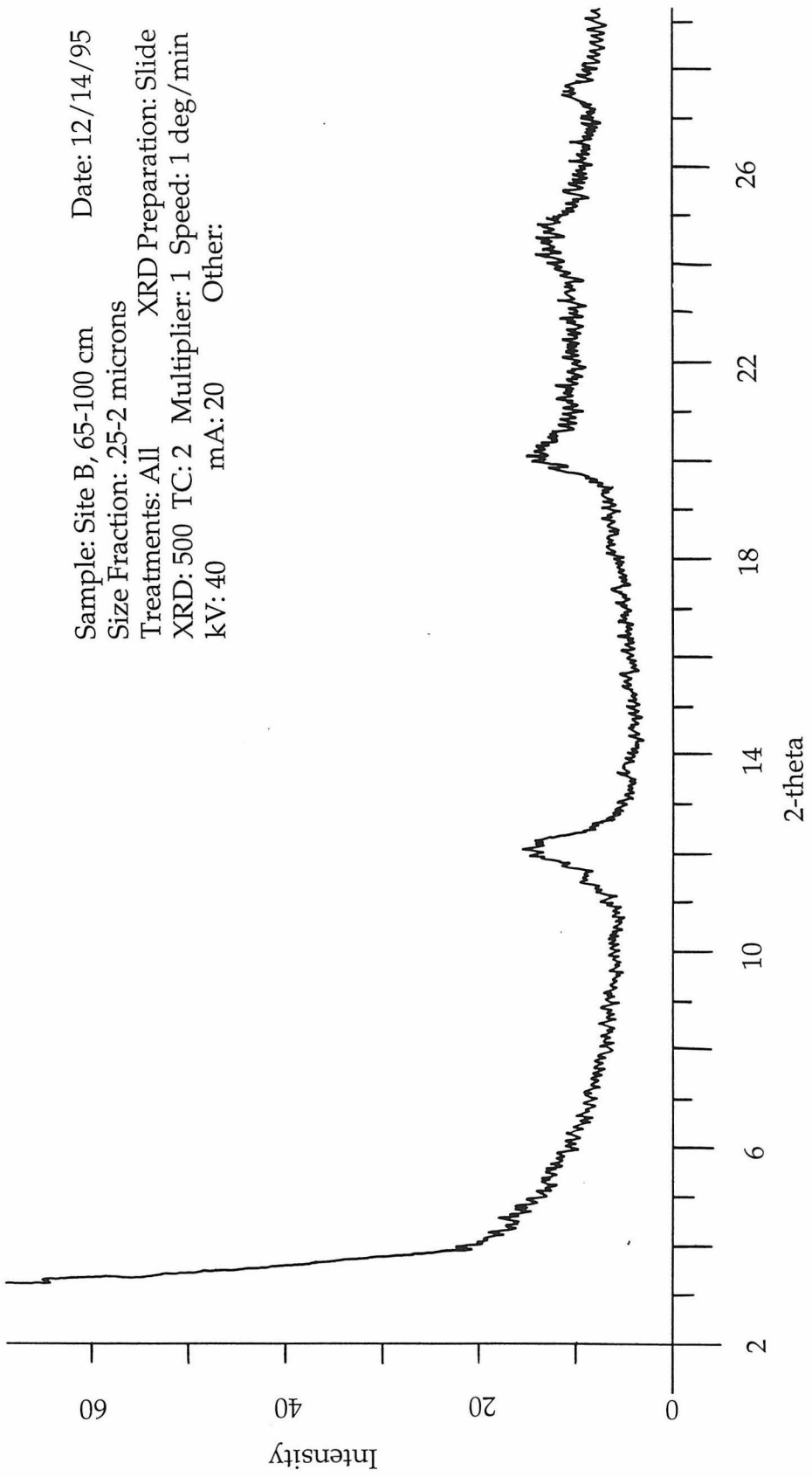
Sample: Site B, 65-100 cm Date: 12/14/95
Size Fraction: .25-2 microns
Treatments: All XRD Preparation: Slide
XRD: 500 TC: 2 Multiplier: 1 Speed: 1 deg/min
kV: 40 mA: 20 Other:
Intensity
0
20
40
60
2
6
10
14
18
22
26
2-theta

JH-8-1 <1 micron

VOLUME-Weighted NICOMP DISTRIBUTION Analysis (Solid Particles)

NICOMP SUMMARY:
Peak Number 1: Mean Diameter = 108.7 nm Volume: 38.83 %
Peak Number 2: Mean Diameter = 419.2 nm Volume: 61.17 %

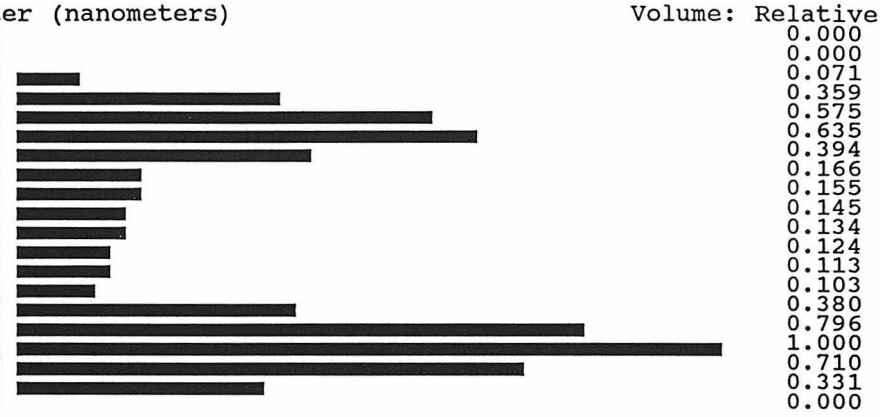

Mean Diameter = 292.7 nm Fit Error = 4.708 Residual = 37.609

NICOMP SCALE PARAMETERS:
Min. Diam. = 10.0 nm Plot Size = 45
Smoothing = 3 Plot Range = 200

Run Time = 0 Hr 11 Min 48 Sec
Count Rate = 339 Khz Temperature = 23 deg C
Channel #1 = 1953.6 K Viscosity = 0.933 cp
Channel Width = 63.0 uSec Index of Ref. = 1.333

GAUSSIAN SUMMARY:
Mean Diameter = 450.4 nm Chi Squared = 152.509
Stnd. Deviation = 267.2 nm (59.3 %) Baseline Adj. = 0.021 %
Coeff. of Var'n = 0.593 Mean Diff. Coeff. = 6.44E-09 cm2/s

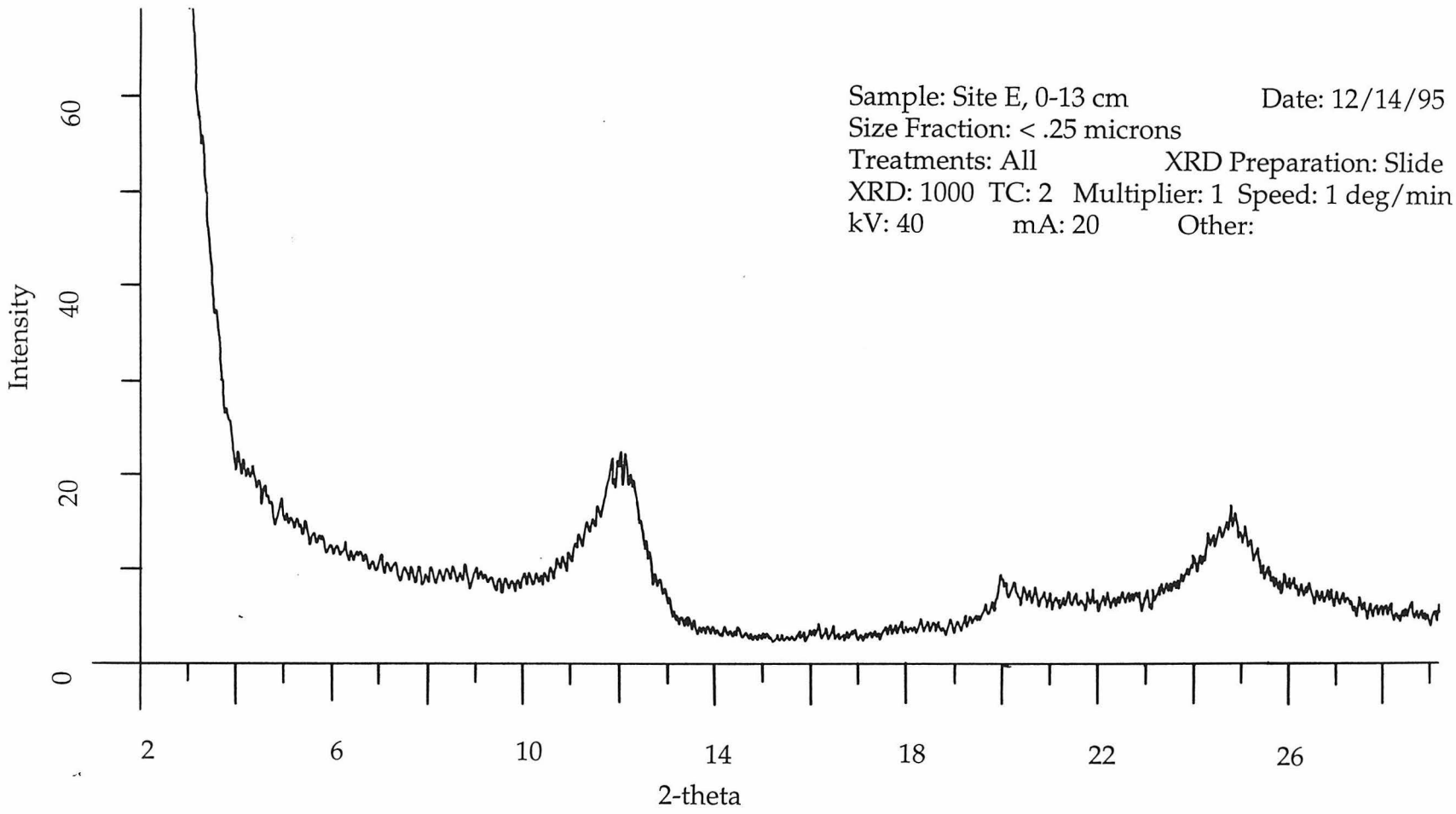
Sample: Site E, 0-13 cm
Date: 12/14/95
Size Fraction: < .25 microns
Treatments: All
XRD Preparation: Slide
XRD: 1000 TC: 2 Multiplier: 1 Speed: 1 deg/min
kV: 40
mA: 20
Other:
Intensity
0
20
40
60
2
6
10
14
18
22
26
2-theta

JH-8-2 < 1 microns, repeat

VOLUME-Weighted NICOMP DISTRIBUTION Analysis (Solid Particles)

NICOMP SUMMARY:
Peak Number 1: Mean Diameter = 113.8 nm Volume: 29.24 %
Peak Number 2: Mean Diameter = 436.8 nm Volume: 70.76 %

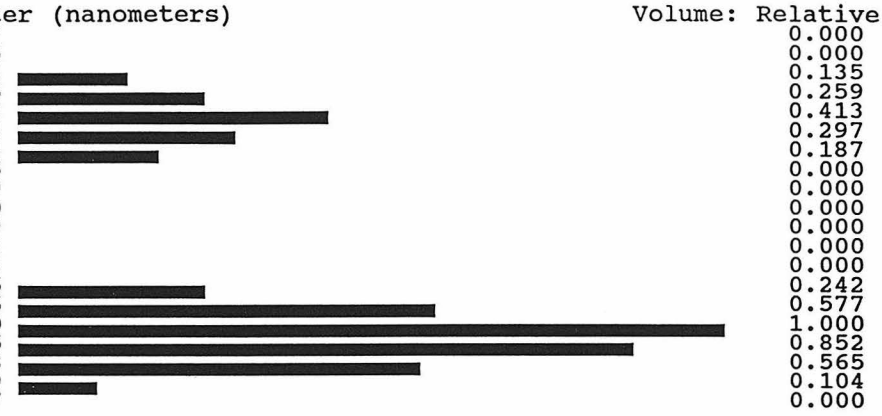

Mean Diameter = 350.3 nm Fit Error = 2.757 Residual = 44.434

NICOMP SCALE PARAMETERS:
Min. Diam. = 10.0 nm Plot Size = 45
Smoothing = 3 Plot Range = 200

Run Time = 0 Hr 10 Min 47 Sec
Count Rate = 190 Khz Temperature = 23 deg C
Channel #1 = 692.3 K Viscosity = 0.933 cp
Channel Width = 53.0 uSec Index of Ref. = 1.333

GAUSSIAN SUMMARY:
Mean Diameter = 586.6 nm Chi Squared = 38.305
Stnd. Deviation = 389.1 nm (66.3 %) Baseline Adj. = 0.000 %
Coeff. of Var'n = 0.663 Mean Diff. Coeff. = 6.44E-09 cm2/s

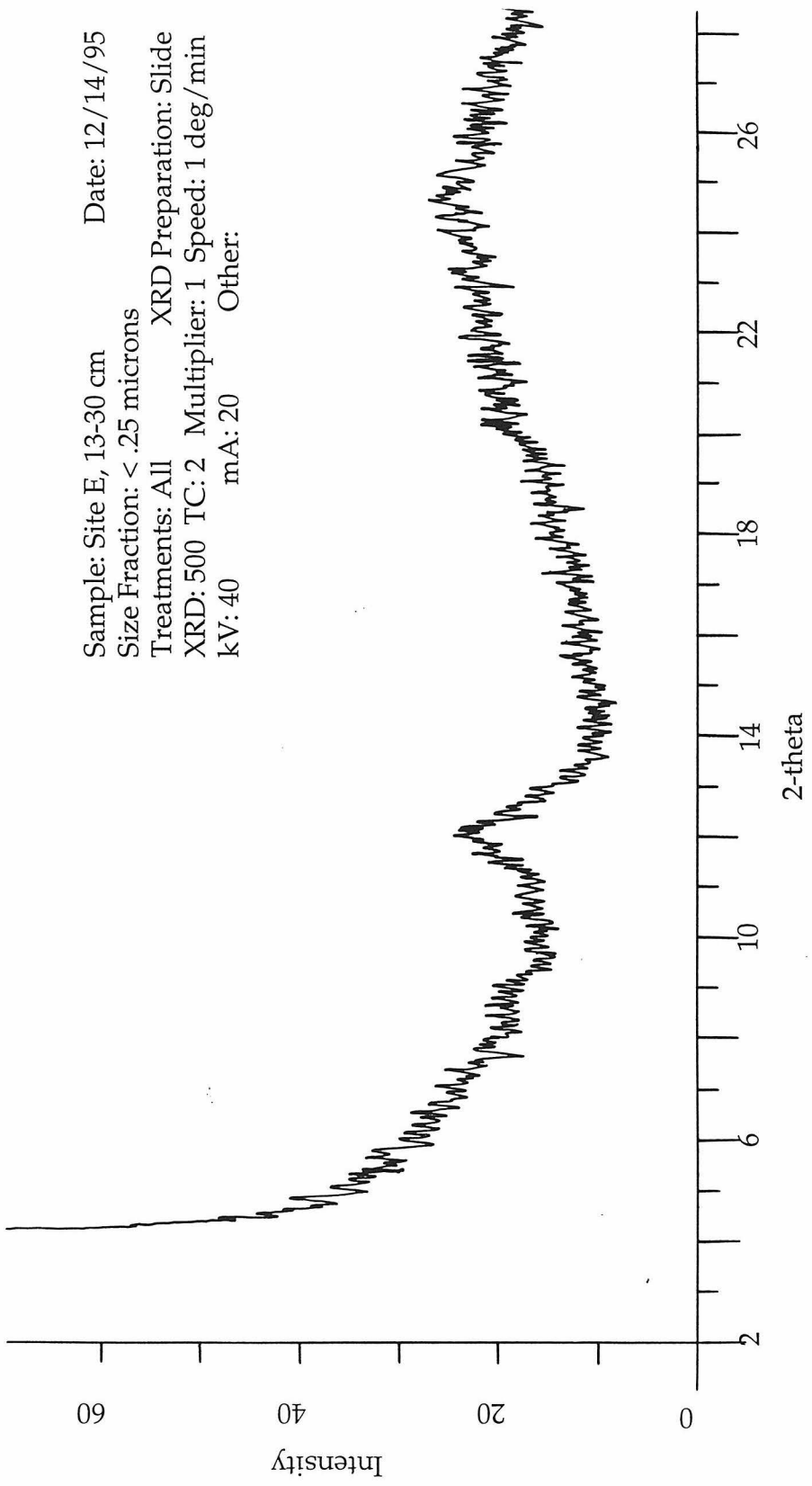
Sample: Site E, 13-30 cm
Date: 12/14/95
Size Fraction: < .25 microns
Treatments: All
XRD Preparation: Slide
XRD: 500 TC: 2 Multiplier: 1 Speed: 1 deg/min
kV: 40 mA: 20 Other:
Intensity
0
20
40
60
2-theta
2
6
10
14
18
22
26

JH-8-3 light colored material

VOLUME-Weighted NICOMP DISTRIBUTION Analysis (Solid Particles)

NICOMP SUMMARY:

Peak Number 1:	Mean Diameter = 85.5 nm	Volume:	12.01 %
Peak Number 2:	Mean Diameter = 316.2 nm	Volume:	14.66 %
Peak Number 3:	Mean Diameter = 2059.4 nm	Volume:	73.33 %

Diameter (nanometers)	Volume: Relative
47.3	0.000
54.5	0.000
62.7	0.048
72.2	0.118
83.2	0.164
95.8	0.130
110.4	0.068
127.1	0.021
146.4	0.000
168.6	0.000
194.2	0.000
223.6	0.059
257.5	0.118
296.6	0.200
341.6	0.181
393.4	0.152
453.1	0.000
521.8	0.000
601.0	0.000
692.2	0.000
797.2	0.000
918.1	0.000
1057.4	0.000
1217.8	0.000
1402.5	0.067
1615.3	0.702
1860.3	0.781
2142.5	1.000
2467.6	0.354
2841.9	0.306
3273.0	0.000

Mean Diameter = 1530.7 nm Fit Error = 2.017 Residual = 0.000

NICOMP SCALE PARAMETERS:

Min. Diam. = 10.0 nm	Plot Size = 45
Smoothing = 3	Plot Range = 500

Run Time	= 0 Hr 12 Min 11 Sec				
Count Rate	= 264	Khz	Temperature	= 23	deg C
Channel #1	= 888.3	K	Viscosity	= 0.933	cp
Channel Width	= 63.0	uSec	Index of Ref.	= 1.333	

GAUSSIAN SUMMARY:

Mean Diameter	= 556.4 nm	Chi Squared	= 89.178
Stnd. Deviation	= 353.7 nm (63.6 %)	Baseline Adj.	= 0.020 %
Coeff. of Var'n	= 0.636	Mean Diff. Coeff.	= 6.44E-09 cm2/s

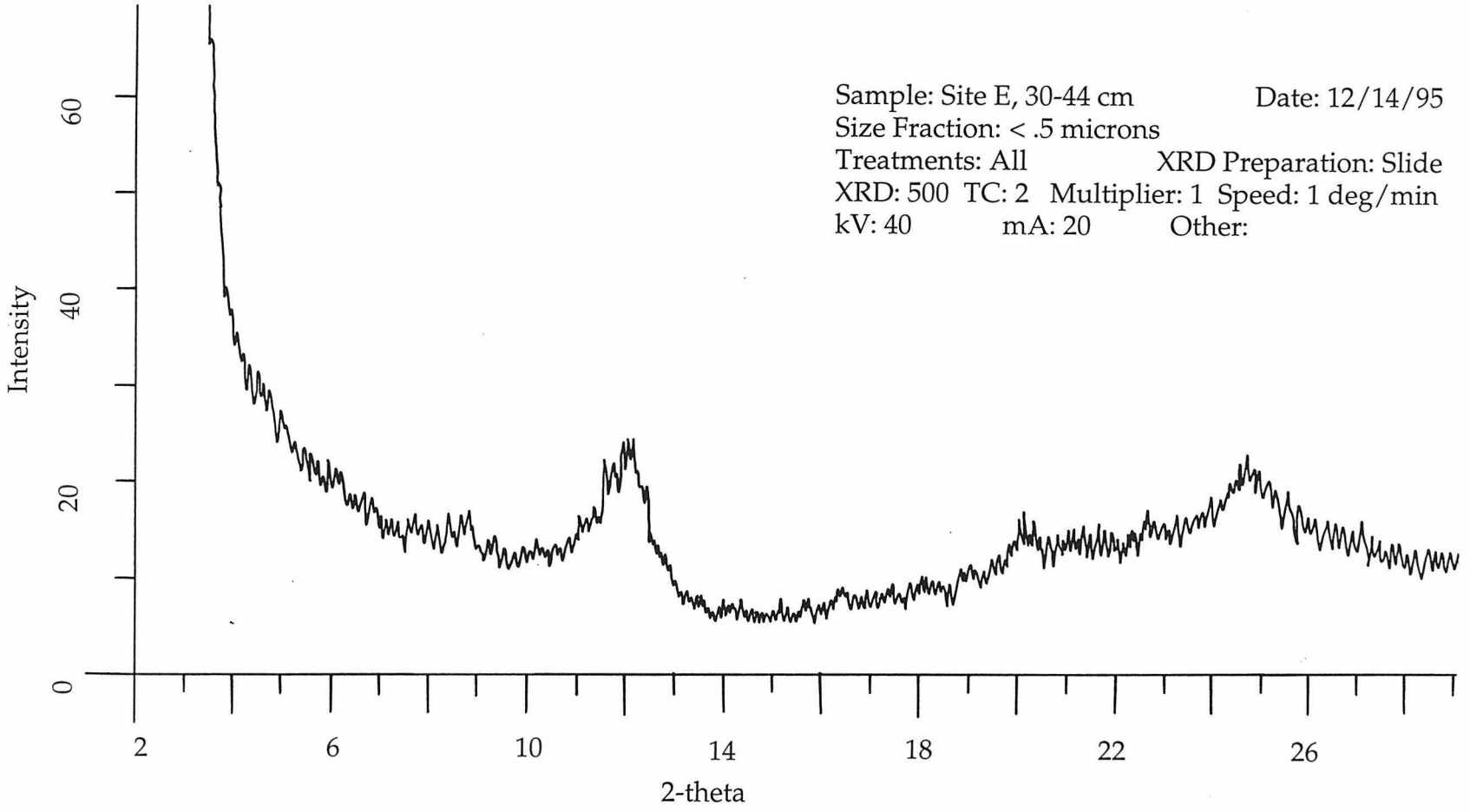
Sample: Site E, 30-44 cm
Date: 12/14/95
Size Fraction: < .5 microns
Treatments: All
XRD Preparation: Slide
XRD: 500 TC: 2 Multiplier: 1 Speed: 1 deg/min
kV: 40
mA: 20
Other:
Intensity
0
20
40
60
2
6
10
14
18
22
26
2-theta

JH-8-4

VOLUME-Weighted NICOMP DISTRIBUTION Analysis (Solid Particles)

NICOMP SUMMARY:
Peak Number 1: Mean Diameter = 35.3 nm Volume: 10.15 %
Peak Number 2: Mean Diameter = 625.1 nm Volume: 13.48 %
Peak Number 3: Mean Diameter = 4486.5 nm Volume: 76.37 %

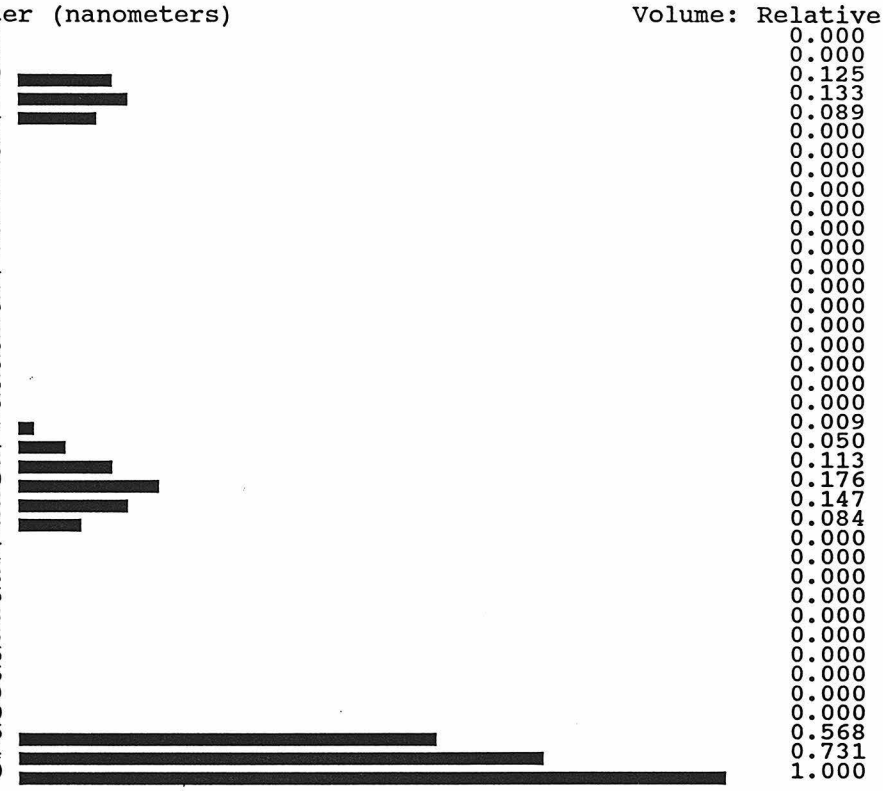

Mean Diameter = 3312.9 nm Fit Error = 3.223 Residual = 65.494

NICOMP SCALE PARAMETERS:
Min. Diam. = 10.0 nm Plot Size = 45
Smoothing = 3 Plot Range = 500

Run Time = 0 Hr 7 Min 37 Sec
Count Rate = 283 Khz Temperature = 23 deg C
Channel #1 = 1159.8 K Viscosity = 0.933 cp
Channel Width = 160.0 uSec Index of Ref. = 1.333

GAUSSIAN SUMMARY:
Mean Diameter = 3028.1 nm Chi Squared = 184.825
Stnd. Deviation = 2697.8 nm (89.1 %) Baseline Adj. = 0.128 %
Coeff. of Var'n = 0.891 Mean Diff. Coeff. = 6.44E-09 cm2/s

JH-8-5

VOLUME-Weighted NICOMP DISTRIBUTION Analysis (Solid Particles)

NICOMP SUMMARY:
Peak Number 1: Mean Diameter = 43.2 nm Volume: 4.44 %
Peak Number 2: Mean Diameter = 482.0 nm Volume: 4.97 %
Peak Number 3: Mean Diameter = 4451.3 nm Volume: 90.58 %

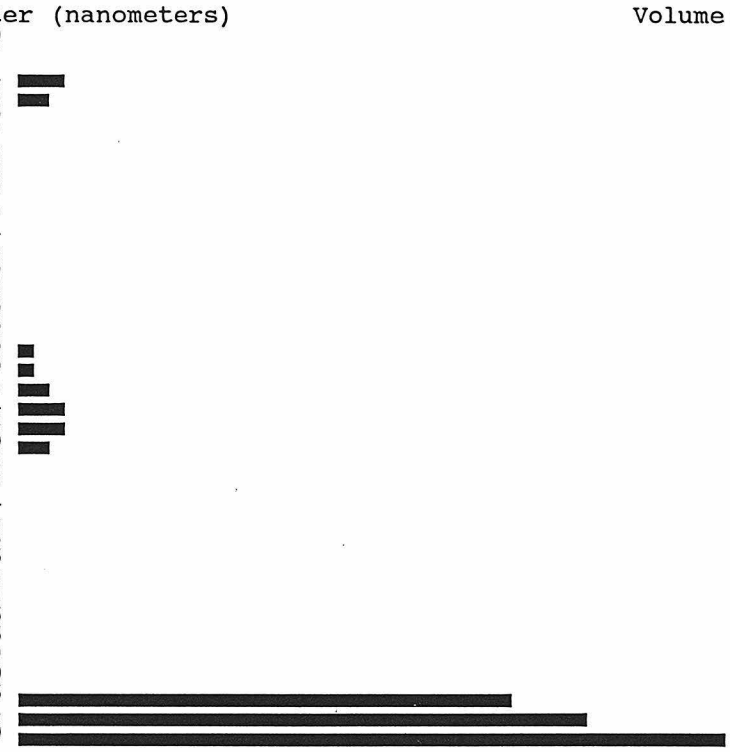

Mean Diameter = 4063.2 nm Fit Error = 2.636 Residual = 23.477

NICOMP SCALE PARAMETERS:
Min. Diam. = 10.0 nm Plot Size = 45
Smoothing = 3 Plot Range = 500

Run Time = 0 Hr 10 Min 37 Sec
Count Rate = 265 Khz Temperature = 23 deg C
Channel #1 = 1832.4 K Viscosity = 0.933 cp
Channel Width = 140.0 uSec Index of Ref. = 1.333

GAUSSIAN SUMMARY:
Mean Diameter = 2514.4 nm Chi Squared = 181.063
Stnd. Deviation = 2140.0 nm (85.1 %) Baseline Adj. = 0.053 %
Coeff. of Var'n = 0.851 Mean Diff. Coeff. = 6.44E-09 cm2/s

JH-J50, < 2micron

VOLUME-Weighted NICOMP DISTRIBUTION Analysis (Solid Particles)

NICOMP SUMMARY:
Peak Number 1: Mean Diameter = 177.9 nm Volume: 3.82 %
Peak Number 2: Mean Diameter = 1090.4 nm Volume: 96.18 %

Mean Diameter = 1046.2 nm Fit Error = 3.621 Residual = 61.376

NICOMP SCALE PARAMETERS:
Min. Diam. = 10.0 nm Plot Size = 45
Smoothing = 3 Plot Range = 500

Run Time = 0 Hr 1 Min 58 Sec
Count Rate = 331 Khz Temperature = 23 deg C
Channel #1 = 392.9 K Viscosity = 0.933 cp
Channel Width = 120.0 uSec Index of Ref. = 1.333

GAUSSIAN SUMMARY:
Mean Diameter = 2661.7 nm Chi Squared = 20.316
Stnd. Deviation = 2188.7 nm (82.2 %) Baseline Adj. = 0.036 %
Coeff. of Var'n = 0.822 Mean Diff. Coeff. = 6.44E-09 cm2/s

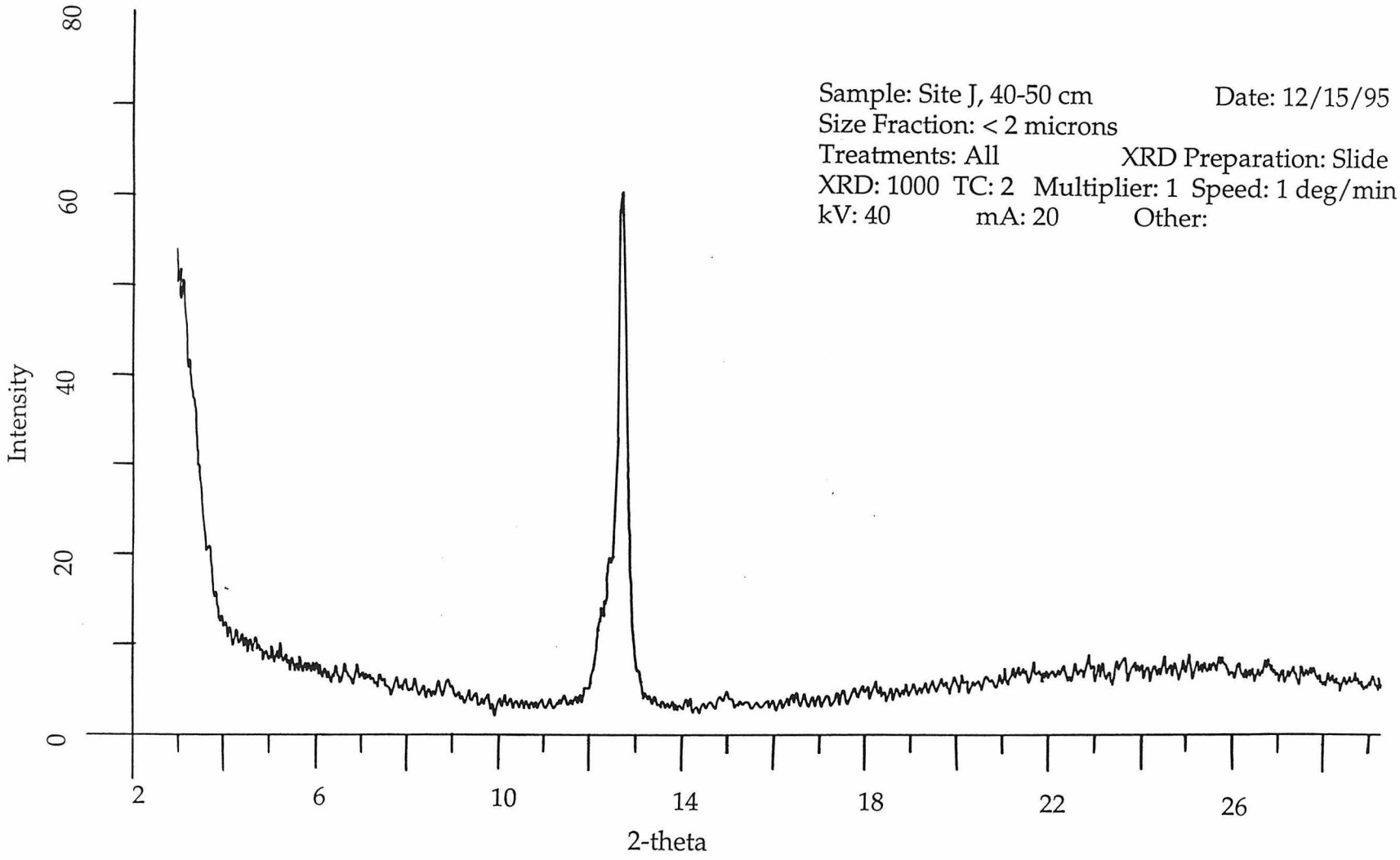
Sample: Site J, 40-50 cm
Date: 12/15/95
Size Fraction: < 2 microns
Treatments: All
XRD Preparation: Slide
XRD: 1000 TC: 2 Multiplier: 1 Speed: 1 deg/min
kV: 40
mA: 20
Other:
Intensity
0
20
40
60
80
2
6
10
14
18
22
26
2-theta

JH-J-70 < 5 microns

VOLUME-Weighted NICOMP DISTRIBUTION Analysis (Solid Particles)

NICOMP SUMMARY:
Peak Number 1: Mean Diameter = 284.5 nm Volume: 5.63 %
Peak Number 2: Mean Diameter = 981.7 nm Volume: 38.62 %
Peak Number 3: Mean Diameter = 4588.3 nm Volume: 55.75 %

Diameter (nanometers)	Volume: Relative
146.4	0.000
168.6	0.000
194.2	0.020
223.6	0.058
257.5	0.099
296.6	0.101
341.6	0.077
393.4	0.005
453.1	0.000
521.8	0.000
601.0	0.140
692.2	0.222
797.2	0.514
918.1	0.692
1057.4	0.693
1217.8	0.365
1402.5	0.000
1615.3	0.000
1860.3	0.000
2142.5	0.000
2467.6	0.000
2841.9	0.000
3273.0	0.000
3769.5	0.333
4341.4	0.563
5000.0	1.000

Mean Diameter = 2306.1 nm Fit Error = 7.147 Residual = 73.996

NICOMP SCALE PARAMETERS:
Min. Diam. = 10.0 nm Plot Size = 45
Smoothing = 3 Plot Range = 500

Run Time = 0 Hr 12 Min 0 Sec
Count Rate = 321 Khz Temperature = 23 deg C
Channel #1 = 2464.1 K Viscosity = 0.933 cp
Channel Width = 250.0 uSec Index of Ref. = 1.333

GAUSSIAN SUMMARY:
Mean Diameter = 2273.6 nm Chi Squared = 2002.529
Stnd. Deviation = 1667.3 nm (73.3 %) Baseline Adj. = 0.217 %
Coeff. of Var'n = 0.733 Mean Diff. Coeff. = 6.44E-09 cm2/s

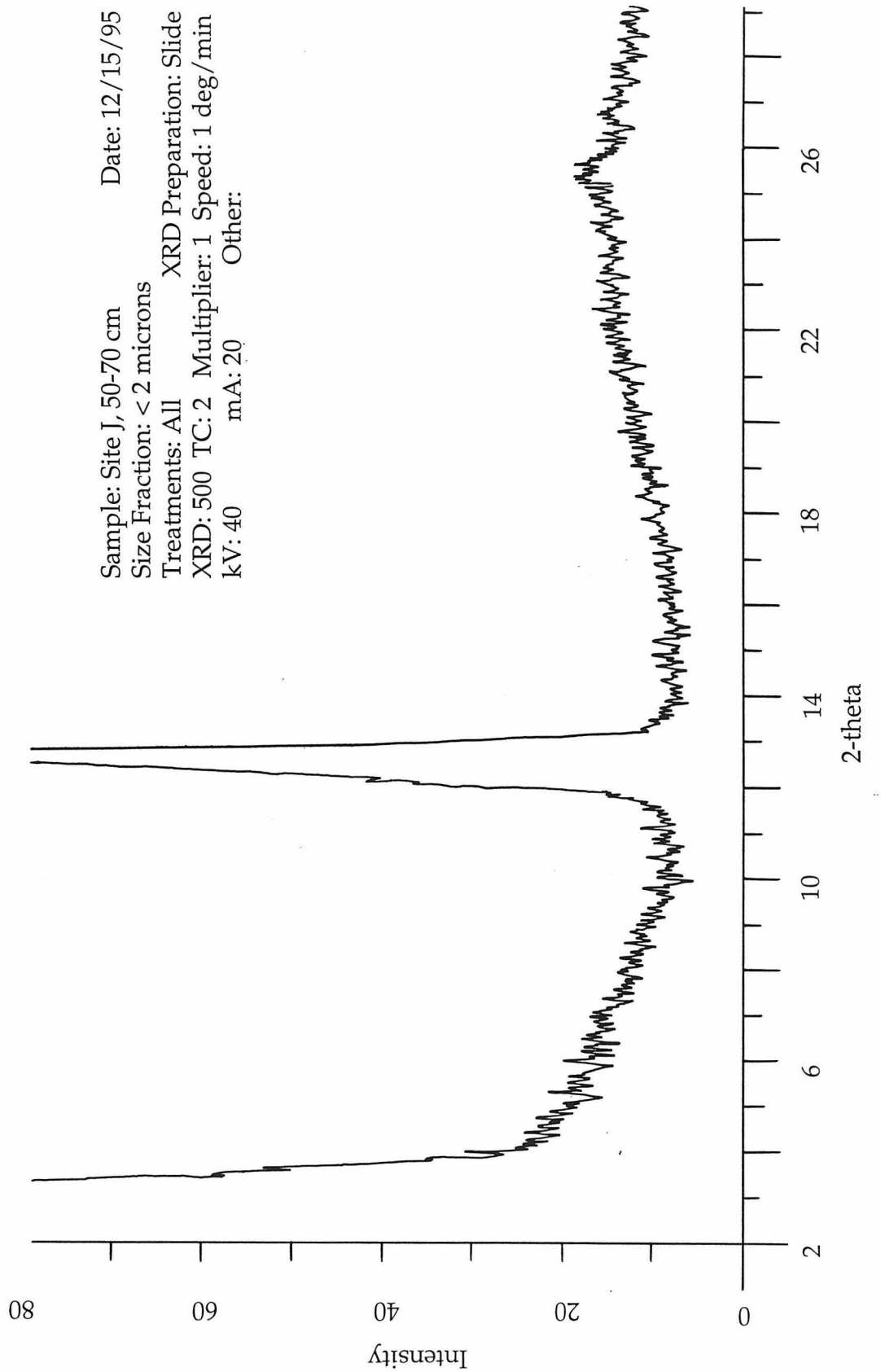
Sample: Site J, 50-70 cm
Size Fraction: < 2 microns
Treatments: All
XRD: 500 TC: 2 Multiplier: 1 Speed: 1 deg/min
kV: 40 mA: 20 Other:
Date: 12/15/95
XRD Preparation: Slide
Intensity
0
20
40
60
80
2
6
10
14
18
22
26
2-theta

HI-001, 5-26 cm

VOLUME-Weighted NICOMP DISTRIBUTION Analysis (Solid Particles)

NICOMP SUMMARY:
Peak Number 1: Mean Diameter = 109.8 nm Volume: 20.44 %
Peak Number 2: Mean Diameter = 464.8 nm Volume: 79.56 %

Diameter (nanometers)	Volume: Relative
70.2	0.000
78.0	0.000
86.6	0.070
96.1	0.156
106.7	0.257
118.5	0.209
131.6	0.126
146.1	0.016
162.2	0.000
180.1	0.000
200.0	0.000
222.1	0.000
246.6	0.000
273.8	0.000
304.0	0.000
337.5	0.055
374.8	0.373
416.1	0.724
462.0	1.000
513.0	0.710
569.6	0.358
632.5	0.000

Mean Diameter = 390.2 nm Fit Error = 1.248 Residual = 27.978

NICOMP SCALE PARAMETERS:
Min. Diam. = 20.0 nm Plot Size = 45
Smoothing = 3 Plot Range = 100

Run Time = 0 Hr 30 Min 55 Sec
Count Rate = 264 Khz Temperature = 23 deg C
Channel #1 = 3942.1 K Viscosity = 0.933 cp
Channel Width = 49.0 uSec Index of Ref. = 1.333

GAUSSIAN SUMMARY:
Mean Diameter = 567.2 nm Chi Squared = 31.549
Stnd. Deviation = 323.8 nm (57.1 %) Baseline Adj. = 0.000 %
Coeff. of Var'n = 0.571 Mean Diff. Coeff. = 6.44E-09 cm2/s

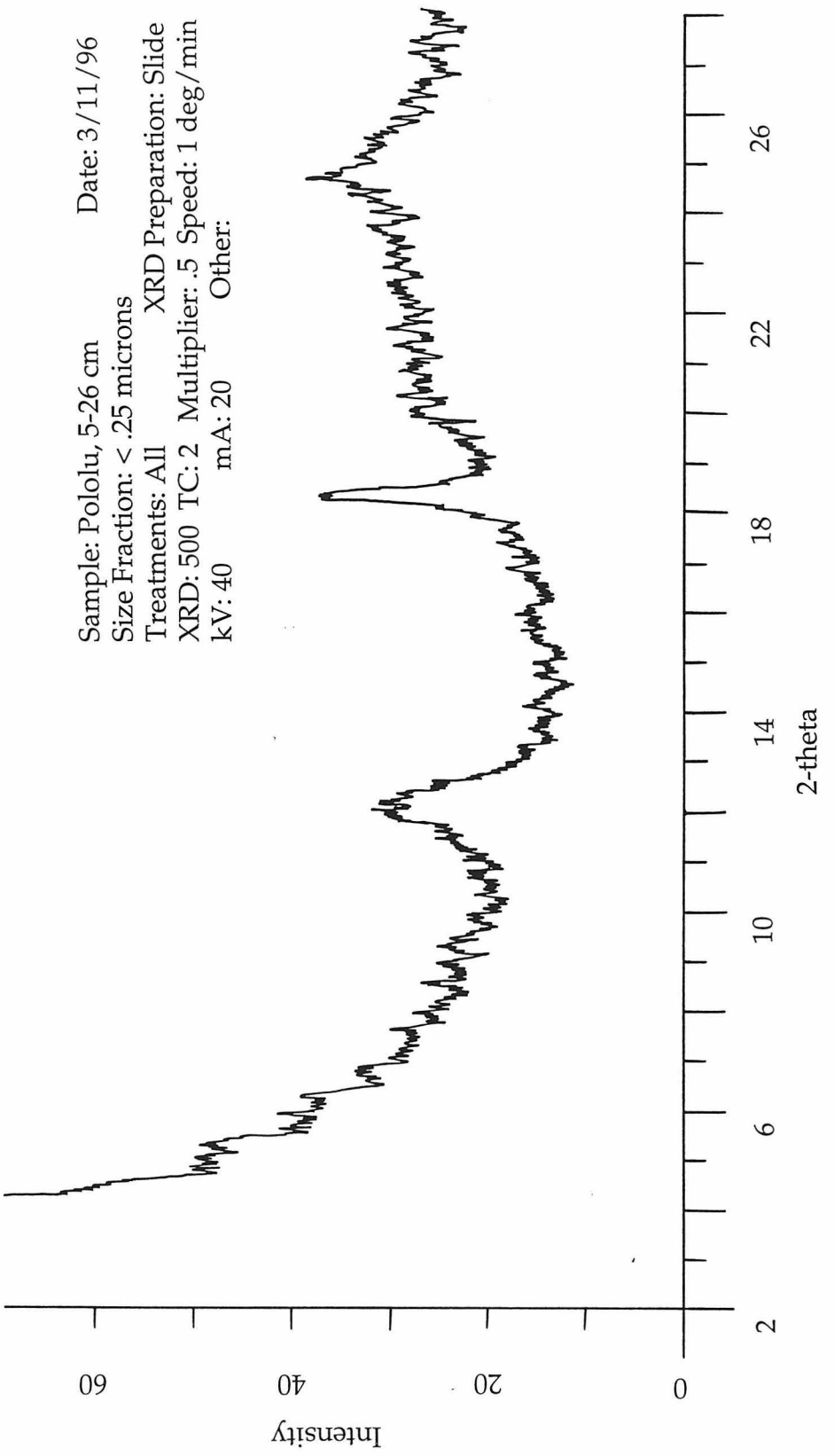
Sample: Pololu, 5-26 cm
Date: 3/11/96
Size Fraction: < .25 microns
Treatments: All
XRD Preparation: Slide
XRD: 500 TC: 2 Multiplier: .5 Speed: 1 deg/min
kV: 40 mA: 20 Other:
Intensity
0
20
40
60
2
6
10
14
18
22
26
2-theta

HI-001, 90-102 cm

VOLUME-Weighted NICOMP DISTRIBUTION Analysis (Solid Particles)

NICOMP SUMMARY:
Peak Number 1: Mean Diameter = 36.9 nm Volume: 24.04 %
Peak Number 2: Mean Diameter = 368.7 nm Volume: 4.83 %
Peak Number 3: Mean Diameter = 1821.7 nm Volume: 71.13 %

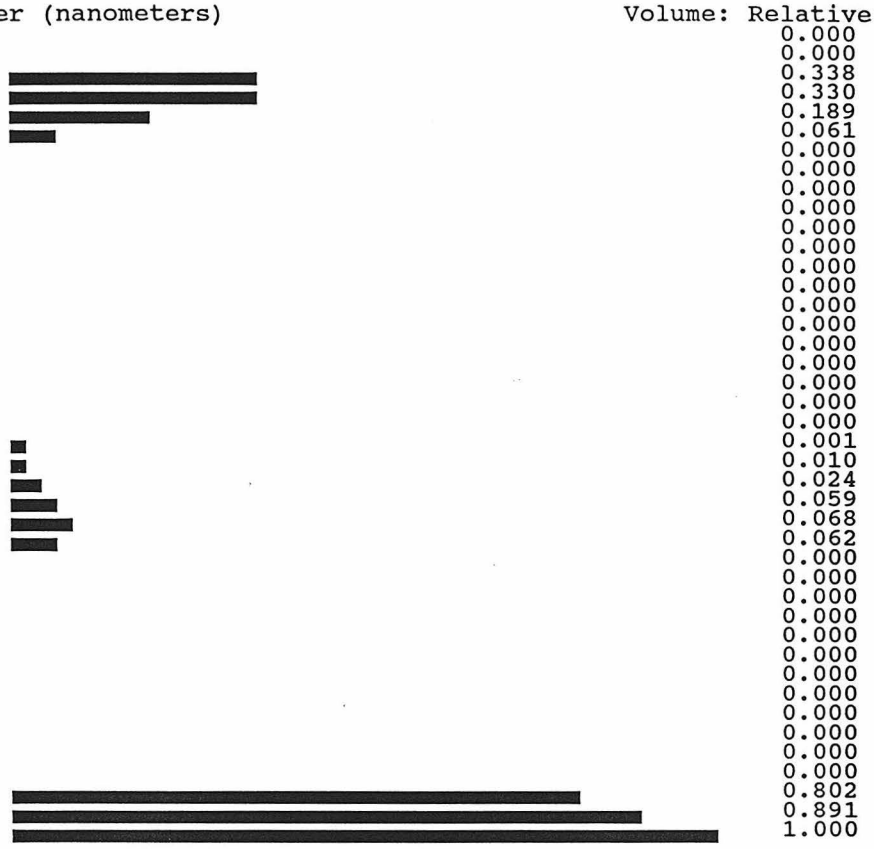

Mean Diameter = 1309.6 nm Fit Error = 4.672 Residual = 17.645

NICOMP SCALE PARAMETERS:
Min. Diam. = 20.0 nm Plot Size = 45
Smoothing = 3 Plot Range = 100

Run Time = 0 Hr 9 Min 42 Sec
Count Rate = 308 Khz Temperature = 23 deg C
Channel #1 = 1604.5 K Viscosity = 0.933 cp
Channel Width = 130.0 uSec Index of Ref. = 1.333

GAUSSIAN SUMMARY:
Mean Diameter = 1598.0 nm Chi Squared = 190.644
Stnd. Deviation = 1080.7 nm (67.6 %) Baseline Adj. = 0.032 %
Coeff. of Var'n = 0.676 Mean Diff. Coeff. = 6.44E-09 cm2/s

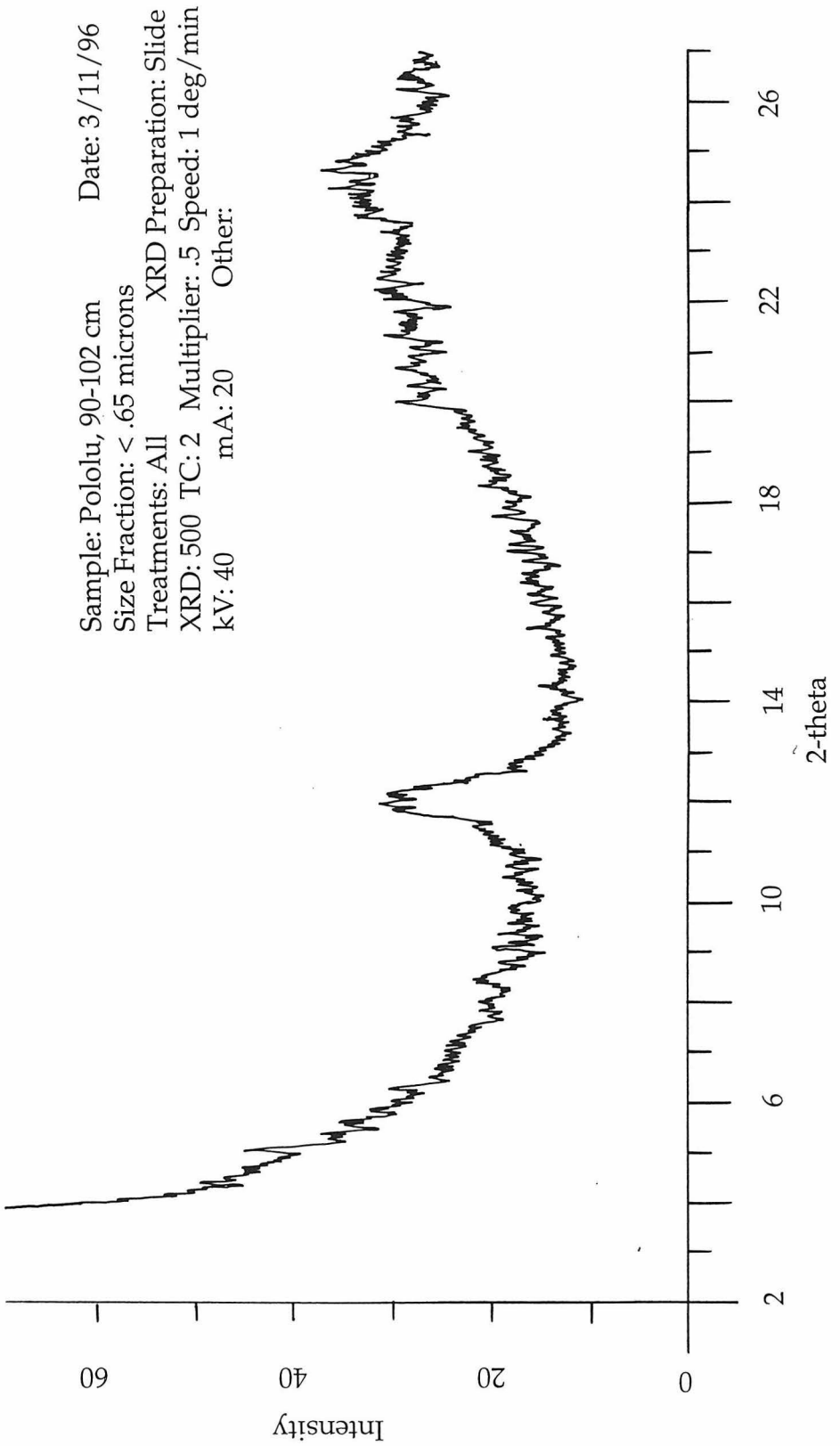
Sample: Pololu, 90-102 cm Date: 3/11/96
Size Fraction: < .65 microns
Treatments: All XRD Preparation: Slide
XRD: 500 TC: 2 Multiplier: .5 Speed: 1 deg/min
kV: 40 mA: 20 Other:
Intensity
0
20
40
60
2
6
10
14
18
22
26
2-theta

HI-001, 102-115 cm

VOLUME-Weighted NICOMP DISTRIBUTION Analysis (Solid Particles)

NICOMP SUMMARY:
Peak Number 1: Mean Diameter = 198.9 nm Volume: 6.30 %
Peak Number 2: Mean Diameter = 1090.8 nm Volume: 93.70 %

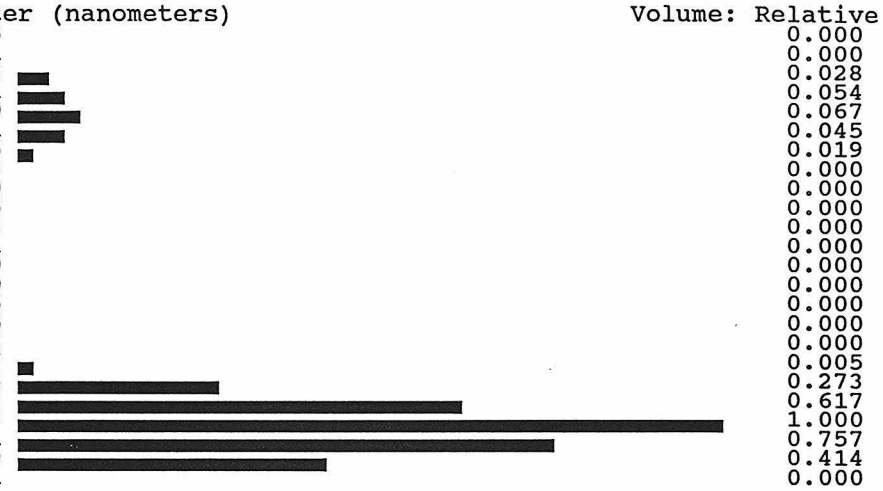

Mean Diameter = 1032.4 nm Fit Error = 5.011 Residual = 39.473

NICOMP SCALE PARAMETERS:
Min. Diam. = 20.0 nm Plot Size = 45
Smoothing = 3 Plot Range = 100

Run Time = 0 Hr 10 Min 56 Sec
Count Rate = 318 Khz Temperature = 23 deg C
Channel #1 = 1657.5 K Viscosity = 0.933 cp
Channel Width = 130.0 uSec Index of Ref. = 1.333

GAUSSIAN SUMMARY:
Mean Diameter = 1577.9 nm Chi Squared = 241.162
Stnd. Deviation = 1050.3 nm (66.6 %) Baseline Adj. = 0.000 %
Coeff. of Var'n = 0.666 Mean Diff. Coeff. = 2.95E-09 cm2/s

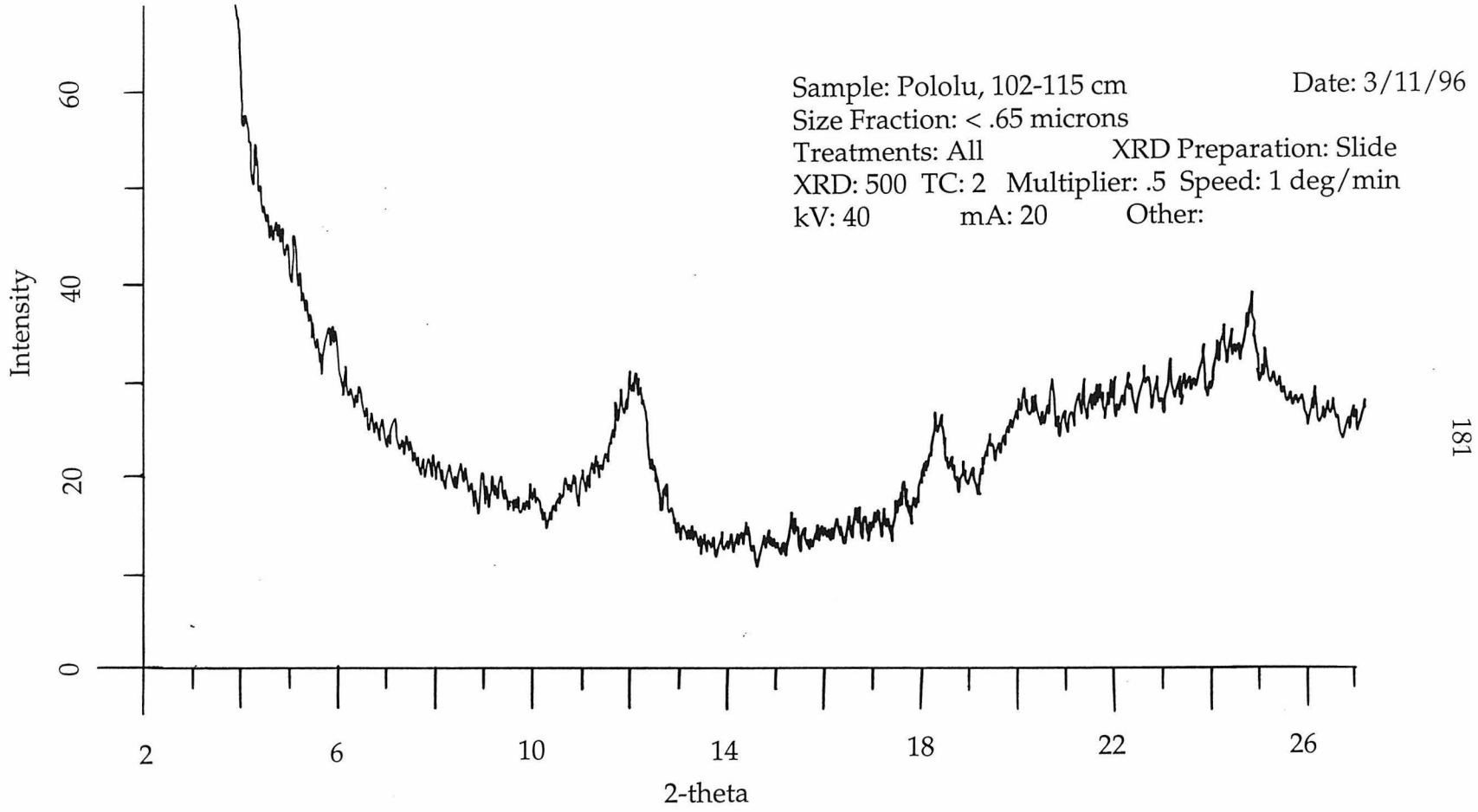
Sample: Pololu, 102-115 cm
Date: 3/11/96
Size Fraction: < .65 microns
Treatments: All
XRD Preparation: Slide
XRD: 500 TC: 2 Multiplier: .5 Speed: 1 deg/min
kV: 40
mA: 20
Other:
Intensity
0
20
40
60
2
6
10
14
18
22
26
2-theta